2023 DRAFT COASTAL MASTER PLAN

ICM-WETLANDS, VEGETATION, AND SOILS MODEL IMPROVEMENTS

ATTACHMENT D2

COASTAL PROTECTION AND
RESTORATION AUTHORITY
150 TERRACE AVENUE
BATON ROUGE, LA 70802
WWW.COASTAL.LA.GOV

COASTAL PROTECTION AND RESTORATION AUTHORITY

This document was developed in support of the 2023 Coastal Master Plan being prepared by the Coastal Protection and Restoration Authority (CPRA). CPRA was established by the Louisiana Legislature in response to Hurricanes Katrina and Rita through Act 8 of the First Extraordinary Session of 2005. Act 8 of the First Extraordinary Session of 2005 expanded the membership, duties, and responsibilities of CPRA and charged the new authority to develop and implement a comprehensive coastal protection plan, consisting of a master plan (revised every six years) and annual plans. CPRA's mandate is to develop, implement, and enforce a comprehensive coastal protection and restoration master plan.

CITATION

Baustian, M. M., Reed, D., Visser, J., Duke-Sylvester, S., Snedden, G., Wang, H., DeMarco, K., Foster-Martinez, M., Sharp, L. A., McGinnis, T., Jarrell, E. (2020). 2023 Draft Coastal Master Plan: Model Improvement Plan, ICM-Wetlands, Vegetation, and Soil. Version I. (p. 155). Baton Rouge, Louisiana: Coastal Protection and Restoration Authority.

ACKNOWLEDGEMENTS

EXECUTIVE SUMMARY

As part of the model improvement effort for the 2023 Coastal Master Plan, the wetland processes captured by the morphology and vegetation models used during previous master plans were reevaluated to assess how Integrated Compartment Model (ICM) subroutines could be improved. This process considered technical reviews, comments, and suggested improvements provided by model developers, advisory groups, and other experts during previous master plan cycles. The availability of new data and information that could be used to make model improvements was also considered. In many cases, the team considered and tested multiple options or approaches. As a result of this effort, recommended improvements are provided here.

The improvements recommended to be included in the 2023 Coastal Master Plan include: adjusting marsh collapse thresholds, refining organic matter accretion calculations, developing an unstructured grid for modeling vegetation, improving flotant marsh and forested wetlands algorithms, creating and applying an updated map of existing vegetation, adjusting model code, and updating the submerged aquatic vegetation (SAV) module.

This report describes the team's work through a series of seven distinct activities to identify and test options for model improvements to ensure the updated ICM used for the 2023 Coastal Master Plan appropriately captures ecological and morphological processes observed in Coastal Louisiana. As appropriate, relevant literature and data are discussed. Test runs to evaluate how changes influence model outputs are also documented. A final list of recommended updates, taking into account consideration of all options and results from test runs, is summarized at the end of the report. A later report will describe the final ICM-LAVegMod and ICM-Morph subroutines for the 2023 Coastal Master Plan, detailing the updates that have been incorporated.

TABLE OF CONTENTS

LIST OF TABLES

LIST OF FIGURES

LIST OF ABBREVIATIONS

1.0 INTRODUCTION

Master plan project selection is driven, in part, by changes in coastal wetland area predicted by the Integrated Compartment Model (ICM). These changes come in the form of an increase or decrease in total wetland area and surface elevation due to environmental drivers and/or restoration projects. Changes in wetland area and elevation simulated by the ICM are influenced by existing wetland area; processes that build new land; relative sea level rise (i.e., the combination of eustatic sea level rise and subsidence); and for each habitat type, the stressors that lead to wetland loss. Positive changes in wetland elevation are also simulated in the ICM by two processes: organic matter accumulation and mineral sediment deposition (for all wetland habitat types except for flotant).

In the predictive models developed for the 2012 Coastal Master Plan and then improved for the 2017 ICM, fresh wetlands converted directly to open water (with an associated loss of elevation, i.e., wetland collapse) if salinities exceeded a two-week threshold. Non-fresh wetlands converted directly to open water if they were subject to inundation thresholds (based on mean annual water depth) for two successive years (Couvillion & Beck, 2013). Salinity patterns and water depths throughout the system were driven by relative sea level rise, which varied by environmental scenario, and by changing system hydrology. An uncertainty analysis conducted for the 2017 Coastal Master Plan found that total wetland area at year 50 was most sensitive to subsidence rate, organic matter accumulation rate (OMAR), and collapse threshold values utilized in ICM-LAVegMod and ICM-Morph as well as water level in ICM-Hydro (Meselhe et al., 2017). The OMAR and marsh collapse threshold values that significantly contributed to landscape change in the 2017 analysis were largely derived from previous work conducted for the 2012 Coastal Master Plan and were further adjusted during calibration and validation of the 2017 ICM (Brown et al., 2017).

Representations of collapse thresholds and OMAR are revisited to ensure the updated ICM used for the 2023 Coastal Master Plan appropriately captures these natural processes and reflects the best available observations and understanding. In addition, representation of flotant and forested wetland extent are re-examined, and an existing condition vegetation map is developed with the addition and removal of some species. The submerged aquatic vegetation (SAV) output from the 2017 ICM is also being validated with more recent field observations to inform possible improvements for the 2023 ICM. Improvements recommended here seek to better represent the ecological and morphological processes in ICM-LAVegMod and ICM-Morph for the 2023 Coastal Master Plan (Figure 1).
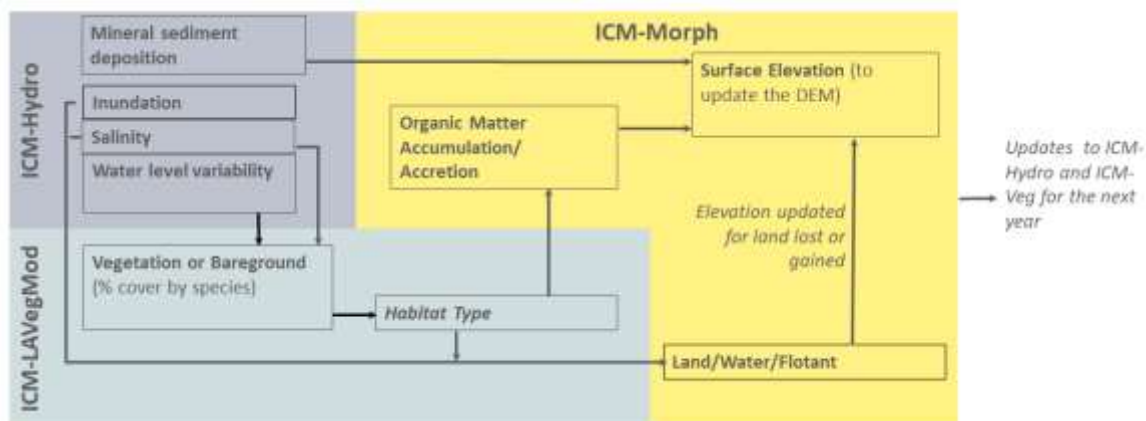
Figure 1. Outline of information flow within an annual cycle of the 2017 Coastal Master Plan ICM subroutines: ICM-Hydro, ICM-Morph, and ICM-LAVegMod. Note that subsidence and sea level rise are also applied annually to adjust the digital elevation model (DEM) and relative water levels.

The development of recommended improvements was organized into a series of activities which explored multiple approaches that included testing model assumptions with CRMS data, calculating organic and mineral matter accumulation rates, assessing significant environmental drivers of OMAR, and developing mortality and establishment tables of additional wetland taxa not included in the 2017 Coastal Master Plan. Peer-reviewed literature was reviewed to inform inundation depth limitations for wetland vegetation, and wetland vegetation responses identified from mesocosm experiments also helped to inform potential responses of soil OMAR to changes in inundation. Recent (2012-2018) field observations for SAV were also gathered by the team for model testing.

Recommended model improvements include use of a new curve that represents water depth limitation by salinity for wetland vegetation; updated look-up tables of soil OMAR and self-packing densities, defined by the ideal mixing model (Adams, 1973) and derived from CRMS data; improvements of flotant representation on the existing conditions map; a revised list of wetland vegetation species and their corresponding mortality and establishment tables; and a plan for validation of SAV output from the 2017 ICM. Recommendations are summarized at the end of this report, and a list of next steps is included to help integrate the model improvements into the ICM framework for the 2023 Coastal Master Plan. To help clarify commonly used terms used throughout this report, a glossary is provided (Table 1).

Table 1. Glossary of commonly used terms in this report.

Term	Definition
Bareground_flt	Areas covered by *Panicum_flt* in the previous year which are not suitable, due to environmental conditions or dispersal rules, for *Panicum* to persist or for *Eleocharis* to establish. Recommended for the 2023 ICM.
Bareground_new	Areas above the water depth limitation for vegetation occurrence where environmental conditions/dispersal rules are such that existing vegetation is unable to persist and on which new vegetation does not establish. Recommended for the 2023 ICM.
Bareground_old	Areas which were *bareground* the previous year and where environmental conditions/dispersal do not allow new vegetation to establish. Recommended for the 2023 ICM.
Collapse thresholds	A set of environmental conditions that, if exceeded in the ICM, result in conversion of wetlands to open water and a loss of elevation. Applied for 2017 ICM, to be replaced by a different approach for the 2023 ICM.
Compartment (or ICM-Hydro compartment)	Grid unit for ICM-Hydro (irregular, to be refined for the 2023 ICM).
CRMS or Coastwide Reference Monitoring System	Monitoring program to assess changing conditions in Louisiana coastal wetlands at over 390 sites (e.g., CRMS0562), with each site having multiple stations (e.g., F01) for collecting land area, hydrologic, vegetation, surface elevation, and soil data.
Dry bulk density	Property of soil calculated by dividing the dry mass of solids by the total volume. Units of g cm^{-3}. Values are used to calculate OMAR.
Elevation for vegetation establishment	Elevation relative to MWL which, if exceeded for two consecutive years, makes areas available for vegetation establishment. Recommended for the 2023 ICM.
FIBS or Fresh, intermediate, brackish, and saline	A classification of marsh habitat types utilized by the ICM-LAVegMod.

Term	Definition
Flotant	Marshes that are permanently underlain by an open water layer that moves up and down as water levels change. Also known as floating marshes or mats; in ICM-LAVegMod, consists of *Panicum_flt* or *Eleocharis_flt*
Grid Cell (or ICM-LAVegMod grid)	Grid unit for ICM-LAVegMod (500 m x 500 m) resolution in the 2017 ICM, to be revised for the 2023 ICM.
Habitat type	An assigned group of vegetation species in the ICM that generally reflects similar environmental conditions (e.g., see FIBS); more generally, may be referred to as vegetation type or community.
HSI or Habitat Suitability Index	Numerical index (between 0 and 1) that represents the capacity of a given habitat to support a species.
ICM or Integrated Compartment Model	Main model used to predict future changes in the landscape and ecosystem for the master plan.
ICM-Hydro	ICM subroutine that simulates changes in water depth, flows, temperature, and salinity in response to boundary conditions and scenarios. Grid is composed of irregular compartments with links that reflect hydrologic exchanges across the coastal zone.
ICM-LAVegMod	ICM subroutine that represents species distribution of wetland vegetation based on niche. Initially developed by Visser and Duke-Sylvester (2013). In the 2017 ICM, the grid was composed of regular 500 m x 500 m grid cells.
ICM-Morph	ICM subroutine that represents soil organic and mineral matter accumulation, vertical accretion, and elevation of the landscape. Grid is composed of 30 m x 30 m pixels.
Ideal mixing model	Calculation that estimates the bulk density of soils based on the organic matter content and the self-packing densities of organic matter and mineral sediment. Recommended application for the 2023 ICM.
Mean Water Level or MWL	Average height reached by water over a given time period. Calculated by the ICM-Hydro.

Term	Definition
MMAR or mineral matter accumulation rate or Q_{sed}	Process of sediment/soils storing mineral matter over time. Units of g cm^{-2} yr^{-1}. Calculated by ICM-Morph.
Net annual primary productivity (NAPP)	Measure of the production of plant biomass in a year that equals carbon uptake for photosynthesis minus carbon lost to respiration. Units of g m^{-2} yr^{-1}.
OMAR or organic matter accumulation rate or Q_{org}	Process of sediment/soils storing organic matter over time. Units of g cm^{-2} yr^{-1}. Calculated by ICM-Morph using look-up table values based on habitat types.
Pixel (or ICM-Morph pixel)	Grid unit for ICM-Morph (30 m x 30 m pixel).
SAV or submerged aquatic vegetation	Rooted vascular plants that grow underwater. Modeled by ICM-LAVegMod.
Salinity	Measurement of dissolved salt content in surface waters or soil porewater with commonly reported units of ppt, psu, and others.
Self-packing density	Bulk densities of organic (k1) and mineral matter (k2) utilized in the ideal mixing model (Adams, 1973). Recommended parameters for the 2023 ICM.
Unvegetated flats	Newly emerging substrates that are available for vegetation establishment.
Vertical accretion, accretion, or vertical accretion rate (VAR)	The process of sediment/soils gaining elevation over time through surficial accumulation of mineral matter and soil organic matter. Units of cm yr^{-1}. Calculated by ICM-Morph.
Water depth limitation for vegetation occurrence	A maximum water depth (m) for vegetation occurrence which varies by salinity. Recommended for the 2023 ICM.

2.0 MODEL IMPROVEMENT ACTIVITIES

The ICM-Wetlands, Vegetation, and Soils Model Improvement Team was tasked with the seven activities described below. They include (1) Provide recommendation for adjusting marsh collapse thresholds; (2) refine the organic matter accretion approach; (3) coordinate with ICM-Integration and Coding Team on development of an unstructured grid for ICM-LAVegMod; (4) explore and recommend options to improve flotant marsh and forested wetland algorithms; (5) coordinate with Model Input Team as needed to create existing conditions vegetation map; (6) coordinate with ICM-Integration and Coding team to adjust model code; and (7) update the submerged aquatic vegetation (SAV) module.

2.1 ACTIVITY 1: PROVIDE RECOMMENDATION FOR ADJUSTING MARSH COLLAPSE THRESHOLDS

ISSUE

In the 2017 ICM, fresh wetland habitat types (bottomland hardwoods, swamps, and attached fresh marshes) converted directly to open water with an associated loss of elevation (i.e., wetland soil collapse) if salinity exceeded a two-week threshold (Table 2). Non-fresh wetland habitat types (intermediate, brackish, and saline marsh) converted directly to open water if they were subject to inundation thresholds (based on mean annual depth) for two successive years. Flotant conversion to open water is discussed in Activity 4. Research shows that for many wetland habitat types, vegetation can be influenced by the combined effects of salinity and inundation stress. Moreover, the assignment of collapse mechanism and threshold tolerance by habitat types make wetland extent sensitive to the classification of these habitat types. *This activity explored whether collapse thresholds should be modified (for example, to reflect the combined influence of salinity and inundation stress) as well as how species are assigned to habitat types.*

BACKGROUND

The collapse thresholds used for the 2017 Coastal Master Plan (Brown et al., 2017) were based on the analysis and advice that supported the 2012 Coastal Master Plan. Collapse thresholds were defined based on water depth, determined by comparing wetland elevation to annual mean water level (MWL), and the maximum two-week mean salinity during each year (Table 2). The collapse thresholds for non-fresh wetland habitat types were chosen by locating the intercept of a polynomial regression of Normalized Difference Vegetation Index (NDVI) values vs. elevation relative to mean water level with two standard deviations below the mean NDVI value for each habitat type (Couvillion & Beck, 2013). Salinity thresholds for fresh wetlands were based on guidance from the 2012 Coastal Master Plan Marsh Collapse Threshold Advisory Panel and suggestions from reviewers of the 2012

ICM effort. A threshold for converting water to land was also defined based on elevation relative to MWL, and the conversion to open water was associated with a loss of elevation of 25 cm (Table 3).

Table 2. Collapse thresholds used in the 2017 ICM-Morph (Brown et al., 2017) for habitat types.

Habitat Type	Collapse Threshold
Fresh Forested Wetlands	Land will convert to open water if it is at, or below, the annual MWL for the year and the maximum two-week mean salinity during the year is above: 7 ppt
Fresh Marsh	Land will convert to open water if it is at, or below, the annual MWL for the year and the maximum two-week mean salinity during the year is above: 5.5 ppt
Intermediate Marsh	Land will convert to open water if the annual mean water depth over the marsh for two consecutive years is greater than: 0.36 m
Brackish Marsh	Land will convert to open water if the annual mean water depth over the marsh for two consecutive years is greater than: 0.26 m
Saline Marsh	Land will convert to open water if the annual mean water depth over the marsh for two consecutive years is greater than: 0.24 m
Bareground	Bareground converts to open water with a loss of elevation (of 25 cm) if MWL for two consecutive years is at least 0.2 m higher than the elevation of the bareground

Table 3. Land gain threshold used in the 2017 ICM-Morph (Brown et al., 2017) for open water habitat type.

Habitat Type	Land Gain Threshold
Open Water	Open water converts to land if MWL for two consecutive years is at least 0.2 m lower than the bed elevation of the open water area

In the ICM, predicted coastal wetlands extent is sensitive to collapse thresholds (Meselhe et al., 2017) due to the role of these thresholds in driving modeled landscape change. As the collapse thresholds are applied by habitat types, the assignment of species to those habitat types also becomes important. The habitat types shown in Table 2 are those used for the 2017 ICM-Morph analysis. The species assigned to each of these habitats for the 2017 Coastal Master Plan are shown in Table 4.

Table 4. Vegetation species mixture for each habitat type in Table 1 and utilized in the 2017 Coastal Master Plan.

Habitat Type	Species
Fresh Forested Wetlands	*Quercus lyrata, Quercus texana, Quercus laurifolia, Ulmus americana, Quercus nigra, Quercus virginiana, Salix nigra, Taxodium distichum, Nyssa aquatica*
Fresh Attached Marsh[1]	*Morella cerifera, Panicum hemitomon, Sagittaria latifolia, Zizaniopsis miliacea, Cladium mariscus, Typha domingensis*
Intermediate Marsh	*Sagittaria lancifolia, Phragmites australis, Schoenoplectus californicus, Iva frutescens, Baccharis halimifolia*
Brackish Marsh	*Spartina patens, Paspalum vaginatum*
Saline Marsh	*Juncus roemerianus, Distichlis spicata, Spartina alterniflora, Avicennia germinans*

[1] The ICM also considered flotant but these were not subject to marsh collapse thresholds in the 2017 Coastal Master Plan and are not included in Table 2.

Each species in the ICM-LAVegMod was uniquely associated with one habitat type (Table 4). This contrasts with the approach used by Chabreck (1970), which identified plant associations rather than individual species for classification. Building on the categorization of species according to their salinity tolerance developed by Penfound and Hathaway (1938) and refined by O'Neil (1949), Chabreck (1970) noted that typical plant associations within any wetland habitat type (fresh, intermediate, brackish or saline – known as FIBS) can include plants found in other types (e.g., *Spartina patens* is found in intermediate, brackish, and saline marshes). The Coastwide Reference and Monitoring System (CRMS) also uses the FIBS classification approach. Visser et al. (1998, 2000) reanalyzed the species data used by Chabreck (1970) with Two Way Indicator Species Analysis and identified seven associations of species, or vegetation types, in the Chenier Plain and nine in the Deltaic Plain. Several species occurred in more than one vegetation type. Snedden and Steyer (2013) analyzed species information from CRMS sites in relation to key environmental variables (i.e., salinity and water level variability) and identified nine associations of species, or communities. Further analysis by Snedden (2019) using self-organizing maps identified eleven vegetation communities. In analyses of Snedden and Steyer (2013) and Snedden (2019), there were some species associated with more than one vegetation community. Given the various classification methodologies outlined in these studies, Activity 1 also considered the appropriate classifications, if any, to use in the model to transition wetlands to open water.

APPROACHES/METHODS

Several approaches were pursued to assess the need to modify collapse thresholds in the ICM for the 2023 Coastal Master Plan and to inform recommendations for updates:

1. Adjust the Couvillion and Beck (2013) relationships to use inundation duration
2. Test collapse threshold assumptions with CRMS data
3. Literature review
4. Reconsider use of collapse thresholds in the ICM

RESULTS

APPROACH 1: ADJUST THE COUVILLION AND BECK (2013) RELATIONSHIPS TO USE INUNDATION DURATION

The inundation thresholds used for intermediate, brackish, and saline marshes in the 2017 ICM were based on depth of flooding over the marsh surface. Inundation duration also reflects the influence of hydrology on vegetation occurrence, and this approach revisited the Couvillion and Beck (2013) analysis to explore if relationships linking marsh collapse with duration could be identified. A time series of water surface elevation was thus needed to calculate inundation duration based on the marsh elevations.

To create a spatially and temporally varying water surface elevation layer, 2018 CRMS water surface elevation data were interpolated spatially for each hour of the year. This exercise was performed separately for each basin, and interpolation was not allowed across major hydrologic barriers, such as the levees of the Mississippi River. The resulting time-varying water surface elevation layer was intersected with a digital elevation model (DEM) at each grid point classified as land for each hour. The number of hours in the year each grid point was submerged (water surface elevation > DEM elevation) was calculated and converted to percent time flooded for the year.

Effectiveness of this approach was assessed by first examining the distribution of percent time flooded for each of the grid points in the brackish zone of Barataria Basin. For all basins and marsh types, the vast majority of sites were flooded over 90% of the time which does not align well with observed values, at CRMS stations, which were mostly in the 40% - 70% range (Figure 2).
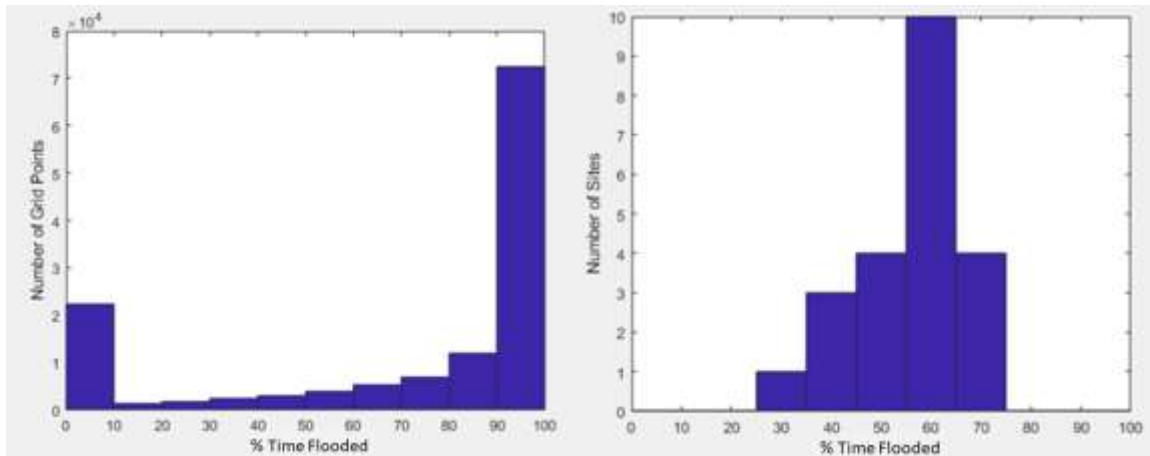
Figure 2. Distribution of modeled and observed values for % time flooded. Left: distribution by grid points (see text for details of approach); right: observed % time flooded at brackish marsh CRMS stations Barataria Basin, 2018.

The spatial domain of the water surface elevation model contained over six million pixels, making hourly interpolations in two dimensions computationally intensive. As a result, extensive effort was required to examine the reasons for the mismatch, and as this was only one of the approaches being pursued for this activity, it was not pursued further. However, a similar approach may be useful in the future for examination of the environmental conditions under which CRMS sites are vegetated or not. This approach would enable marsh collapse thresholds to be based on % time flooded rather than depth of flooding. The % time flooded approach may be more appropriate, given that soil redox and oxygen conditions that influence wetland collapse may be more responsive to flood duration than depth (e.g., Visser & Peterson, 2015).

APPROACH 2: TEST MODEL ASSUMPTIONS WITH CRMS DATA

Existing CRMS data were used to test the 2017 ICM wetland collapse criteria (Table 2) and evaluate wetland vegetation occurrence. This task included assessing a) the change in marsh vegetation cover (% total cover) if environmental data (e.g., salinity, water level) showed that collapse thresholds were exceeded, b) the extent and frequency of wetland collapse, c) occurrence of forested wetlands in areas where environmental data exceeded the collapse threshold, and d) evidence of a water depth limitation for vegetation occurrence. Those four assessments are listed below.

CHANGE IN MARSH VEGETATION COVER

The change in vegetation cover (% total cover) was evaluated at CRMS sites and for multiple stations within a CRMS site. For this analysis, it was assumed that if % total cover decreased by 50% within a five-year period that the marsh could be experiencing collapse-like conditions. The salinity and water

level observations were only available at the site level and were used to compare to the change in % total cover. The results from the analysis (Appendix A) suggested that most observations of collapse-like loss of vegetation cover are temporary. There was little evidence from the existing CRMS data that marsh collapse occurs commonly across the landscape. Appendix A provides details about the data analysis and examples of stations from CRMS sites that experienced fluctuations in % total cover and salinity.

EXTENT AND FREQUENCY OF WETLAND COLLAPSE

An alternative technique to examining the change in % total cover was to assess when the collapse thresholds were exceeded at the CRMS sites and whether this resulted in loss of % total cover. Examination of CRMS data showed that 144 stations from 17 CRMS sites (4% of all CRMS sites) exceeded the flooding threshold for their respective marsh type (Table 2). These site observations were distributed across intermediate, brackish, and saline habitat types. Some stations have been inundated to depths above the collapse threshold associated with their respective vegetation type (Table 2) for the entire monitoring period. Though both flooding and salinity of the collapse thresholds were met repeatedly at CRMS sites, very few sites experienced the predicted vegetation loss. Flood stress rarely caused a change in vegetative cover, and salinity stress did impact cover in fresh marshes but the vegetation almost always recovered. Observations of permanent vegetation loss mostly occurred in coastal fringe sites experiencing erosion of otherwise healthy salt marsh. This evaluation supports the need to reconsider the use of collapse thresholds in the ICM (see Approach 4 below).

OCCURRENCE OF FORESTED WETLANDS EXPERIENCING COLLAPSE THRESHOLD

In the 2017 ICM, the collapse threshold for forested wetlands was triggered if a maximum two-week mean salinity level of 7 ppt was achieved. To assess if forested wetlands at CRMS sites experience this collapse threshold, the canopy cover of forested wetlands from 2007 to 2018 was utilized, which is an equivalent measure to % total cover in emergent marshes of CRMS sites. There were 57 CRMS swamp sites, each with three stations that contain these data, for a total of 171 stations. Of those, 68 stations from 29 swamp sites have canopy cover below 50% at some point. Overall, the salinity threshold was exceeded at 2.5% of the swamp sites but a decline in % canopy cover was not observed; therefore, this collapse threshold should be removed or modified. See Appendix A for more details.

WATER DEPTH LIMITATION FOR VEGETATION OCCURRENCE

Water level variability rather than water level or water depth is used in ICM-LAVegMod to determine species mortality and establishment. Once vegetation establishes, mean annual depth could change considerably within a simulation and mortality would not occur if water level variability remained within the appropriate range for the species with no changes in salinity. In the 2017 ICM-Morph subroutine, wetlands converted to open water with a loss of elevation if the mean water level (MWL) for two

consecutive years was at least 0.2 m higher than the elevation of the marsh (Table 2). CRMS data were examined to explore whether there was a threshold depth above which vegetation does not occur regardless of its habitat type and variation of salinity. If there are no vegetation coverage observations above an inundation and salinity limit, then the ICM should not assume that vegetation can survive above that upper limit.

Mean annual water depth for herbaceous vegetation coverage at CRMS marsh sites was plotted against mean annual salinity for each year of observation (Figure 3). Because of extensive scatter in the data, a curve defining a relationship between the two variables was fit with a 2.5th and 97.5th quantile of the data. See Appendix A for more details on this analysis of CRMS data.
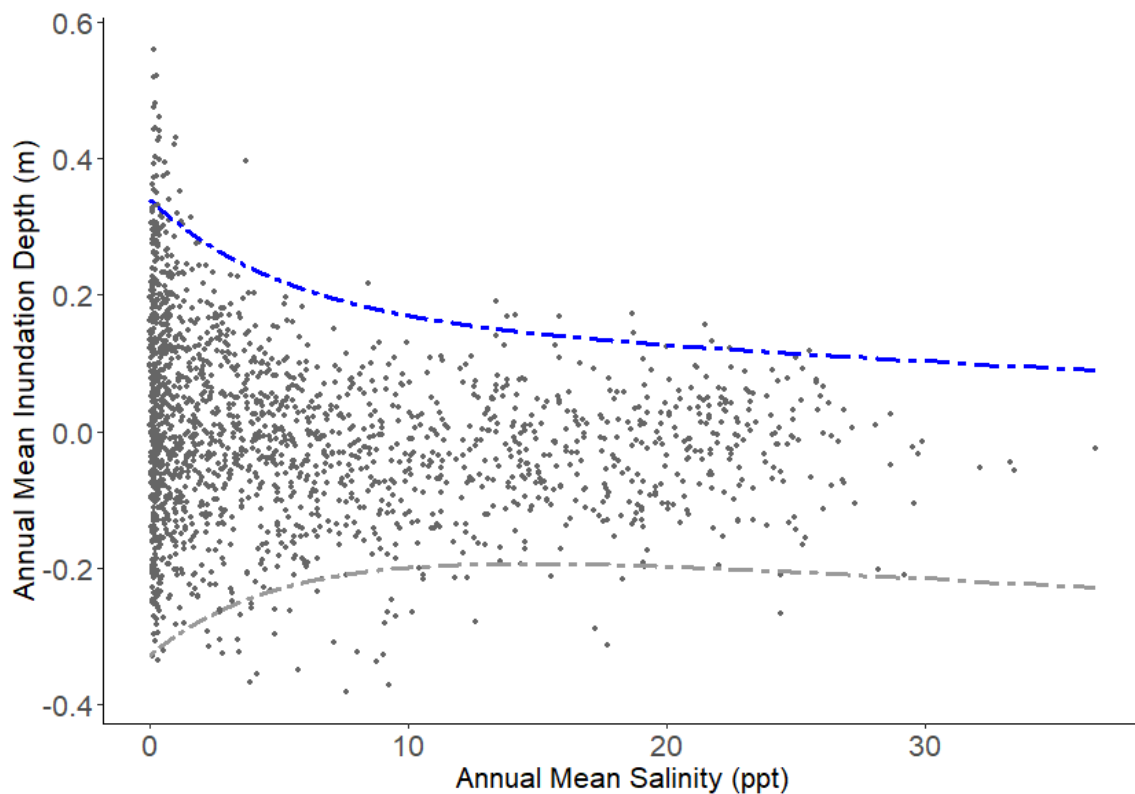
Figure 3. Salinity and water depth distribution of vegetation occurrence in coastal Louisiana with blue line at 97.5th quantile. Each point represents mean salinity and depth for a single CRMS station (2010-2017), n = 1944. The grey line represents the 2.5th quantile from the quantile regression analysis.

The blue curve in Figure 3 could be used to identify a maximum depth, varying by salinity, above which established vegetation would not be considered to survive (i.e., a threshold for transition from

vegetated land to open water in the ICM). The blue curve in Figure 3 fits the notion that as salinity stress increases, plants become more vulnerable to flooding stress. Previous studies have shown that plant biomass decreases and mortality increases as plants experience multiple stressors (Slocum & Mendelssohn, 2008; Visser et al., 2006). Yearly water level and salinity data plotted by station in Figure 4 were classified according to vegetation communities (Snedden, 2019) to determine if there were any clear patterns that would suggest the need to apply a salinity-varied depth threshold by vegetation type. No clear pattern or grouping by vegetation type was apparent, in contrast to the threshold by habitat type approach used in the 2017 ICM.
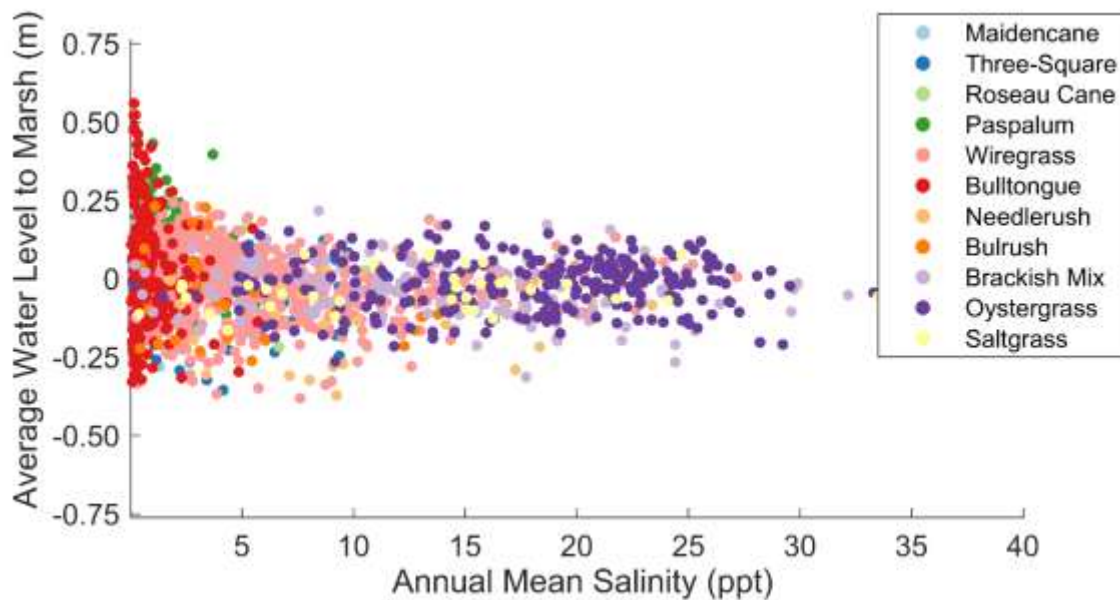
Figure 4. Water depth and salinity distribution by vegetation community in coastal Louisiana by community type. Each point represented mean salinity and depth for a single CRMS station for a single year (2010-2017), n=1944. Eleven vegetation communities are dominated by the following indicator species: Maidencane = *Panicum hemitomon*, Three square = *Schoenoplectus americanus*, Roseau cane = *Phragmites australis*, Pasaplum = *Paspalum vaginatum*, Wiregrass = *Spartina patens*, Bulltongue = *Sagittaria lancifolia*, Needlerush = *Juncus roemerianus*, Bulrush = *Bolboschoenus robustus*, Oystergrass = *Spartina alterniflora*, Saltgrass = *Distichilis spicata*, and Brackish mix = none. Communities here are defined following Snedden (2019).

APPROACH 3: LITERATURE REVIEW

A literature review was conducted to identify current understanding of substrate elevation change and vegetation response to inundation and other environmental conditions. These studies were examined for evidence of collapse thresholds and how to conceptualize the land loss and land gain in the ICM.

FORESTED WETLANDS

Appendix B summarizes recent and relevant literature in relation to documented collapse thresholds or criteria for forested wetlands. There was evidence from lab experiments (mostly with seedlings) and field measurements (response of adult trees to Hurricane Sandy) that mortality occurs at high salinity. For example, Conner (1994) showed that bald cypress seedlings died after exposure to salinities of 10 ppt for two weeks. However, plants survived a simulated storm surge with salinities of 21 ppt for 48 hours, followed by a slow decrease to 2.5 ppt (over ~1 week). Studies in the Maurepas swamp in Louisiana (Hoeppner et al., 2008; Shaffer et al., 2009) used annual soil salinity measurements which limits a direct association with the collapse threshold approach that uses a two-week surface water salinity (Table 2). The highest annual soil salinity noted was 4-5 ppt during the 1999-2000 drought when tree mortality occurred.

MARSHES – CAUSES AND CONSEQUENCES OF MORTALITY

Few papers directly address the collapse of marshes in terms of the conditions that kill vegetation or the consequences of vegetation loss for the marsh substrate. Chambers et al. (2019) provide a useful overview of peat collapse, which is similar to wetland collapse as represented in the ICM. They define peat collapse in a wetland as when highly organic soils (> 20% organic matter by mass) lose elevation within the root zone and create an open water/pond or a mudflat area. The chronic stressors that cause peat collapse can be inundation, nutrient enrichment, and salinity intrusion. They note that once vegetation dies, peat collapse can occur between 5 months to 3 years later, and elevation decreases up to 15 cm. DeLaune et al. (1994) measured a 15 cm peat collapse over a 2-year period in a Louisiana *S. patens* marsh. While the authors suggested that the collapse was due to excessive inundation, water levels were not monitored.

Exposed outdoor mesocosms were used by Li and Pennings (2019) to experimentally subject fresh marsh vegetation to three salinity levels (3, 5, and 10 ppt) crossed with five exposure durations (5, 10, 15, 20, and 30 days per month), plus a freshwater control treatment. Results supported the hypothesis that the responses and recovery of tidal marsh vegetation were directly related to the salinity and duration of saline pulses. Higher-salinity, longer-duration saline pulses caused community composition shifts towards more salt-tolerant species, as well as towards lower species richness and lower aboveground biomass. Communities experiencing low-salinity and short-duration saline pulses recovered due to the regrowth of salt-sensitive species. Community composition of heavily salinized treatments did not recover, but aboveground biomass did indicate that species transition rather than mortality can occur in response to salinity stress. Outdoor mesocosms were used by Charles et al.

(2019) to examine the effect of elevated salinity (~9 ppt) on fresh marsh vegetation (*Cladium jamaicense)* from the Florida Everglades. While there was some effect of the salinity treatment on elevation (a decrease of ~3 cm yr^{-1}), the plants survived.

Lane et al. (2016) simulated wetland loss by applying herbicide to vegetation in plots in fresh, brackish, and saline Louisiana marshes. Elevation surveys found decreases in elevation at all the treatment plots compared to the surrounding wetland elevation. Over the 1.5 years of the study, the fresh site had an average decrease in elevation of −4.24 ± 0.57 cm compared to the surrounding wetland. This rate of elevation loss was significantly greater than experienced at the brackish and saline sites, which had relative elevation losses of −1.56 ± 0.35 cm and −1.48 ± 0.34 cm, respectively. However, other studies which experimentally killed vegetation saw no change in elevation. McKee and Vervaeke (2018) used wrack to kill *Spartina alterniflora* and freeze treatments to kill *Avicennia* in a study in south Louisiana. No effects on surface elevation change were found associated with the experimental mortality. Reed et al. (2009) incorporated a lethal treatment into their field experiment in a brackish marsh community dominated by *S. patens* and *Schoenoplectus americanus* (Northshore of Lake Pontchartrain in Louisiana). The lethal treatment was found to have no significant effect on surface elevation change. Elevation change in bare plots, where *S. alterniflora* had previously been killed due to brown marsh dieback, was tracked over five years (starting six years after the dieback) by Baustian et al. (2012). They measured 9.4 mm yr^{-1} of surface lowering over the 5-year study in dieback areas (i.e., 5-10 years following the initial vegetation loss).

Several studies have examined elevation change following burning of marshes. Cahoon et al. (2004) noted elevation loss of 2-3 cm in six months following burning of *S. patens*. However, their study in coastal Texas showed that unburned marsh declined faster than burned marsh (67.9 mm yr^{-1} vs. 36.9 mm yr^{-1} of elevation loss). The elevation decline not associated with burning was attributed to death and breakup of the *S. patens* mat following prolonged flooding. McKee and Grace (2012), also working in coastal Texas in *S. patens* marshes, found that experimentally burned plots gained elevation faster than plots which were not burned.

VEGETATION ESTABLISHMENT ON NEWLY BUILDING LAND

Several studies of seed germination and flooding were identified. Keddy and Ellis (1985) show that there was at least 25% seed germination at 5 cm of flooding for 11 different freshwater wetland species including *Polygonum punctatum*, *S. americanus*, and *Sagittaria latifolia*. Baldwin et al. (2001) conducted a seedbank study and show that many species from a freshwater wetland germinated in water 3-4 cm deep.

In addition, observational and remote sensing studies of newly establishing areas of vegetation in the Bird's Foot Delta and the Wax Lake Delta were reviewed. Relevant information regarding the elevation, depth, or flooding conditions for vegetation types is summarized in Table 5. Olliver and Edmonds (2017) did not examine specific species but examined the transitions from either open water or bare sediment to vegetation, based on remote sensing data.

Table 5. Summary of observed elevation, relative elevation, depth, and flooding values associated with vegetated deltaic areas in Louisiana.

Vegetation or land cover classification	Carle et al. (2013)[^] Elevation (cm, NAVD88)	Olliver & Edmonds (2017) [#] Elevation (cm, NAVD88)	Shaffer et al. (1992)[&] Elevation (cm, NAVD88)	White (1993)[%] Relative Elevation (cm)	Cahoon et al. (2011) Time flooded* (%)	Flood depth (cm)	Johnson et al. (1985)[$] Height above MWL (cm)
Potamogeton nodosus	-1						
Nelumbo lutea	11						
Polygonum spp.	37						
Colocasia esculanta	47			<-11			
Salix nigra	53			0	6	3.67	21(2) - 9(8)
Sagittaria latifolia			-37.8		94	16.53	9(2) - 6(3)
Typha latifolia							17(4) - 4(3)
Schoenoplectus spp.				-11	50	6.31	
Colonizing mudflat					99	28.24	
Water to sediment[#]		-12					
Water to vegetation[#]		-9					
Sediment to vegetation[#]		12					

^ *Mean substrate elevations by vegetation class from 2009 LIDAR data (low tide); vegetation measurements from 2010-2011*
# *median surface substrate elevations by land-cover class from LIDAR data; land-cover classes defined by the difference in maximum and minimum biomass during 2014; mean lower low water and mean sea level approximately -0.215 m NAVD88 and 0.116 m NAVD88 at the delta apex*
* *percent time flooded calculated over a 340-day period*
& *substrate elevation = 5 cm (NAVD29) was converted to -37.8 cm (NAVD88) using NOAA's VDatum tool online*
% *relative elevation determined during 2 days of extreme flooding; on average,* Scirpus *(i.e.,* Scheoneoplectus*) sites were 11 cm lower than* Salix *sites.* Colacasia *sites were assumed to be even lower*
$ *mean with standard error*

APPROACH 4: RECONSIDER USE OF COLLAPSE THRESHOLDS IN THE ICM

The identification of new threshold values to replace those in Table 2 may not be needed if aspects of how wetland extent are simulated in the 2017 ICM are modified. This approach builds on the information developed through examination of CRMS data (Approach 2) and literature studies (Approach 3) to leverage other aspects of the existing ICM subroutines to model transitions from vegetated wetlands to open water and vice versa.

The mortality and establishment tables in ICM-LAVegMod already account for the transition of vegetation species under varying hydrological conditions, including transition to bareground. These tables consider both salinity and hydrology (specifically, water level variability). In the 2017 ICM, bareground converts to open water with a loss of elevation if the MWL for two consecutive years is at least 0.2 m higher than the elevation of the bareground (Table 2). Bareground occurs in ICM-LAVegMod when environmental conditions (salinity and water level variability) result in mortality of the existing species but conditions are not suitable to establishment of any species within a proximity defined by the dispersal algorithm (Visser & Duke-Sylvester, 2017). The 2017 ICM application of the collapse thresholds to vegetated areas makes the transition directly from vegetated to deeper open water without a bareground phase.

Few direct studies of wetland collapse are available (see Approach 3). Chambers et al. (2019) note that the loss of elevation due to collapse can occur between five months and three years following vegetation death. Lane et al. (2016) showed a loss of elevation of less than 5 cm in 1.5 years following treatment of marshes with herbicide. Given this, the collapse threshold approach applied for vegetated areas in the 2017 ICM may be too aggressive.

POTENTIAL OPTIONS TO TEST

Based on the previous analysis, adjusting the way in which vegetated land converts to open water, and vice versa, may address the issues with sensitivity to the collapse thresholds and allow the combined effect of salinity and inundation to influence land loss. Activity 4 discusses adjustments to transitions within flotant and fresh forested wetlands that align with the approach presented here for attached marshes.

Three sets of processes need to be considered in revision to the 2023 ICM:

- **Gradual Transitions:** Rather than specific collapse thresholds that immediately convert vegetated areas to open water, transitions should be more gradual and for most vegetation types could include a bareground phase when vegetation could be re-established depending on environmental conditions
- **Water Depth Limitation for Vegetation:** There should be a depth limit that varies by salinity for vegetation occurrence

- **Elevations Enabling Establishment:** An elevation relative to MWL is needed to identify substrate which is eligible for vegetation establishment (note that a threshold was used in the 2017 ICM, but the team suggests re-visiting the value)

The ICM operates on an annual time step with decisions made each year on whether an area is land or water and whether land is vegetated and how its elevation changes. The cover types involved in the processes described above are proposed in Table 6. The distinction between new and old bareground and the addition of unvegetated flats require changes to the 2017 ICM.

Table 6. Proposed 2023 ICM land cover types considered as part of the transitions between vegetated areas and water.

Cover Type	Description
Vegetated	Areas covered with emergent vegetation. Vegetation type determined by ICM-LAVegMod
Bareground_new	Unvegetated areas where the bed elevation relative to MWL is above the elevation for vegetation establishment AND were vegetated in the previous year
Bareground_old	Unvegetated areas where the bed elevation relative to MWL is above the elevation for vegetation establishment AND were bareground (old or new) in the previous year
Unvegetated flats	Unvegetated areas where the bed elevation relative to MWL is above the elevation for vegetation establishment AND were not vegetated or bareground (old or new) in the previous year
Open water	Areas where the bed elevation relative to MWL is below the elevation for vegetation establishment

The proposed pathways of transition among cover types are shown in Figure 5 which also indicates how the three processes outlined above control the transitions. Each set of processes is described here, followed by a table that shows how they are applied together.
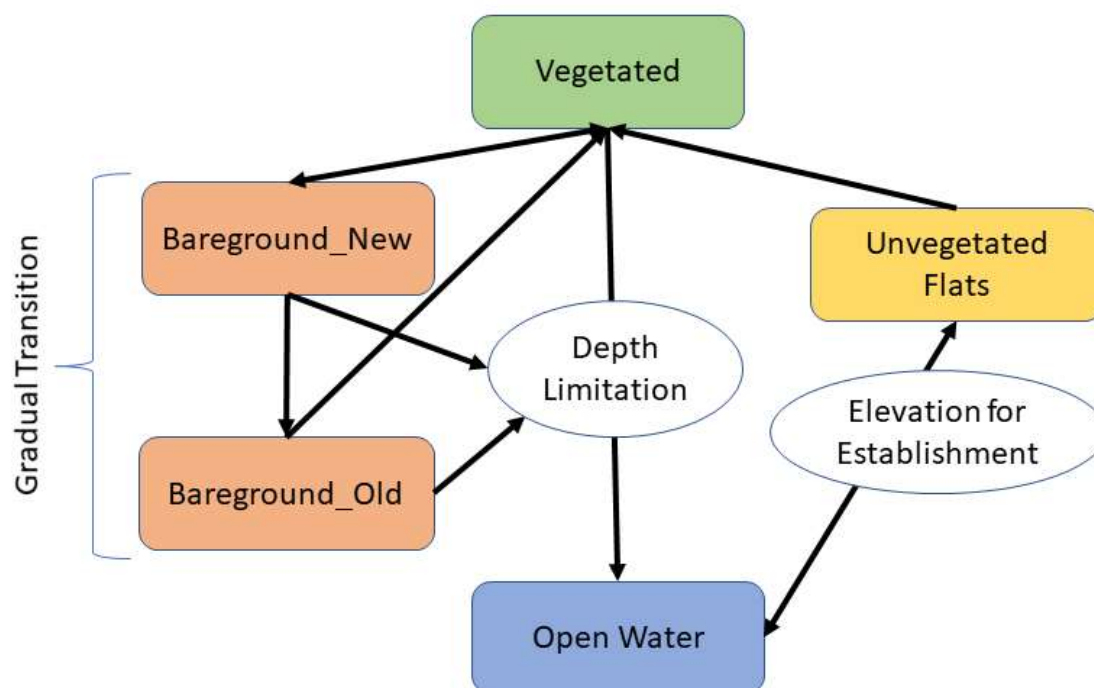
Figure 5. Transitions among cover types with the three sets of processes proposed to transition between vegetated land and open water for the 2023 ICM.

GRADUAL TRANSITIONS

ICM-LAVegMod determines whether an area that was vegetated remains vegetated (and, if so, the % cover by species). The result can be vegetated land or bareground with no vegetation cover. Bareground occurs when no species within the dispersal range were able to establish based on the previous year's salinity and water level variability. Bareground is available for vegetation to establish based on rules of establishment and dispersal in the following year. In the first year, for *bareground_new*, no changes in elevation are made (except those associated with mineral sediment deposition and subsidence). However, after the first year, for *bareground_new* that has not become either *vegetated* or transitioned to *open water* (see Water Depth Limitation below) will become *bareground_old*. The elevation of *bareground_old* will be progressively reduced, in addition to changes in elevation associated with mineral sediment deposition and subsidence. Based on the literature and limited available studies and data, *bareground_old* elevation change will initially be tested using a decrease of 5 cm yr^{-1}. These changes in elevation may be offset to some extent by sediment deposition, but there will be no organic accumulation in the soil for bareground. The rate of elevation decrease for *bareground_old* for test runs was defined based on data from existing literature discussed above (e.g., Lane et al., 2016; Cahoon et al., 2004; Baustian et al., 2012) and best

professional judgement. Both *bareground_new* and *bareground_old* remain eligible for vegetation establishment until water depth exceeds the Water Depth Limitation criteria.

Two additional changes to the 2023 ICM are associated with these transitions:

- ICM-LAVegMod needs to be updated to allow for acute stress to impact vegetation (see Approach 4 above). The change is needed to allow for a two-week increase in salinity to impact fresh marshes (floating and non-floating). The values for collapse thresholds in the 2017 ICM (Table 2) can be used, but the result should be *bareground_new* rather than *open water*.
- Changes are to be made to the dispersal rates so that they vary by species; initially with three dispersal classes to be tested for the wetland vegetation species (see
- Table 7). Note that in the 2017 ICM, all species were only allowed to move to an adjacent grid cell.

Table 7. Dispersal class characteristics to be tested for potential use for the 2023 ICM. Note that wetland vegetation species can only establish if the environmental conditions are met in ICM-LAVegMod grid cells and are established proportional on how well they adapt.

Dispersal Class	Species	Annual Dispersal Rate
Low	*Quercus lyrata, Quercus texana, Quercus laurifolia, Ulmus americana, Quercus nigra, Quercus virginiana, Taxodium distichum, Nyssa aquatica, Panicum hemitomon (*attached and flotant), *Spartina alterniflora*	Can only move to an adjacent grid cell
Medium	*Eleocharis baldwinii, Morella cerifera, Cladium mariscus, Sagittaria lancifolia, Eleocharis cellulosa, Iva frutescens, Paspalum vaginatum, Schoenoplectus californicus, Spartina patens, Schoenoplectus americanus, Spartina cynusuroides, Juncus roemerianus, Distichlis spicata*	Can move two grid cells
High	*Salix nigra, Sagittaria latifolia, Zizaniopsis miliacea, Colocasia esculenta, Polygonum punctatum, Phragmites australis, Typha domingensis, Avicennia germinans*	Can move to any grid cell

WATER DEPTH LIMITATION

While water depth was used in the 2017 ICM collapse thresholds (in ICM-Morph), ICM-LAVegMod uses water level variability, rather than water depth, to determine species composition of the available area determined by ICM-Morph. A model test was designed using the curve in Figure 3 (built from CRMS data) to determine a maximum water depth for vegetation occurrence which varies by salinity. This curve allows for a direct transition from vegetation to open water and thus replaces the collapse thresholds used in the 2017 ICM and eliminates the dependence of the loss of marshes in the classification on habitat type. If the annual mean inundation depth and annual mean salinity put vegetated land below this limit, then the area will remain vegetated. If the limit is exceeded, then the area will convert to open water. Note that there should not be a change in elevation associated with the conversion to open water. If the marsh was subject to this amount of flooding, it should already be low in the tidal frame. Also, the change to open water means the substrate will no longer receive organic matter accumulation as a contribution to vertical accretion. Thus, it should continue to be lower relative to surviving marshes. This water depth limitation will also be applied to bareground as shown in Figure 5 but does not apply to flotant or associated flotant bareground (see Activity 4).

ELEVATION FOR VEGETATION ESTABLISHMENT

Within the ICM framework, open water substrate can only convert back to vegetated area if mineral sediment deposition increases elevation above a threshold for vegetation establishment (or water levels are persistently lowered). Open water does not transition to bareground because this is rarely observed in coastal Louisiana wetlands. Vegetation tends to establish quickly once elevation increases to the point where plants can grow. The information in Table 5 from Carle et al. (2013) and Olliver and Edmonds (2017) can be used to determine elevation positions relative to MWL for vegetation colonization and transition from open water to vegetated land. Due to the limited data available, two elevations relative to MWL should be initially tested to assess the effects on land gain within the ICM framework:

- Bed elevation relative to MWL = MWL. This was approximately the point where Olliver and Edmonds (2017) identify the sediment-vegetation transition.
- Bed elevation relative to MWL = 10 cm above MWL. This was within the range of elevations identified by Carle et al. (2013) for the lower limit of marsh elevation (5.5 cm accuracy on LIDAR survey).

In addition, the modifications to the dispersal rates (Table 7) that vary by species should enable certain deltaic species to establish from propagules in river water. These are also subject to testing to assess the resulting vegetation distribution and the effect on land gain in the ICM.

MODEL IMPROVEMENT TESTING

Suggested improvements were assessed with test runs that were compared to G400, the future with action run from the 2017 ICM (i.e., with master plan projects in place), run with the medium environmental scenario (S04) from the 2017 Coastal Master Plan. These test runs (G020, G021, and G022) are summarized in Table 8 along with some additional tests that may be needed as improvements are integrated with other updates for the 2023 ICM.

Table 8. Model runs suggested to test the Activity 1 recommendations. Runs marked G### are suggested for future testing.

Name	Issue to be Tested	Description of Test
Water depth limitation (G020)	Maximum depth for vegetation and bareground	Remove collapse thresholds and add a depth limitation by salinity for all vegetation (except forested wetlands) and bareground.
New land 1 (G021)	New land establishment	Replace 2017 ICM land gain threshold with bed elevation = MWL as the threshold for allowing vegetation establishment.
New land 2 (G022)	New land establishment	Replace 2017 ICM land gain threshold with bed elevation = 10 cm above MWL as the threshold for allowing vegetation establishment.
Bareground lowering 1 (G###)	Gradual transition of land-water via bareground lowering	Remove collapse thresholds for forested wetlands and FIBS. Retain collapse threshold for bareground and land gain threshold. Add distinction between *bareground_new* and *bareground_old* and lower elevation of *bareground_old* by 5 cm yr^{-1}.
Bareground lowering 2 (G###)	Gradual transition of land-water via bareground lowering	As for Bareground lowering 1 but do not lower elevation of bareground, i.e., test of lowering = 0 cm yr^{-1}
New dispersal (G###)	Change in dispersal rates by species	Replace existing dispersal distance (1 grid cell) with three dispersal classes (by species). See Table 7.

WATER DEPTH LIMITATION (G020)

A model test (G020) was undertaken to assess replacing the collapse thresholds used in previous

master plans with a water depth limitation for vegetation occurrence which varies by salinity. In the model test, the collapse thresholds were only removed for FIBS. No change was made for swamp and bareground, and all other aspects of 2017 ICM remain the same. The water depth limitation shown in Figure 3 was applied based on a single year of hydrology. The test run was compared to a future with master plan projects run using the 2017 ICM (G400).

There are key differences between this proposed approach and the collapse approach used in 2017 ICM. While the curve applied imposes limiting depths similar to those previously used for intermediate, brackish, and saline marshes (Table 2), the previous collapse thresholds required exceedance for two consecutive years. In addition, previously fresh marshes were not subject to any water depth limitation and were subject to a maximum two-week salinity in any year.

Prior to the test, run effects were hypothesized, and the results were examined for such effects. Appendix C includes discussion of the results of this test. The results are summarized here:

- Loss patterns for G020 were similar to G400, but the large loss areas associated with sudden collapse were eliminated (e.g., Year 33 in Mermentau from G400). The sudden collapse of fresh marshes due to single-year salinity effects seemed to be eliminated.
- There are still periods of rapid land loss, but initial inspection indicates these losses may be associated with progressive increase in water levels that crossed the depth limit. Notably, these land losses were observed in fresh marshes which was not observed with the previous approach.
- Restoration projects that are designed to address salinity effects were not specifically investigated. Future model runs should identify an area that experiences a salinity decline in the future without action using the 2017 ICM (G300), which tests restoration project influences in G400. The water depth limitation could then be imposed in the 2017 ICM G300 run so that project effects could be more specifically identified.

This test has shown that the approach that uses the water depth limitation, which varies by salinity, for vegetation occurrence shows intuitive results. By replacing the previous threshold for fresh marshes, this approach addresses the issue of sudden loss due to single-year events. Despite being applied to single-year exceedance, as opposed to the two consecutive years previously required, the loss patterns do not appear to be responding to extreme years. However, subjecting a marsh to high water levels for two years in a row prior to loss was likely more consistent with field experience.

This approach increases land loss in many areas of the coast, perhaps more than anticipated. The Predictive Modeling Technical Advisory Committee (PM-TAC) noted that developing the relationship for water depth limitation by salinity based on CRMS sites may introduce a 'survivorship bias' (i.e., the data was from marshes that survive, not those that are lost). However, CRMS data indicate that using a 97.5th quantile to account for this may cause land to be lost under conditions where they currently

occur. For example, if fresh marsh CRMS sites were flooded on a mean annual basis with 35 cm of water (a general estimate based on Figure 3) for two years in a row then only vegetated stations at 10 CRMS sites would have experienced these conditions. According to observations, only six of those sites had stations that lost more than 50% cover (Figure 6).
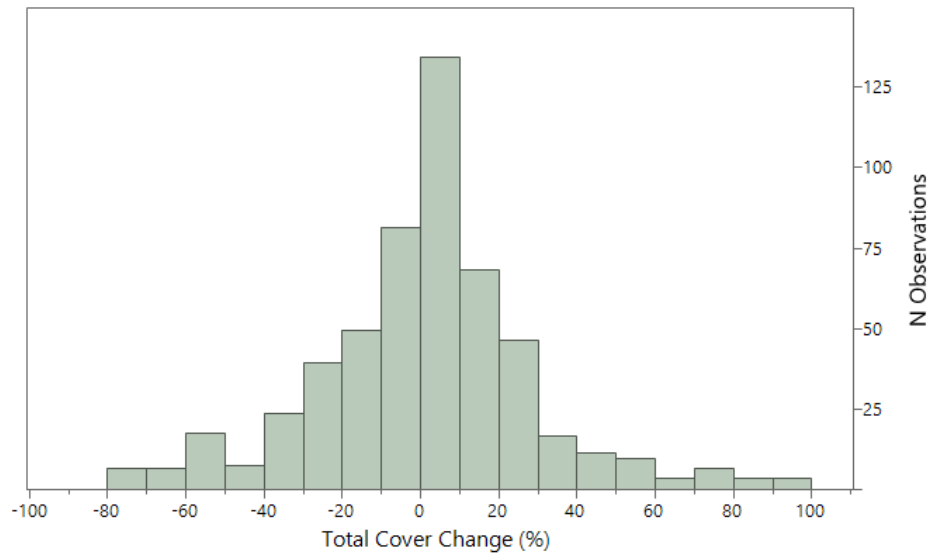
Figure 6. CRMS vegetation stations that experienced > 35 cm of flooding for two consecutive years by % cover change.

Several of these sites were observed to support fresh marsh vegetation which does not appear to show stress. The curve applied in the G020 test was based on 97.5th quantile of the data, and for fresh marshes may impose too low a depth limit on vegetation occurrence. Percentiles that include higher depth limits for fresh marshes and only minor changes for non-fresh marshes (e.g., the 99.5th quantile in Figure 7) could be tested.

An additional refinement would be to assess the water depth at the scale of the land-water mapping in ICM-Morph with 30 m x 30 m pixels, rather than the 500 m x 500 m grid cells in ICM-LAVegMod. As the application of the water depth limitation does not require information regarding habitat type, it can be applied at the scale at which elevation used for water depth calculations is tracked. If this approach is taken, it will be necessary to ensure the water depth limitation is not applied to flotant or forested wetland areas for reasons discussed above.
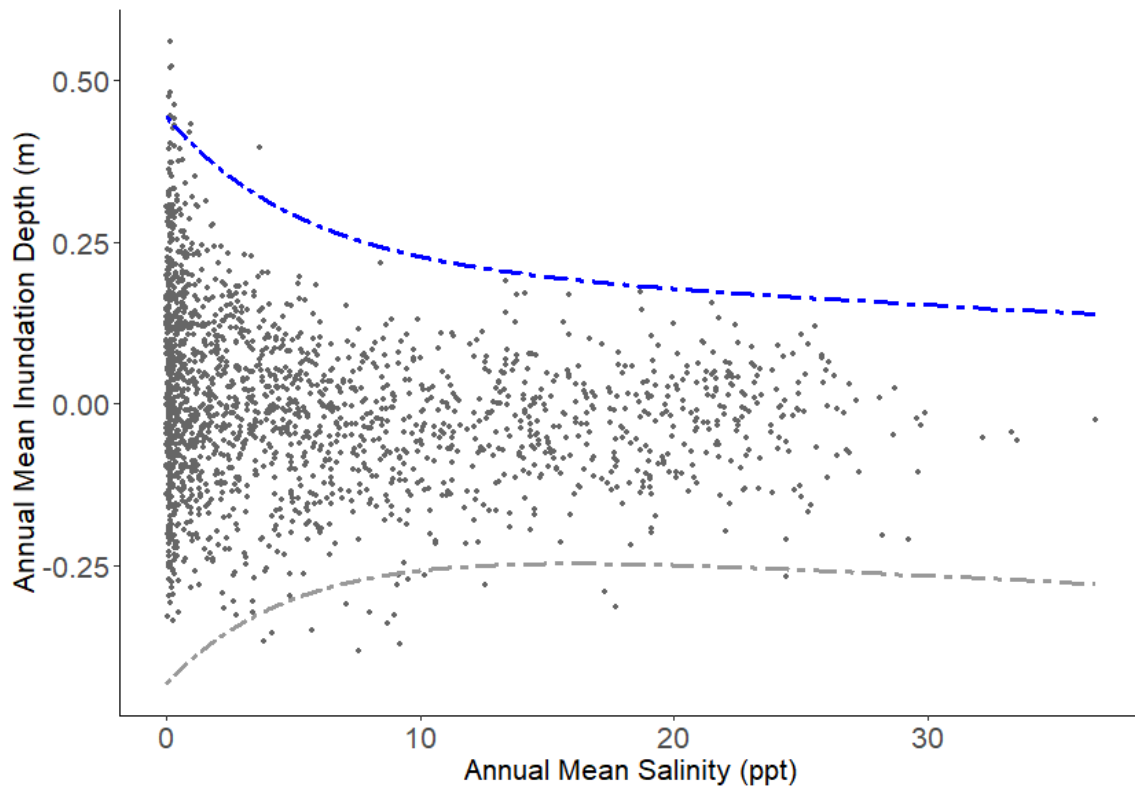
Figure 7. Salinity and water depth distribution of vegetation occurrence in coastal Louisiana with blue line at 99.5th quantile. Each point represents mean salinity and depth for a single CRMS station (2010-2017), n = 1944 (Figure 3). The grey line represents the 0.5th quantile from the quantile regression analysis.

ELEVATION FOR VEGETATION ESTABLISHMENT (G021 AND G022)

Two model tests (G021 and G022) were undertaken to explore the appropriate elevation relative to annual MWL at which vegetation can establish. Three runs are compared with different elevation thresholds:

- G021: Establishment elevation = MWL
- G022: Establishment elevation = MWL+10 cm
- G400: Establishment elevation = MWL+20 cm (Base run reflecting the 2017 ICM approach)

In each run the elevation relative to MWL has to be met or exceeded for two consecutive years before the area becomes eligible for vegetation establishment. All other conditions in the 2017 ICM remain,

so any new land resulting from the change in establishment elevation represents land that was lost due to the collapse thresholds used in the 2017 ICM.

Prior to the test, run effects were hypothesized, and the results were examined for such effects. Appendix D includes discussion of the results of this test. The results are summarized here:

- Consistently across the coast, land area was greatest with G021, followed by G022 and G400. This is shown clearly in time series plots (Appendix D). Areas of active sediment deposition show that this effect increases over time, suggesting that delta building was more effective when the elevation for vegetation establishment was lowest in relation to MWL. For non-deltaic areas, G021 still shows greater land area as a result of early year spin-up issues; there was not an increase in land area over time (Appendix D).
- While there may be some isolated small areas of land gain, likely associated with slight irregularities in the DEM (Appendix D), for the most part additional new land gained in delta building areas in G021 and G022 was contiguous with existing land masses.
- In areas without active subaqueous deposition, there was some difference in land area between G021, G022, and G400. However, these are not progressive increases in land area and result from differences in realignment of initial conditions during the first few years of the simulations (Appendix D).

In addition, inspection of land change maps showed that some shallow channels and small ponds infilled in G021, relative to their condition in G400. The effect was less evident in G022. This was also to be expected when the elevation for vegetation establishment was increased. Any areas above that elevation for two consecutive years would become eligible for vegetation establishment and thus convert from open water to land. Model simulations based on any type of threshold condition are always subject to minor perturbations above and below the threshold. Another modification being considered, the imposition of a water depth limitation for vegetation occurrence, would ensure that areas of vegetation established do not unduly persist as water depths increase.

The changes to the elevation for vegetation establishment tested here would also interact with potential adjustments to vegetation dispersal rates. Change in land area for current tests requires not only that substrate elevation has exceeded to the level appropriate for establishment, but also that wetland vegetation is available to establish. Thus, a fuller test would also include recommended changes in wetland vegetation dispersal rates (three proposed classes), which would allow some species to establish in any area (Table 8).

RECOMMENDATIONS AND NEXT STEPS

The team puts forth the following recommendations:

1. Remove the two-week salinity collapse threshold for swamps as there was no evidence of such sudden loss occurring in fresh forested wetlands in Louisiana.
2. Land change aspects of the ICM should be modified to reflect:
    a. Gradual Transitions
        i. Consider the approach to bareground lowering described in this report and determine the rate of lowering based on model tests (proposed tests at 0 cm and 5 cm per year).
        ii. Modify ICM-LAVegMod to convert fresh marsh that meets a two-week salinity mortality threshold to bareground to reflect acute effects of salinity on vegetation. Assuming no other species establish, bareground would then be available for vegetation establishment the following year.
    b. Water Depth Limitation
        i. Replace collapse thresholds for FIBS habitat types with the water depth limitation by salinity for vegetation occurrence.
        ii. Apply the water depth limitation based on two consecutive years.
        iii. Calculate depth at the scale of the 30 m x 30 m pixel.
        iv. Explore the effects of water depth limitation using a curve based on the 99.5th quantile of the CRMS data.
    c. Elevation for Vegetation Establishment
        i. Use an elevation for vegetation establishment of MWL+10 cm (G022) and retest with the updated dispersal rates.

2.2 ACTIVITY 2: REFINE THE ORGANIC MATTER ACCRETION APPROACH

ISSUE

Wetland surface elevations in the natural environment change over time due to a suite of physical and biological factors with complicated interactions that are not yet well understood. Wetland elevation can increase due to accumulation of organic and/or mineral sediment, while decreases in elevation can occur as a result of surface erosion, soil compaction, soil organic matter decomposition, or a combination of these processes. Drivers of these processes include frequency and duration of inundation and changes to salinity, temperature, soil properties, vegetation type and cover, etc. The ICM attempts to capture the net results of elevation change and resulting land loss over time without accounting for all contributing processes and drivers. The flow of related information in the 2017 ICM (Couvillion et al., 2013; Meselhe et al., 2013; Steyer et al., 2012) is shown in Figure 1. Organic matter accumulation is combined with mineral sediment accumulation (provided by ICM-Hydro) to estimate total annual vertical accretion rate (VAR). Capturing organic matter accumulation is particularly

important for coastal Louisiana, where wetland soils often have a limited supply of mineral sediment, and organic matter can contribute > 80% to vertical accretion (Morris et al., 2016; Nyman et al., 1993, 2006). Additionally, land loss results from the 2017 ICM were shown to be sensitive to organic matter accretion as well as mineral sedimentation (Meselhe et al., 2017). In the ICM, wetland elevation increases result from a combination of soil mineral matter accumulation rate (MMAR or Q_{sed}) and organic matter accumulation rate (OMAR or Q_{org}), but OMAR does not respond dynamically and explicitly to hydrological processes. For the 2017 ICM, organic matter accumulation was defined by wetland habitat type and hydrologic basin using look-up tables with annual equivalents for mass/area (and for bulk density) derived from CRMS soil properties data (following from the approach outlined in Steyer et al., 2012). ***This activity is focused on refining the approach to model organic matter accumulation, including identification and assessment of a relatively simple but ecosystem process-driven option to predict OMAR based on changing environmental conditions (e.g., inundation, water level variation, etc.).***

BACKGROUND

This activity involved an extensive review of existing literature and data related to OMAR to determine, for example, whether OMAR within a wetland habitat type (Activity 1) varies with environmental conditions and how OMAR varies spatially across coastal Louisiana. The activity also required consideration of how observations and data could feasibly be incorporated into the ICM framework, for example, how to utilize OMAR and mineral sediment deposition to calculate VAR in a manner that accounts for the highly disparate densities at which organic and mineral matter accumulate in situ. For use in the ICM, procedures for modeling soil organic matter accumulation need to be a) responsive to inputs provided by other ICM subroutines; b) tractable within the ICM simulation framework, which by design simplifies many complex ecological interactions; and c) grounded in an understanding of coastal Louisiana wetland soils and processes. While the main focus of this activity was on organic matter accumulation, adjustments to other related model assumptions were also considered. New approaches to vegetation classification methodology were evaluated, both for development of look-up tables and for post-processing of model output. In addition, an assumption from the 2017 ICM that vertical accretion would not occur in areas with no mineral sediment deposition, determined based on the extent of flooding of the wetland surface, was re-visited. It is possible that a marsh may not flood in any specific year, but wetland vegetation may still contribute to net vertical accretion through primary production.

Extensive data are now available through CRMS to provide context for this activity (e.g., soil properties data, including a second CRMS soil properties survey from 2014 and 2018; VAR estimated with 10+-year-old marker horizons; and 10+ years of water level, salinity, and vegetation species composition data). For the 2023 Coastal Master Plan analysis, subsidence, including 'shallow subsidence' (Cahoon et al., 1995), will be considered separately and will vary by environmental scenario. Thus, in analyzing the CRMS data, it was important to separate processes that inform organic matter accumulation as described in Figure 1, from those considered elsewhere in the ICM. Figure 8 parses out potential steps

in calculating vertical accretion and surface elevation change relative to existing ICM calculations and CRMS data.
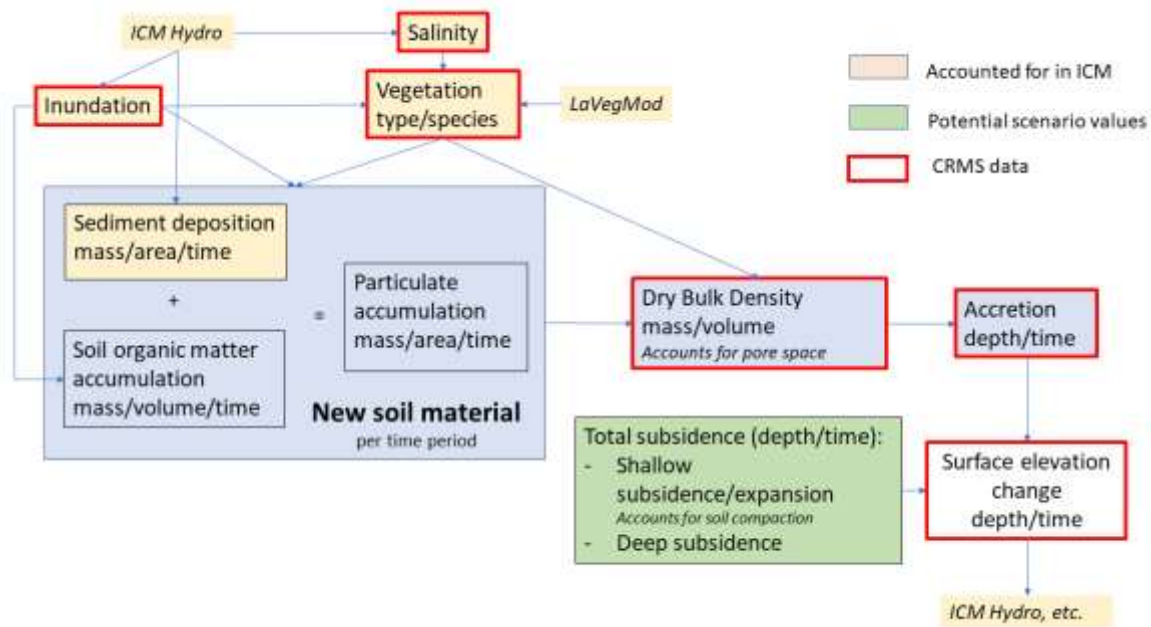
Figure 8. Potential flow of information in relation to organic matter accumulation illustrating role of CRMS data and subsidence scenarios. Red box outlines indicate CRMS data, and green boxes indicate information associated with scenarios.

Additional data to inform refinement of the approach to model OMAR are available from other studies, but the observations are not always easily applicable within the ICM framework. Many of these studies utilize measurements of bulk soil accumulation over time, applying a variety of techniques from marker horizons to radiometric dating (e.g., ^{137}Cs and ^{210}Pb) to estimate overall rates of accumulation, and estimating soil bulk density and organic matter content to calculate OMAR (Baustian et al., 2017; Cahoon & Reed, 1995; Callaway et al., 1997; Couvillion & Beck, 2013; Neubauer, 2008; Nyman et al., 1990). Most of these studies report organic matter accumulation in gravimetric terms, often with some conversion to volume contributions based on assumptions regarding specific gravity of organic matter. More recently, studies have measured soil carbon directly to assess soil carbon accumulation rates (Ouyang & Lee, 2014).

For this activity, the team identified methods to reduce uncertainty in estimating OMAR using existing bulk density/organic matter look-up tables, which provide single values by basin and do not allow consideration of variability in bulk density/organic matter within vegetation types or over time. The team also explored potential methods to increase the responsiveness of soil OMAR to changing soil

conditions within the ICM framework, which would represent a move toward more mechanistic representation of organic accretion. While a fully mechanistic approach to modeling processes related to OMAR is not consistent at this time with the goal of coastwide, long-term predictions for the 2023 Coastal Master Plan, more mechanistic modeling approaches may be further explored for future master plan efforts. More mechanistic modeling approaches could, for example, determine OMAR values based on biological processes such as belowground productivity, root/shoot allocation, and decomposition of various pools of soil organic matter (e.g., labile and refractory). These biological processes are closely related to physical conditions including subsidence, salinity, inundation (depth, duration, frequency, etc.), nutrient availability, suspended sediment concentration, light, and temperature; thus, OMAR can be directly linked and modeled to these physical processes (Baustian et al., 2018b; Snedden et al., 2015). For example, the soil cohort based relative elevation model (Kairis & Rybczyk, 2010) estimated organic matter accumulation via root biomass distribution and decomposition of organic matter (labile and refractory fractions) for seagrass habitats in Padilla Bay, WA in combination with mineral input, sediment compaction, eustatic sea level rise, and subsidence to determine elevation dynamics.

APPROACHES/METHODS

Several approaches were assessed to attempt to increase the responsiveness of OMAR to inundation in the ICM and to inform recommendations for updates. These approaches included revising how vertical accretion was calculated in the 2012 and 2017 predictive models and how OMAR might be more responsive to inundation.

Approaches:

1. Update the existing coastal master plan look-up tables
2. Develop OMAR look-up table to apply with the ideal mixing model
3. Utilize regression analyses from CRMS data to quantify OMAR-inundation response functions
4. Derive OMAR-inundation response functions from previously published in situ or laboratory mesocosm studies.

APPROACH 1: UPDATE THE EXISTING COASTAL MASTER PLAN LOOK-UP TABLES

The soil organic matter and bulk density values utilized in the 2012 and 2017 predictive models were derived from the 2007-2008 soil core collection campaign at the initiation of the CRMS sites (Table 9). A second soil core collection effort occurred in 2014 and 2018, and those data are available to update look-up table values (Table 10). This approach was not pursued further because other approaches the team explored that do not rely on a look-up table of bulk density and organic matter values to calculate VAR are preferred.

Table 9. Final calibrated values of bulk density and organic matter (%) content of various habitats and basins utilized in the 2012 Coastal Master Plan. Habitat types: F- Fresh Marsh, I – Intermediate Marsh, B-Brackish Marsh, S- Saline Marsh. Bulk Density is in g cm-3. This table is copied from Table 8 in Steyer et al. (2012) and was adjusted for the 2017 Coastal Master Plan during calibration (see Appendix E).

Basin	Delta	F	I	B	S	Swamp	Other
Bulk Density (g cm^{-3})							
Calcasieu/Sabine		0.08[c]	0.13[c]	0.23[a]	0.4[c]		0.24[d]
Mermentau		0.04[a]	0.19[b]	0.38[a]	0.41[b]		0.24[d]
Teche/Vermilion		0.25[d]	0.16[b]	0.21[b]	0.53[c]	0.36[b]	0.24[d]
Atchafalaya	0.65[b]	0.25[b]	0.42[b]	0.21[d]		0.21[b]	0.24[d]
Terrebonne		0.11[b]	0.18[a]	0.32[a]	0.32[c]	0.33[c]	0.10[b]
Barataria		0.05[a]	0.08[b]	0.15[b]	0.28[a]	0.41[c]	0.10[d]
Mississippi River Delta	0.46[b]	0.05[d]		0.23[d]	0.75[c]		0.10[d]
Breton Sound		0.05[d]	0.11[d]	0.23[a]	0.53[a]		0.10[d]
Pontchartrain		0.05[d]	0.11[b]	0.23[c]	0.44[c]	0.30[c]	0.10[d]
Organic Matter (%)							
Calcasieu/Sabine		61[c]	58[c]	33[a]	19[c]		32[d]
Mermentau		82[a]	40[b]	16[a]	14[b]		32[d]
Teche/Vermilion		30[d]	47[b]	37[b]	14[c]	18[b]	32[d]
Atchafalaya	7[b]	30[b]	13[b]	37[d]		37[b]	32[b]
Terrebonne		59[b]	42[a]	22[a]	25[c]	48[c]	62[b]
Barataria		79[a]	68[b]	49[a]	26[a]	38[c]	62[d]
Mississippi River Delta	11[b]	79[d]		33[d]	9[c]		62[d]
Breton Sound		79[d]	59[d]	33[a]	8[a]		62[d]
Pontchartrain		79[d]	59[b]	35[c]	19[c]	41[c]	62[d]

[a]calibrated from LCA S&T data; [b]calibrated from CRMS data; [c]assumed equal to CRMS 0-24 cm average; [d]assumed the same as the type in the nearby basin.

Table 10. An updated look-up table developed from the second CRMS soil properties survey. Habitat types: F- Fresh Marsh, I – Intermediate Marsh, B- Brackish Marsh, S- Saline Marsh. The table was built to resemble the look-up table used for the 2012 ICM (Table 9), but using newer data collected in 2014 and 2018. Due to limited data availability, the "Deltaic" and "Other" habitat types were not included in this table.

Basin	F	I	B	S	Swamp
Bulk Density (g cm^{-3})					
Calcasieu/Sabine	0.09	0.20	0.23	0.54	
Mermentau	0.17	0.17	0.25	0.34	
Teche/Vermilion	0.20	0.24	0.29		0.07
Atchafalaya	0.25				0.32
Terrebonne	0.09	0.16	0.21	0.31	0.28
Barataria	0.09	0.12	0.21	0.29	0.56
Mississippi River Delta	0.59	0.49			
Breton Sound	0.30	0.27	0.31	0.34	
Pontchartrain	0.18	0.16	0.34	0.41	0.35
Organic Matter (%)					
Calcasieu/Sabine	62.08	45.67	39.02	16.93	
Mermentau	61.04	49.62	30.64	24.10	
Teche/Vermilion	47.22	35.24	30.00		83.13
Atchafalaya	25.99				27.55
Terrebonne	66.09	40.00	39.92	21.22	47.51
Barataria	74.03	57.39	33.88	27.69	21.90
Mississippi River Delta	10.71	11.68			
Breton Sound	33.85	33.51	24.25	20.98	
Pontchartrain	32.63	46.64	25.63	19.09	41.35

APPROACH 2: DEVELOP OMAR LOOK-UP TABLE TO APPLY WITH THE IDEAL MIXING MODEL

Approach 2 calculated OMAR using OM (%), bulk density (BD; g cm^{-3}), and VAR (cm yr^{-1}). OM and BD were averaged from soil cores collected for CRMS in 2018 (cores were 24 cm deep, sectioned into six

4-cm depth increments). Vertical accretion rates were calculated using regression analyses (using slope of the line and not forced through a zero intercept) for observed data from feldspar marker horizon plots established (from years 2007 through 2010 for most sites) at the initiation of the CRMS sites. OMAR was estimated according to:

$$OMAR = OM \times BD \times VAR$$ Eq. 1

Some variation in mean OMAR was noted among habitat types (Table 11), suggesting that these pooled groupings could provide baseline OMAR values that could be used as a basis for further analysis of environmental conditions as indicators of system stress (see Approach 3, below, for more discussion on drivers of variation). Accretion data are not collected at flotant sites, therefore those habitats are not included in this analysis.

Table 11. Organic matter (OM), bulk density (BD), vertical accretion (VAR), and organic matter accumulation rates (OMAR) by habitat type using data from the second CRMS soil properties survey. Data were collected in 2014 and 2018. This information could be applied for a refined look-up table approach.

	Fresh (n=44)		Intermediate (n=95)		Brackish (n=78)		Saline (n=54)		Swamp (n=40)	
	Mean	S.D.	Mean	S.D.	Mean	S.D.	Mean	S.D.	Mean	S.D.
OM	0.527	0.264	0.426	0.182	0.338	0.145	0.226	0.102	0.384	0.231
BD	0.186	0.181	0.209	0.136	0.247	0.141	0.336	0.160	0.357	0.238
VAR	1.350	0.750	0.940	0.576	0.970	0.566	1.440	1.172	1.150	0.567
OMAR	0.089	0.051	0.062	0.033	0.063	0.035	0.093	0.086	0.107	0.066

As described in the conceptual model for the 2017 ICM (Figure 1), the mineral and organic contributions to surface elevation change were additive and used single estimates of OM and BD for each basin. This approach does not account for the highly disparate self-packing densities of organic and mineral matter (the densities at which mineral and organic matter tend to accumulate in situ). Values for BD were established a priori by basin in the look-up table.

APPLICATION OF THE IDEAL MIXING MODEL

An alternative approach would be to apply the ideal mixing model (Morris et al., 2016), described below, that accounts for disparate self-packing densities of organic and mineral matter without explicitly needing total soil dry BD. This could reduce the uncertainty in estimated vertical accretion due to the large variation in BD among and within habitat types (Table 11). Using this approach, OMAR calculations (Equation 1) based on CRMS data, ICM-Hydro derived MMAR, and self-packing densities could be utilized to estimate VAR.

Stewart et al. (1970) postulated that in soils containing a mixture of mineral and organic matter, a relationship exists between soil bulk density and organic matter content, essentially that the bulk volume of such a soil mixture approximates to the summed self-packing volumes of the organic and mineral components. As such, it follows that the bulk densities of pure organic matter (i.e., soils with OM = 1) and pure mineral matter (i.e., soils with OM = 0) are fixed values, and the organic and mineral volumetric components of a mixed soil are additive (Federer et al., 1993). Taking a mixed soil with dry weights W_o and W_i of organic and inorganic matter with corresponding self-packing densities of k_1 and k_2, and volumes $V_o = W_o/k_1$ and $V_i = W_i/k_2$, when the two components are mixed, the resulting bulk density was given by:

$$BD = \frac{W_o + W_i}{\frac{W_o}{k_1} + \frac{W_i}{k_2}} \qquad \text{Eq. 2}$$

The mixture has an OM content of:

$$OM = \frac{W_o}{W_o + W_i} \qquad \text{Eq. 3}$$

Rearranging and substituting provides estimates of bulk density:

$$BD = \frac{1}{\frac{OM}{k_1} + \frac{1 - OM}{k_2}} \qquad \text{Eq. 4}$$

Equation 2 is known as the ideal mixing model by Adams (1973) and was applied to wetland soils by Morris et al. (2016). When OM = 0 (pure mineral), Equation 4 reduces to BD = k_2, and it reduces to BD = k_1 when OM = 1 (pure organic). As such, coefficients k_1 and k_2 are the bulk, self-packing densities of pure organic and mineral matter, respectively. These densities, and their corresponding volumes, include pore space, which is why k_1 and k_2 are typically less (much less for k_1) than the true particle densities of organic and mineral matter (commonly taken as 1.14-1.20 g cm^{-3}; 2.60-2.65 g cm^{-3}, respectively; see Nyman et al., 1990) used when calculating % soil volume occupied by mineral matter, organic matter, and pore space. Fitting the ideal mixing model through soil properties data from soil surveys conducted at CRMS site establishment (2006 to 2008) gives values for k_1 and k_2 of 0.076 ± 0.0009 and 2.106 ± 0.06 g cm^{-3}, respectively (Figure 9). The k_1 and k_2 values obtained from the CRMS site establishment surveys were similar to values reported in the literature obtained from fitting the model through national datasets (k_1 = 0.085 to 0.098 g cm^{-3}; k_2 = 1.67 to 1.99 g cm^{-3} (Holmquist et al., 2018; Morris et al., 2016). These values could be modified by using BD and OM values from additional soil samples to ensure the self-packing densities used reflect coastal Louisiana environments not well sampled by CRMS including newly forming deltas. This may be especially important for the coastal master plan as new sediment diversion projects are expected to increase the extent of newly emerging deltaic environments.
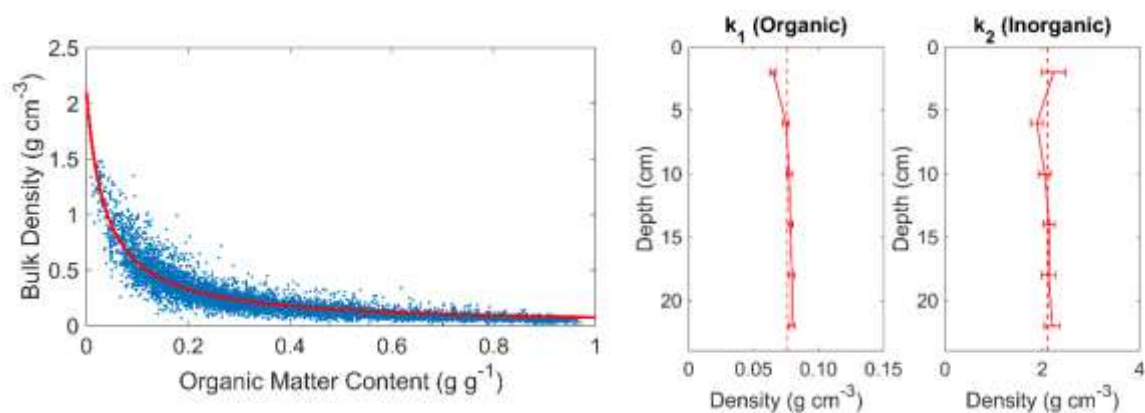
Figure 9. Ideal mixing model fit and self-packing densities from the second CRMS soil properties survey data. Left: fit of Ideal Mixing Model (red line, r^2 = 0.84) to CRMS bulk density and organic matter (OM) data (blue dots) from CRMS soils survey (n=6412 soil samples collected from 375 CRMS sites). Right: mean (dots) and standard errors (horizontal bars) of organic (left) and inorganic (right) self-packing densities as a function of depth. Dashed vertical lines indicate values averaged over the entire 24 cm soil core (k_1 = 0.076; k_2 = 2.106).

Estimates of the self-packing densities (k_1 and k_2) are useful because they allow for back-calculation of accretion from MMAR and OMAR, accounting for density differences between accumulated mineral and organic matter mass and the corresponding volumetric (and thus vertical accretion) disparities between the two. Thus, accretion can be calculated based on MMAR (from ICM-Hydro) and OMAR (the subject of this Activity) for wetland habitat types (herbaceous and forested) as shown in Figure 10 without the need to utilize BD values from look-up tables (Tables 9 & 10). Further details and examples of this approach applied to sample data from coastal Louisiana are provided in Appendix F, which also shows that mixing model approach can reliably predict total accretion based on CRMS data (Figure F2).
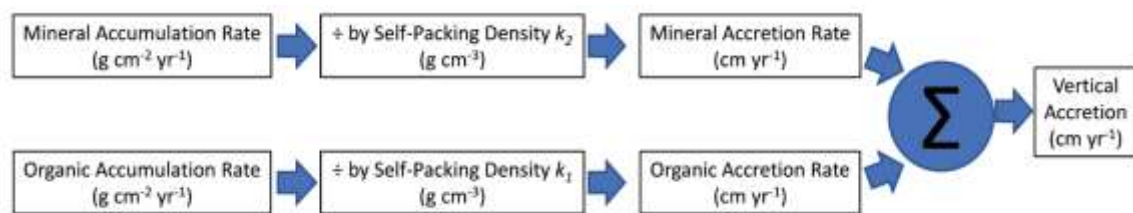
Figure 10. Proposed calculation of total vertical accretion rate for the Integrated Compartment Model used for the 2023 Coastal Master Plan.

The issue in the 2017 ICM that vertical accretion was zero when no mineral sediment deposition occurred can also be addressed with this approach. As mineral accretion and organic accretion are additive (Figure 10), vertical accretion should still occur even when MMAR is zero as calculated by the ICM. The 2023 ICM should remove the inundation requirement for OMAR. Note, however, that the ideal mixing model only applies for areas covered by emergent vegetation and bareground, and changes in elevation due to mineral sediment deposition in open water areas should be handled separately.

APPROACH 3: UTILIZE REGRESSION ANALYSES FROM CRMS DATA TO QUANTIFY OMAR-INUNDATION RESPONSE FUNCTIONS

An exploratory analysis of CRMS data was suggested to test for relationships between OMAR and % time flooded at various CRMS sites. Although most communities demonstrated a negative relationship, initial results did not show a strong governing effect of inundation duration on OMAR (Figure 11). This finding was somewhat unexpected given that a number of studies have quantified strong inverse relationships between inundation duration and belowground biomass/production with field studies (Kirwan & Guntenspergen, 2015; Schile et al., 2017; Snedden et al., 2015; Voss et al., 2013; Watson et al., 2017) and laboratory and mesocosm approaches (Naidoo et al., 1992; Pezeshki & DeLaune, 1996; Spalding & Hester, 2007; Visser & Sandy, 2009).

Figure 11. Organic matter accumulation rates (OMAR) for eleven vegetation communities in relation to mean annual time flooded. Inundation/time flooded is calculated as a percentage based on years 2010 through 2017; red dots indicate CRMS sites in the Deltaic Plain, and blue dots indicate CRMS sites in the Chenier Plain; dashed lines indicate 95% confidence intervals. All available data was used. Eleven vegetation communities are dominated by the following indicator species: Maidencane = *Panicum hemitomon*, Three square = *Schoenoplectus americanus*, Roseau cane = *Phragmites australis*, Pasaplum = *Paspalum vaginatum*, Wiregrass = *Spartina patens*, Bulltongue = *Sagittaria lancifolia*, Needlerush = *Juncus roemerianus*, Bulrush = *Bolboschoenus robustus*, Oystergrass = *Spartina alterniflora*, Saltgrass = *Distichilis spicata*, and Brackish mix = none. Communities are defined following Snedden (2019).

It is possible that there exists no strong effect of inundation duration on OMAR in Louisiana coastal marshes. This lack of correspondence could occur if, for example, even though belowground production was inhibited by inundation stress, the effect was offset due to concurrent inhibition of decomposition. Currently this issue is largely unresolved, with some studies showing such inhibitory

impacts of inundation to decomposition (Acharya, 1935; Day & Megonigal, 1993; Tate, 1979; Tenney & Waksman, 1930) and others showing no clear effect (Blum, 1993; Hackney, 1987; Hackney & De La Cruz, 1980; Janousek et al., 2017; Stagg et al., 2017). Kirwan et al. (2013) put forth that organic matter decomposition in semi-saturated wetland soils is not strongly regulated by elevated hydroperiods.

Another possible explanation for the lack of correspondence between inundation duration and OMAR is that there may be other controlling variables that regulate OMAR that are either unmeasured or not included in the regression model. This notion is supported by conflicting results between mesocosm/marsh organ studies versus field (in situ) studies examining inundation-biomass relations. Mesocosm and marsh organ studies (e.g., Kirwan & Guntenspergen, 2015; Snedden et al., 2015; Visser & Sandy, 2009; Watson et al., 2017) can isolate the inundation effect while holding other variables constant and have consistently identified high inundation duration driving reduced belowground production. In contrast, an in situ field study designed to quantify inundation effects at CRMS sites spanning tens to hundreds of km (Stagg et al., 2016) found no inundation effect, possibly due to the presence of other, unmeasured variables driving production (e.g., nutrients) that varied across the landscape. Yet another possible explanation for the high degree of residual OMAR variation may be that substantial amounts of organic matter in the soil profile are the result of allochthonous import from other locations during either routine (e.g., cold front passage) or punctuated (e.g., hurricane storm surge) transport events (Mariotti et al., 2020).

Finally, it is also possible that no significant trends were identified due to the high degree of variability in the OMAR data. Given that OMAR = BD × OM × VAR, the variability of each of the terms can be examined in attempt to identify the source of the OMAR variation. As BD and OM are inversely related (see discussion of the ideal mixing model above), one would expect that their product, organic matter density, would exhibit relatively similar values across the suite of CRMS sites used in the analysis. Indeed, nearly 70% of the 311 sites where organic matter density was quantified exhibit values between 0.05 and 0.07 g cm^{-3} (Figure 12, left). This finding suggests that the variation in OMAR arises from the remaining term, VAR, which was supported by the fact that 25% of the sites exhibit rates below 0.6 cm yr^{-1}, while 25% of the sites exhibit rates that are twice as high (>1.31 cm yr^{-1}; Figure 12, right).
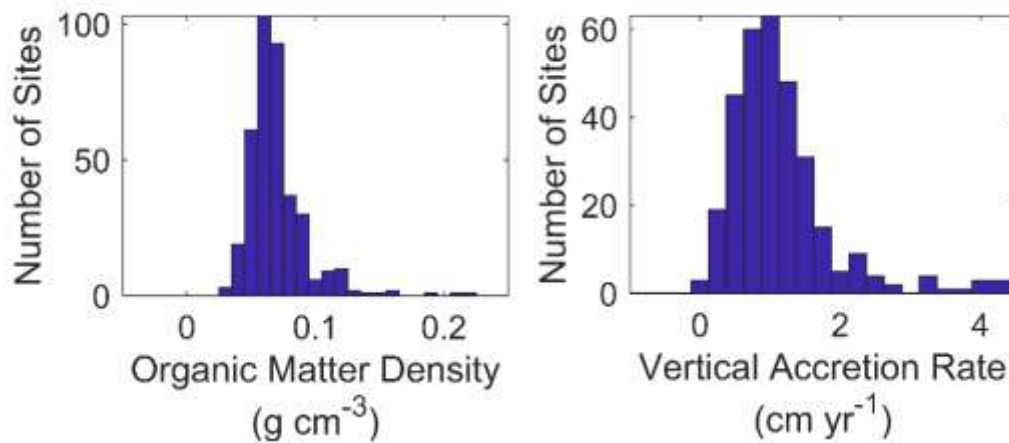
Figure 12. Distribution of organic matter density (left) and vertical accretion rates (right) for the 311 CRMS sites examined in preliminary analysis.

It is possible that the variation in VAR is real (i.e., the spatial decorrelation length in the field is small) or that it arises from measurement error associated with the method itself. Given that VAR is calculated as the slope of the regression line that fits depth to marker horizon to time elapsed since marker horizon deployment, the r^2 values of those regressions were examined to determine if there were sites with anomalously low r^2 values that could indicate that the accretion rates derived from them may be unreliable. The histogram of the 311 r^2 values indicates a bimodal distribution exists with a break around $r^2 = 0.5$, with approximately 20% of the stations exhibiting r^2 values below 0.5 (Figure 13).
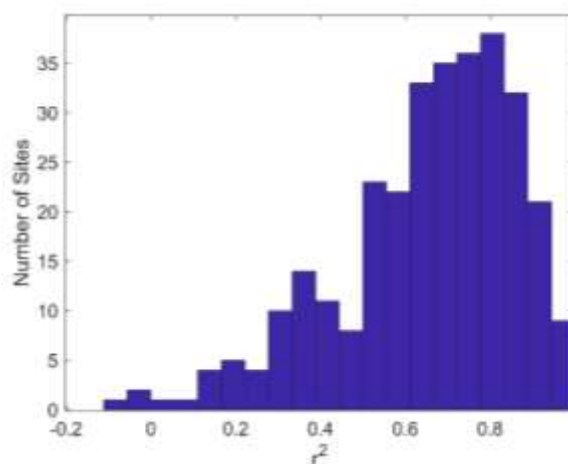
Figure 13. Distribution of the coefficient of determination (r^2) from 311 CRMS sites examined for a preliminary analysis.

Another contributing factor to the variability in the OMAR-inundation response functions by vegetation community (Figure 11) may be the manner in which sites were classified to community type in the preliminary analysis shown above. For that analysis, sites were assigned a community type based on how they were classified in the most recent year of the dataset, 2018. However, many of these sites are not static through time with respect to community type. Table 12 indicates how many sites were classified to the same community type for varying number of years in the nine-year dataset.

Table 12. The number of CRMS sites that were consistently classified in each community type. See Figure 4 for indicator species of these community types. Communities here are defined following Snedden (2019).

Community Type	Number of years in 9-year dataset (2010-2018) site was consistently classified					
	9	8	7	6	5	4
Maiden Cane	14	19	20	22	25	26
Three-square	2	4	6	9	15	18
Roseau Cane	0	1	1	2	5	7
Paspalum	3	4	5	5	8	9
Wiregrass	65	83	97	109	119	125
Bulltongue	33	46	50	58	62	63
Needlerush	2	5	6	6	7	7
Bulrush	0	0	1	3	4	4
Brackish Mix	4	6	11	14	19	20
Oyster Grass	26	31	35	35	40	40
Saltgrass	0	1	2	2	6	6
Total	149	200	234	265	310	325

The team explored whether OMAR-inundation response functions by vegetation community-type could be improved by including only sites that were consistently classified to the same community type in the majority of years observed (e.g., seven or more of the nine years in the dataset). Forested wetlands also needed to be added to this data set. Thus, the data set was refined to include (1) only sites where r^2 values for vertical accretion regressions exceed 0.5 and (2) only sites that were consistently classified to the same community type at least seven of the nine years in the dataset, with the understanding that these two measures, while modestly decreasing sample size, may reduce some of the variation in the dataset and provide clearer OMAR-inundation response functions. Results indicate that the refined data set (n = 125 CRMS sites) did not have less variation and that the environmental drivers still did not significantly account for the OMAR variation (Figure 14). Thus, given the finding that neither of these criteria appreciably increased the fit of the OMAR/inundation regressions by community type, the analysis of the original dataset with 311 CRMS sites (Table 11) is recommended for estimates of OMAR per habitat type.
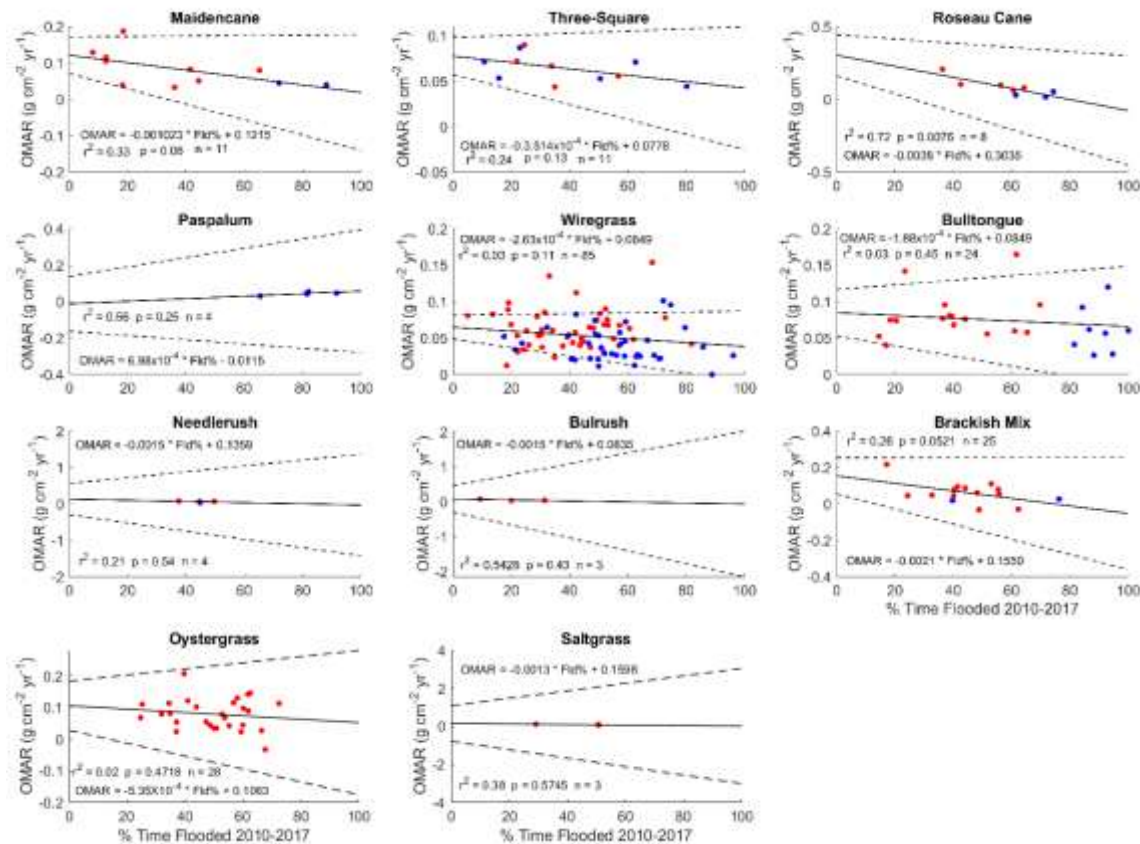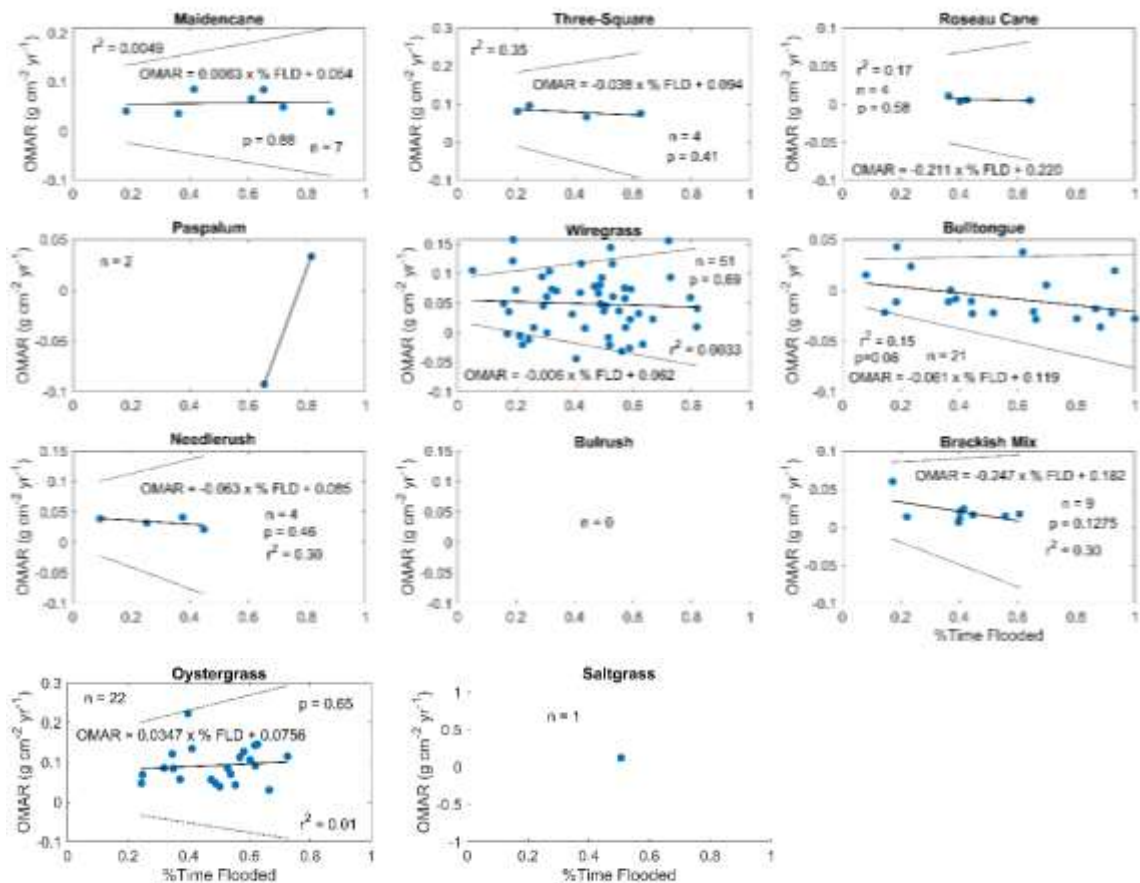
Figure 14. Organic matter accumulation rates (OMAR) for eleven vegetation types in relation to mean annual time flooded. Inundation is calculated as a percentage, based on data from 2010 through 2017; dashed lines indicate 95% confidence intervals; samples restricted to reduced dataset. Eleven vegetation communities are dominated by the following indicator species: Maidencane = *Panicum hemitomon*, Three square = *Schoenoplectus americanus*, Roseau cane = *Phragmites australis*, Pasaplum = *Paspalum vaginatum*, Wiregrass = *Spartina patens*, Bulltongue = *Sagittaria lancifolia*, Needlerush = *Juncus roemerianus*, Bulrush = *Bolboschoenus robustus*, Oystergrass = *Spartina alterniflora*, Saltgrass = *Distichilis spicata*, and Brackish mix = none. Communities are defined following Snedden (2019).

APPROACH 4: DERIVE OMAR-INUNDATION RESPONSE FUNCTIONS FROM PREVIOUSLY PUBLISHED IN SITU OR LABORATORY MESOCOSM STUDIES

In situ mesocosms (or marsh organ experiments) have been used to explore the effect of varying hydroperiod or salinity on vegetation and soils (Janousek et al., 2016; Kirwan & Guntenspergen, 2015; Langley et al., 2013; Morris et al., 2013; Mozdzer et al., 2016; Peng et al., 2018; Snedden et al., 2015; Watson et al., 2015, 2017; Wigand et al., 2016). While these studies typically did not examine OMAR directly, variation in belowground biomass across elevation and inundation gradients was commonly measured. Examining these studies and making assumptions about the relationship between belowground production and OMAR could provide a foundation for assessing relationships with OMAR and environmental stressors like inundation. Information and functions were synthesized from in situ mesocosm studies to examine trends in vegetation and soils response to salinity and inundation. For example, findings from Visser and Sandy (2009) are corroborated by findings of Snedden et al. (2015) for *S. patens* and *S. alterniflora* (Figure 15, top panels), and findings from other mesocosm studies (Watson et al., 2017; Kirwan & Guntenspergen, 2015) are also consistent for those species (Figure 15, bottom panels).
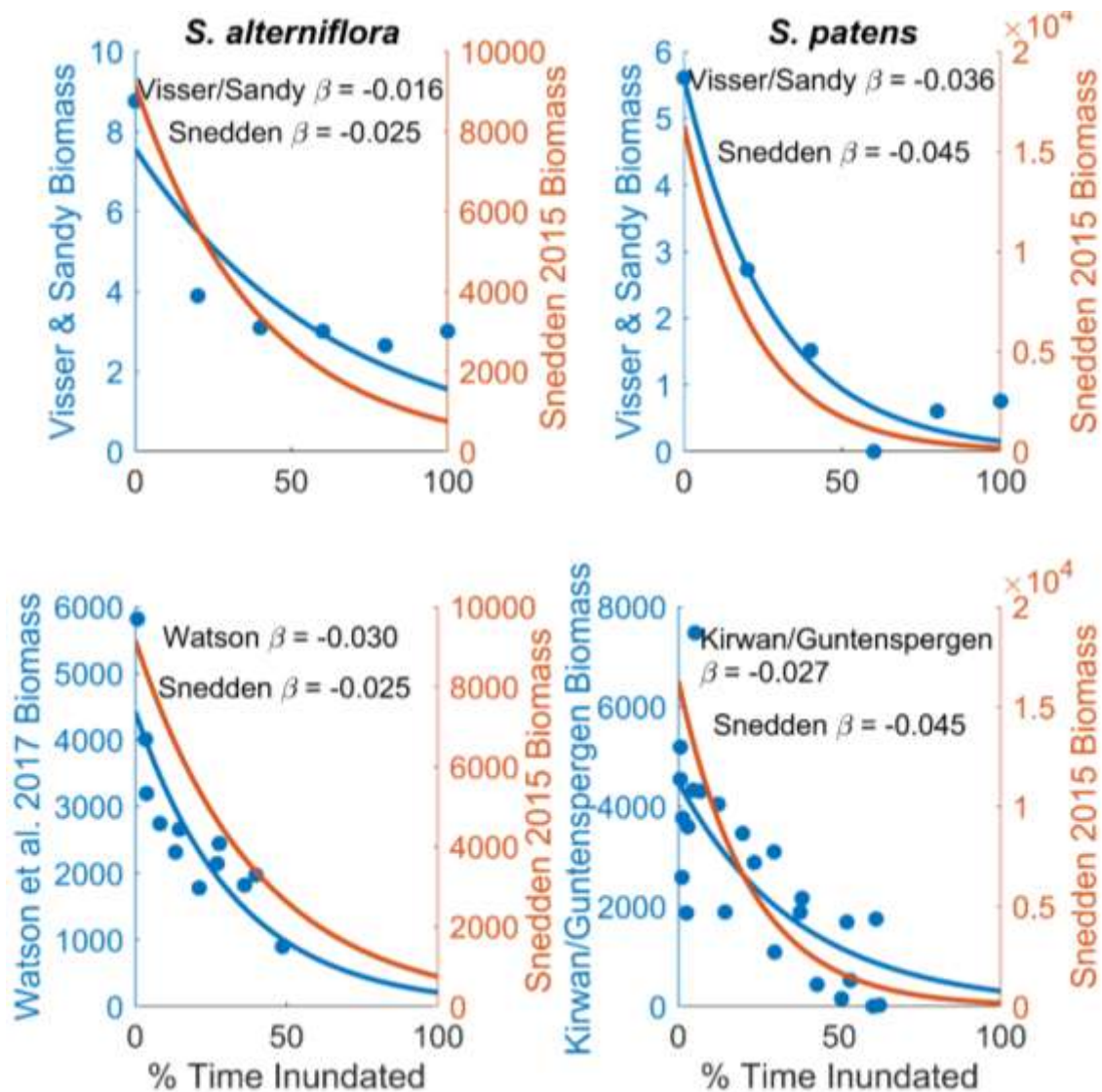
Figure 15. Comparison of mesocosm findings for biomass relative to inundation. Results from Snedden et al. (2015) are shown in orange; results from previous mesocosm experiments for *S. alterniflora* (left) and *S. patens* (right), fit with exponential regressions (belowground biomass = $Ae^{\beta x}$ where A is the intercept term, β is the decay coefficient in the regression equation, and x is % time flooded) are shown in blue. Note that belowground biomass was reported in units of g m^{-2} for Snedden, Watson, and Kirwan and Guntenspergen and in units of g for Visser and Sandy.

After accounting for intercept differences, which may be attributable to differences in initial planting protocols or geographic differences in climate (e.g., temperature), biomass-inundation response functions for *S. alterniflora* and *S. patens* observed in Snedden et al. (2015) are remarkably similar to those put forth by Watson et al. (2017) and Kirwan and Guntenspergen (2015), respectively. It follows that fitting exponential regressions through the belowground biomass response for *Sagittaria lancifolia* and *P. hemitomon* observed in Visser and Sandy (2009) may, with reasonable accuracy, describe the belowground inundation biomass response for those taxa as well. Visser and Sandy (2009) observed modest decreases in belowground biomass with increasing inundation for *S. lancifolia*, and no significant relationship was found between the two variables for *P. hemitomon* in potted containers (Figure 16). The lack of significant relationship between inundation and biomass for *P. hemitomon* was interpreted as that taxon being unaffected by inundation; this lack of flooding effect on production has been observed in other investigations (e.g., Visser & Peterson, 2015; Willis & Hester, 2004).
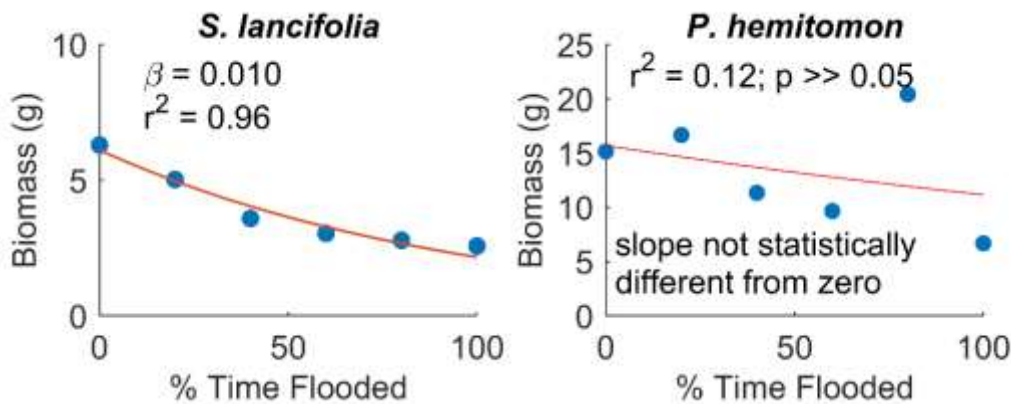
Figure 16. Exponential regressions fit through belowground biomass response of *Sagittaria lancifolia* and *Panicum hemitomon* observed by Visser and Sandy (2009).

It was further assumed that the mean belowground net annual primary productivity (NAPP; g m^2 yr^{-1}) by marsh type (intermediate = 4,679; brackish = 5,609; saline = 4,593) (Stagg et al., 2016, Figure 17) are reflective of the average inundation conditions observed at those CRMS sites and that they will be observed when the % time flooded corresponds to those average inundation conditions (intermediate = 66%; brackish = 51%; saline = 54%). It is important to note that these average inundation conditions are derived from field data and that the average inundation produced for current conditions by the ICM may differ. By marsh type, baseline NAPP rates were set to the corresponding mean % time flooded values to solve for the intercept term A in the exponential equation $NAPP = Ae^{\beta x}$, where β was the decay coefficient observed in Snedden et al. (2015) for *S. patens* (-0.045 g m^2 yr^{-1}) and *S. alterniflora* (-0.025 g m^2 yr^{-1}) or obtained in an exponential regression

from Visser and Sandy (2009) for *S. lancifolia* (-0.01 g m² yr-1). In short, this procedure produces belowground NAPP responses to % time flooded that are informed by experimentation, under the assumption that biomass and NAPP are linearly related (Figure 18). Because Visser and Sandy (2009) found no relation between belowground biomass and % time flooded for *P. hemitomon*, it was assumed NAPP was constant across the inundation gradient and OMAR for fresh marshes was taken as the mean OMAR observed across fresh marsh sites. Because there were no conclusive studies linking OMAR to inundation variability in swamp settings, OMAR for swamps was also taken as the mean OMAR observed across swamp sites.

Using these assumptions and regressions, the approach of Morris et al. (2016) was followed, where only the refractory component, taken as 10% of NAPP, was assumed to contribute to vertical accretion over the long term. Thus, all NAPP values are multiplied by 0.1 to obtain the annual refractory organic matter input to the soil profile. This 10% assumption could be further tested and adjusted during ICM calibration. The resulting refractory OMAR values can then be divided by the self-packing density of organic matter (0.076 g cm^{-3}) to estimate the organically-derived VAR (Figure 9 and Figure 10).
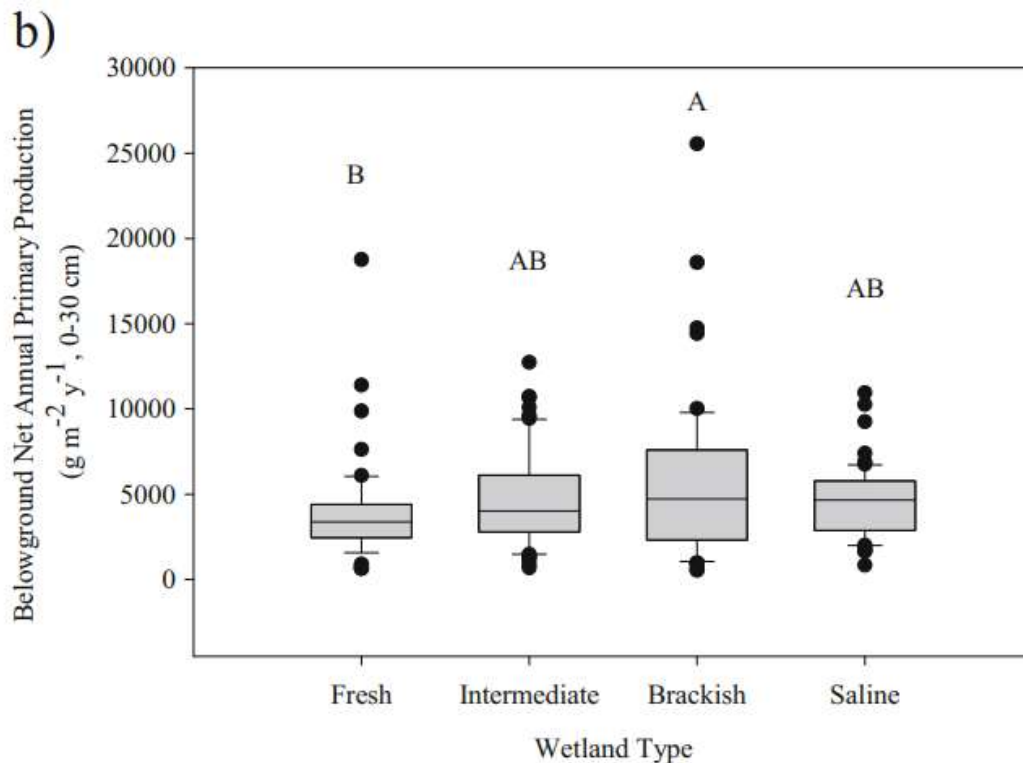
Figure 17. Mean belowground Net Annual Primary Production for fresh (*Panicum hemitomon*), intermediate (*Sagittaria lancifolia*), brackish (*Spartina patens*), and saline (*Spartina alterniflora*) marshes in coastal Louisiana, taken from Stagg et al. (2016).
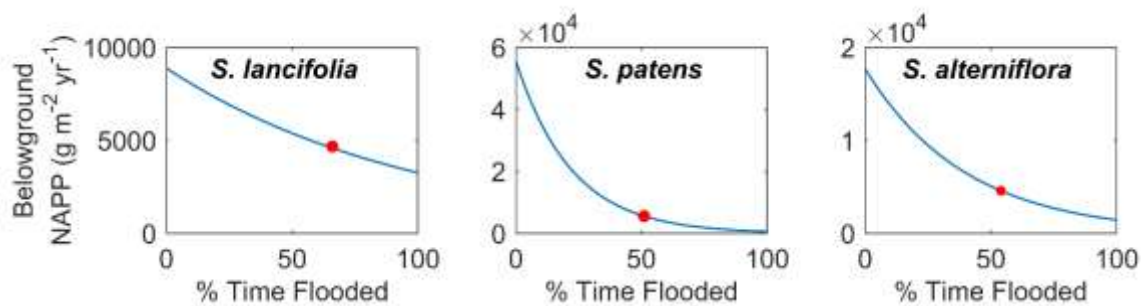
Figure 18. Belowground Net Annual Primary Production (NAPP) rates as a function of inundation duration. Rates were obtained by applying exponential regression decay parameters observed under Visser and Sandy (2009; *Sagittaria lancifolia*) and Snedden et al. (2015; *Spartina patens*, *Spartina alterniflora*). Note that *Panicum hemitomon* is not shown as that regression was not significant. The red dot in each regression represents the average belowground NAPP rate observed by Stagg et al. (2016), set at corresponding mean inundation rates for each marsh type.

The mean belowground NAPP value for *S. patens* observed by Stagg et al. (2016) of around 5,000 g m^{-2} yr^{-1} can be translated into an organic accretion rate (Table 13) and compared with typical observed values in coastal Louisiana. Converting 5,000 g m^{-2} yr^{-1} to cm^{-2} gives 0.5 g cm^{-2} yr^{-1}. Keeping only the refractory component gives 0.05 g cm^{-2} yr^{-1}. Dividing 0.05 g cm^{-2} yr^{-1} by 0.076 g cm^{-3} (the self-packing density of organic matter or k_1 (Figure 10) gives 0.66 cm yr^{-1}. Applying the ideal mixing model to an existing marsh soil core dataset collected across Breton Sound, LA (Snedden, 2021; n=25) indicates the mean organically-derived VAR across the basin was 0.61 cm yr^{-1} (Figure 19), which compares well with applying the method described above. In addition, other coastal Louisiana marsh studies have shown a range of ^{137}Cs or ^{210}Pb based accretion rates of 0.7 to 1.4 cm yr^{-1} (DeLaune et al., 2018; Nyman et al., 1993, 2006). Mean accretion rates of 0.6 to 0.8 cm yr^{-1} based on ^{137}Cs radionuclide activity were also observed across fresh to saline marshes in Barataria Basin (Hatton et al., 1983). Accretion rates measured at the same CRMS sites as observed for the Stagg et al. (2016) study (Figure 17) suggest mean accretion rates of 0.5 to 0.6 cm yr^{-1} based on ^{137}Cs or ^{210}Pb radionuclide dating (Baustian et al., In review) and are near the accretion values estimated by this proposed approach. Comparing this approach to ^{137}Cs or ^{210}Pb based accretion rates can be relevant for 50 year simulations conducted for master plan analysis. Additionally, OMAR modeled with this approach using observed CRMS inundation rates (2010-2017 averaged across all years) as inputs produce similar distributions to CRMS observed OMAR (Figure 20). Future modeling improvements should evaluate the use of short-term and long-term accretion rates for representation of annual time steps and 50-year estimates of OMAR.

Table 13. Organic matter accretion estimates based on mesocosm experiments that measured belowground production (BGP, from Stagg et al., 2016) and inundation stress (> 50%). These formulas could be utilized for a refined look-up table that includes inundation response.

Habitat Type	Organic Matter Accretion (cm yr^{-1}) Formula	Reference
Fresh	Not applicable – use values from OMAR look-up table with ideal mixing model	Visser and Sandy 2009
Intermediate	= [0.10* (0.8887*exp(-0.010*%fld])]/k$_1$	Visser and Sandy 2009
Brackish	= [0.10* (6.371*exp(-0.045*%fld)]/k1	Snedden et al. 2015
Saline	= [0.10* (1.772*exp(-0.025*%fld)]/k1	Snedden et al. 2015
Delta	Not applicable – use values from Approach 2	NA
Swamp	Not applicable – use values from Approach 2	NA
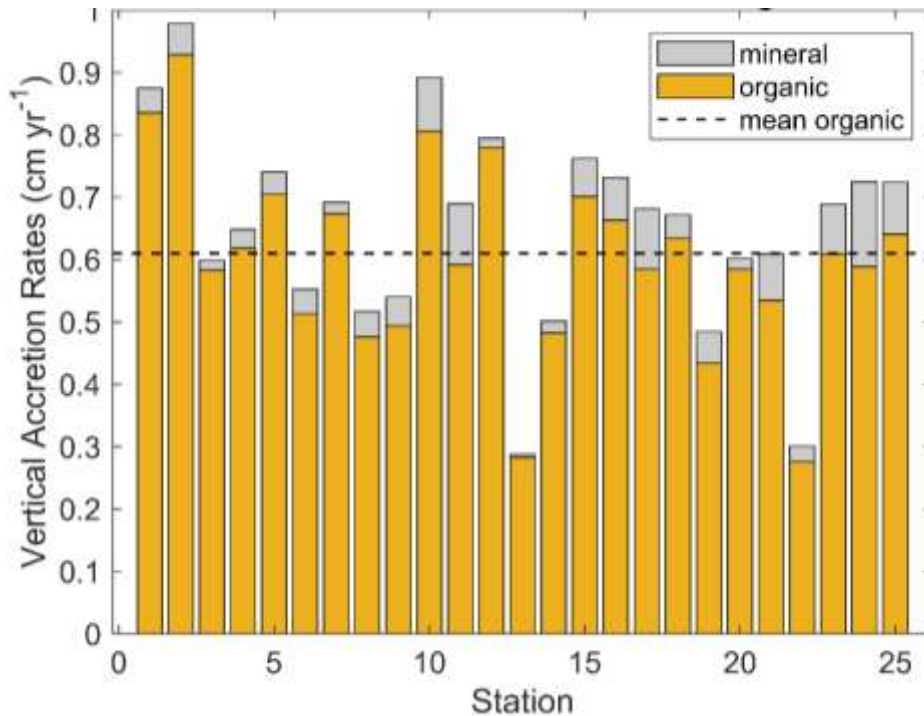
Figure 19. Organic and mineral contributions to the vertical accretion rate. Contributions were obtained by applying the ideal mixing model to 25 cores collected across Breton Sound Basin in 2008-2013 (Snedden, 2021).
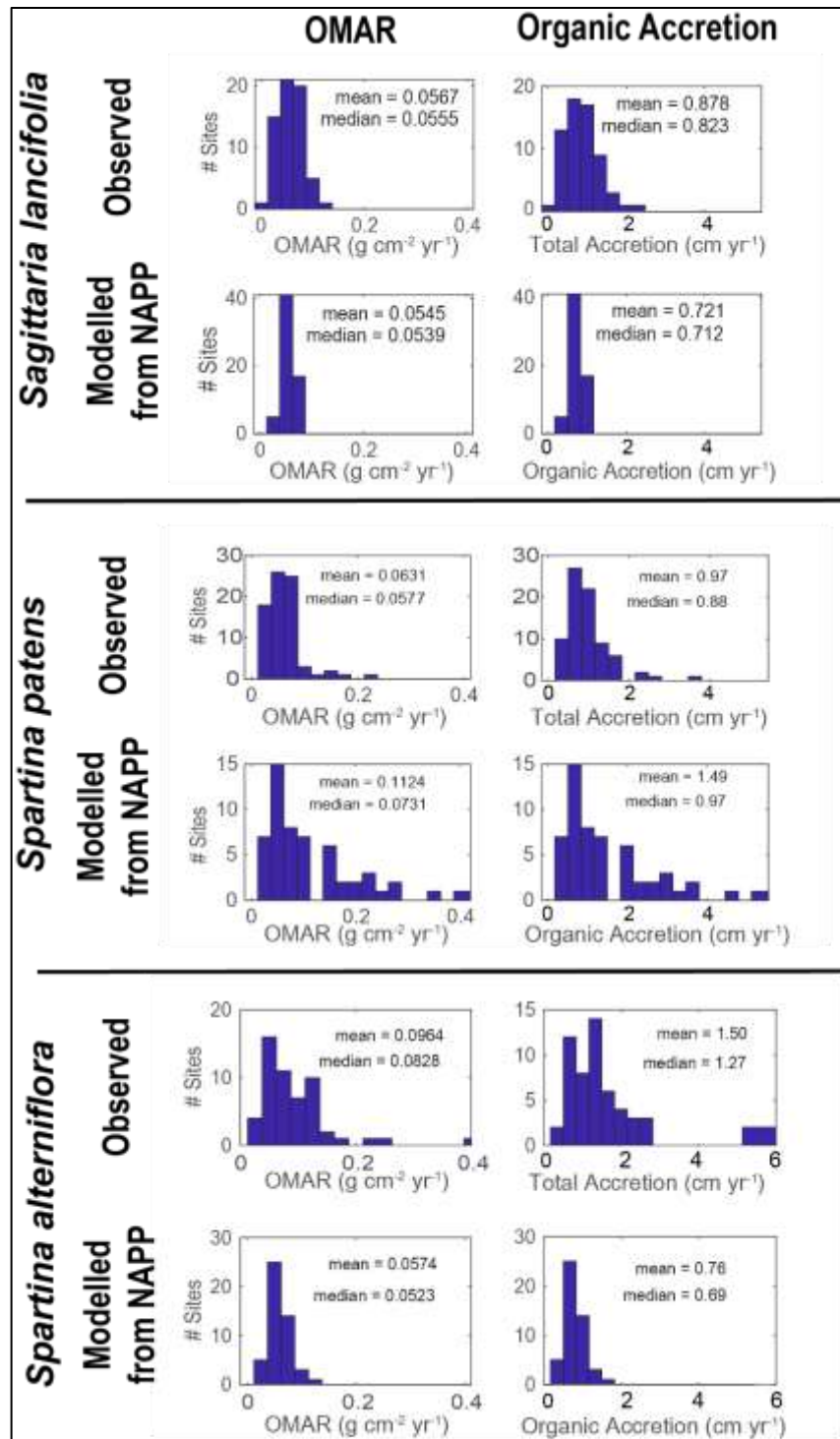
Figure 20. Distribution of observed versus modeled organic matter accumulation rates (OMAR) and organic accretion rates. Results are shown for *Sagittaria lancifolia* (intermediate marsh), *Spartina patens* (brackish marsh), and *Spartina alterniflora* (saline marsh). Observed organic accretion rates are from feldspar marker horizons. Observed average inundation at CRMS sites, 2010-2018, was used as the model input data.

MODEL IMPROVEMENT TESTING

Model tests (G027, G024, and G026) were conducted and compared to a run with the 2017 ICM (G400) that included all the projects included in the 2017 Coastal Master Plan to assess how the proposed approaches would influence ICM results. In the 2017 ICM, organic matter accretion is added to mineral matter accretion, which occurs in areas where wetlands are flooded. Organic matter and mineral matter accretion are added together in ICM-Morph, and together they impact the elevation of the marsh platform, inundation depth, and thus land loss for non-fresh marshes (Table 2). Model tests included the following (see Appendix G for details):

- **G027:** Test Approach 2 that utilized the OMAR look-up table based on 2018 CRMS soil survey data and longer-term vertical accretion with the ideal mixing model by habitat type.
- **G024:** Test Approach 4 that used belowground production estimates that were adjusted to reflect inundation duration stress (e.g., % time flooded) to estimate OMAR by habitat type, after which the ideal mixing model was applied to translate mass accumulation rates to organic accretion.
- **G026**: Test feasibility of Approach 4 by assessing the characteristics of inundation duration conditions by habitat type.

The method for modeling accretion in the 2012 and 2017 predictive models uses a look-up table that requires BD values to be determined a priori by basin/habitat types. In situations where the relative contributions of mineral and organic matter accumulation can change over time while the vegetation classification remains static, a single BD by type by basin may be unresponsive to these temporal variations. For example, in situations where diversion operations change the marsh classification from brackish to fresh, the BD values under G400 actually decrease, as look-up table values for fresh marshes come from fresh peat marshes in the upper reaches of the basin (note that the 2017 ICM does not utilize the Deltaic category identified in Table 10 for the 2012 Coastal Master Plan). In reality, BD should increase in this situation due to increased input of mineral material. Because BD values are low for fresh marshes in Barataria and Breton Basins (0.05 g cm^{-3}) under the G400 model test run (Appendix F), the volumetric leverage is inflated and accretion is overestimated. A transition to BD values nearly an order of magnitude higher in fresh marshes in deltaic settings and diversion outfall areas has been observed at CRMS3169 (Figure 21), which is situated in the immediate outfall of the Davis Pond freshwater diversion.
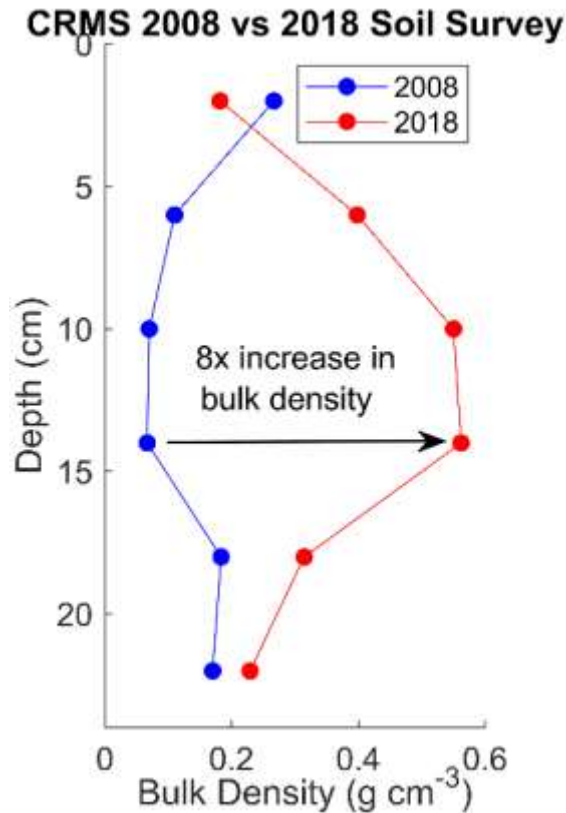
Figure 21. Bulk density profiles at CRMS3169. Data from 2008 is shown in blue, and data from 2018 is in red. CRMS3169 is in the immediate vicinity of the Davis Pond diversion outfall.

The ideal mixing model approach proposed here eliminates the need to designate a value for BD, as it solves for it through an equation based on the overall physical relationship between organic matter content and mineral matter content in soils at CRMS sites that uses the relative contributions of mineral and organic mass accumulation rates as input variables. The accretion response in areas dominated by mineral matter accumulation, particularly (but not restricted to) those areas where mineral matter is increasing from initial conditions through time (e.g., diversions), will be overestimated using the 2017 ICM approach. Thus, when comparing approaches utilizing the ideal mixing model (G027, G024 model test runs) vs G400, fluvially-dominated regions such as deltas and diversion receiving areas should show less accretion with the G027/G024 approach than with the 2017 Coastal Master Plan approach, as shown on difference maps that compare the test runs to G400 (see Appendix G).

It was hypothesized that land area at the end of the model run for G024 would be less than that for either G400 or G027, as this model approach is sensitive to inundation, which one would expect to increase due to subsidence and eustatic sea level rise (0.63 m) for these 50-year model runs. However, G024 showed

the greatest overall land area at the end of the model run (despite the lower accretion in deltaic/diversion receiving areas relative to G400 described above). This outcome is likely a result of the low inundation durations produced by ICM-Hydro compared to those observed in the CRMS dataset. With G026 output indicating that 40% of the model domain exhibits inundation rates under 15%, much of the model domain would exhibit organic accretion rates much higher than current field observations, as the belowground production rates in this approach drive organic accretion, would all fall on the far left of the inundation-production curves for intermediate, brackish, and saline marsh classifications (Figure 18).

RECOMMENDATION AND NEXT STEPS

A revised approach was recommended by the team to simulate VAR in the ICM for the 2023 Coastal Master Plan. This revised approach utilizes the ideal mixing model to derive the additive mineral and organic components of vertical accretion from mineral and organic matter mass accumulation rates. Mineral mass accumulation rates will be provided by ICM-Hydro and ICM-Morph, and OMAR will be determined as described above for Approach 2. Self-packing densities, derived from CRMS data, will be used to convert accumulation to accretion.

Given that an approach rooted in the ideal mixing model gets around some of the issues related to BD estimation presented by the 2017 ICM, two options were explored with test runs: (1) utilizing a look-up table approach for Q_{org} (OMAR), to be used as input data in conjunction with Q_{sed} (MMAR) data provided by ICM-Hydro (G027); and (2) utilizing an approach in which Q_{org} is sensitive to inundation for certain marsh classifications (G024). Considering that model runs will include 50 years of relative sea level rise, the team concluded it would be useful to incorporate inundation effects on organic matter accretion into the model. However, given the lack of strong correspondence between observed inundation durations at CRMS sites and those output from ICM-Hydro, inundation duration should not be considered as a driving factor at this time (Appendix G). The apparent underestimation of inundation duration in ICM-Hydro could be due to several factors. Inundation duration results from the interaction of water surface elevation with marsh elevation, so the quality of the digital elevation model that represents marsh elevation in the model domain could be a cause. A new digital elevation model is being developed to initialize the ICM for 2023 Coastal Master Plan and examining intersecting marsh elevation survey points in the CRMS database with their corresponding points on the DEM would be a useful way of exploring that. In addition, the compartments within ICM-Hydro have been refined and additional detail on the nature of hydrologic links between compartments has been included, which may result in further improvements in inundation duration calculations.

As inundation output from ICM-Hydro improves in the future, the prospect of utilizing Approach 3, as tested in G024, to account for inundation influences on organic accretion appears promising. Using observed CRMS inundation as inputs, modeled OMAR by marsh classification matches the observed OMAR well (Figure 20). The distribution of the observed and modeled median values compared well (given the log-normal qualities of the distribution, comparing mean values is inappropriate). The actual median values for observed *Spartina patens* and *Spartina alterniflora* OMAR do differ from their modeled counterparts by roughly 30%; however, these differences may improve as the model is improved for use in the 2023 Coastal Master Plan. It is important to note that belowground production rates were multiplied by 0.1 to

estimate the refractory component of soil organic matter that is retained for soil development. This value was based on the value reported by Morris et al. (2016), but the refractory portion of soil organic matter may vary based on the taxa involved and also by geographic location. The team recommends a thorough literature review be conducted to determine if the 0.1 factor is appropriate for these taxa and soil conditions in coastal Louisiana. Future iterations of the ICM could also be better informed by marsh mesocosm studies that not only examine belowground production but also decomposition and OMAR.

Taking the above considerations into account, the team recommends that:

1. The ideal mixing model should serve as the foundation for converting mass accumulation rates into vertical accretion rates, using Q_{sed} (MMAR) produced by ICM-Hydro and Q_{org} (OMAR) obtained from a marsh classification lookup table as inputs (e.g., Table 11). This approach should be the path forward for modeling organic matter accumulation and organic and mineral components of vertical accretion in the 2023 ICM.
2. The GO24 approach, or another approach that considers inundation duration influences on OMAR, should be implemented if inundation outputs from ICM-Hydro are well validated. Efforts should be made to ensure that refractory organic soil components are appropriate for the taxa modeled in in the ICM in coastal Louisiana.

2.3 ACTIVITY 3: COORDINATE WITH ICM- INTEGRATION AND CODING TEAM ON DEVELOPMENT OF UNSTRUCTURED GRID FOR ICM-LAVEGMOD

ISSUE

For the 2017 Coastal Master Plan, ICM-LAVegMod used a grid of 500 m x 500 m grid cells to divide the landscape. This partitioning of space required extensive computation to rescale data from both ICM-Morph and ICM-Hydro. ICM-Morph operated at a 30 m x 30 m spatial resolution that had to be aggregated up to the 500 m x 500 m resolution used by ICM-LAVegMod. The ICM-Hydro subroutine used an irregular mesh of compartments that ranged in size from 0.5 km^2 to more than 100 km^2. Having to rescale from two different spatial resolutions to the 500 m x 500 m resolution used by ICM-LAVegMod required a substantial amount of computation. Typically, the overall ICM used more time converting data between scales than the time required to complete the computations to update ICM-LAVegMod. ***This activity focused on consideration of redrawing ICM-LAVegMod grid cells so that the 2023 ICM is more computationally efficient.***

BACKGROUND

The goal for the 2023 ICM is to attempt to remove the substantial computation overhead required to support ICM-LAVegMod by adjusting model grids so that ICM-LAVegMod grid cells nest cleanly within ICM-Hydro compartments and the 30 m x 30 m ICM-Morph pixels nest cleanly within ICM-LAVegMod grid cells. An additional goal is to eliminate vegetation cells from the areas of the domain where wetland vegetation

is not expected to change. For example, those areas of the domain could include deep areas (e.g., greater than 5 m water depth) found in the Gulf of Mexico and high upland areas (e.g., greater than 5 m elevation). These inactive ICM-LAVegMod grid cells are computationally intensive and should be reduced or eliminated in the 2023 ICM.

APPROACHES/METHODS

It was proposed that ICM-LAVegMod grid cells be defined via strict subdivision of ICM-Hydro compartments (after refinement for the 2023 ICM). Strict subdivision means that each grid cell will be located completely within a single compartment. In addition to being nested with the compartments, it was proposed that, where possible, the ICM-LAVegMod boundaries used to subdivide a compartment be coincident with the boundaries of the ICM-Morph pixels. The goal was to ensure that pixels nest within the proposed ICM-LAVegMod grid cells.

A draft calculation indicates that each ICM-LAVegMod grid cells will be composed of a grid of 23 x 23 ICM-Morph pixels (23 * 23 = 529 pixels * 900 m^2/grid cell = 476,100 m^2 = 0.4761 km^2). A draft calculation indicates that subdividing compartments into ~0.5 km^2 sub-units results in each compartment being divided into 59 sub-units (on average) and yielding a total of 47,302 grid cells. This number was an overestimate since it does not exclude some of the larger ICM-Hydro compartments from the 2017 ICM that cover the upper Atchafalaya Basin. There are two scenarios regarding the way the spatial units for ICM-Hydro, ICM-Morph, and ICM-LAVegMod interact. In the simpler of the two scenarios, an ICM-LAVegMod grid cell was a square 690 m on a side with an area of 0.4761 km^2 and was completely contained within a single ICM-Hydro compartment. In this scenario, the ICM-LAVegMod grid cell contains 529 ICM-Morph pixels that are perfectly nested within the vegetation grid cell. Figure 22 illustrates the second scenario where a 0.4761 km^2 grid cell intersects the boundary between two ICM-Hydro compartments. The boundary between two compartments is shown as a thick gray line. Note that at the scale of the illustration, only a portion of the compartment is viewable. The 30 x 30 m mesh of ICM-Morph is shown as thin black lines. Two ICM-LAVegMod grid cells are shown, one outlined in red and the other outlined in blue. The red grid cell is entirely nested within the lower left ICM-Hydro compartment while the blue grid cell is nested entirely within the upper right ICM-Hydro compartment. The ICM-Morph pixels to be associated with the red grid cell are shaded red while those to be associated with the blue grid cell are shaded blue. The left and bottom (western and southern) boundaries of the red grid cell are coincident with the ICM-Morph mesh. Similarly, the right and top (eastern and northern) boundaries of the blue grid cell are coincident with the ICM-Morph mesh.
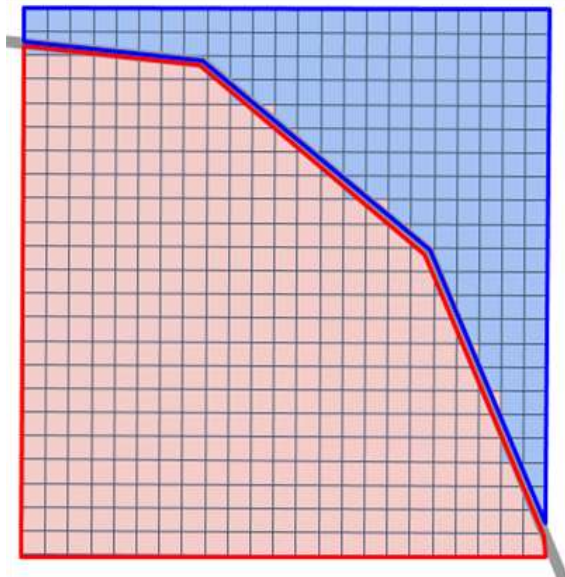
Figure 22. Relationship between ICM-Hydro compartments, ICM-Morph pixels, and the proposed ICM-LAVegMod grid cells. The grey line shows the boundary of an ICM-Hydro compartment; ICM-Morph pixels are shown in blue and red shading; and proposed ICM-LAVegMod grid cell boundaries are shown with darker blue and red lines.

Note that some ICM-Morph pixels intersect the boundary of ICM-Hydro compartments and are associated with two different compartments. There were several approaches to dealing with these kinds of pixels. The simplest approach was to associate each pixel with exactly one compartment with which it has the greatest area of intersection. Assigning pixels in this way simplifies the aggregation of values (elevation, land/water, etc.) from ICM-Morph to ICM-LAVegMod grid cells. A more accurate approach would be to weight an ICM-Morph pixel's contribution based on the area of intersection. However, this can be computationally expensive. The proposed approach will introduce a degree of potential error. However, the error is expected to be small overall relative to other sources of uncertainty in the ICM-LAVegMod framework. The increased potential error introduced is traded against reduced computational complexity and ICM run time.

This approach may produce some ICM-LAVegMod grid cells that are smaller than 0.4761 km², which should not be a problem from the perspective of ICM-LAVegMod. However, it is possible that this approach will produce some grid cells that are "slivers". If a grid cell has an area less than 0.25 km², then it is suggested to be merged with an adjoining grid cell located within the same enclosing compartment.

RECOMMENDATIONS AND NEXT STEPS

This unstructured grid approach was compatible with the grid changes being made to ICM-Hydro and ICM-Morph for the 2023 ICM. The team concluded that the proposed changes to the grid would likely simplify the rescaling ICM-Hydro and ICM-Morph data to a spatial resolution that is compatible with ICM-LAVegMod that likely will result in faster run times. Next steps are to test this new configuration. The work by ICM-Integration and Coding Team will continue to evaluate the feasibility of implementing possible unstructured grid improvements. An additional approach to consider includes examining computational efficiency if the ICM-LAVegMod domain is restricted to areas only where wetland vegetation is expected to change.

2.4 ACTIVITY 4A: EXPLORE AND RECOMMEND OPTIONS TO IMPROVE FLOTANT MARSH ALGORITHMS

ISSUE

In the 2017 ICM, flotant marsh is less dynamic than other wetland habitat types. The 2017 ICM results showed that flotant marshes persisted in areas even as salinity increased. This was most likely the result of miscommunication between the ICM-LAVegMod and ICM-Morph. At the initial condition, there was no crosscheck between areas identified as flotant in the initial land/flotant/water map used by the ICM-Morph subroutine and areas dominated by potential flotant species in ICM-LAVegMod. As a result, areas identified as flotant in the existing conditions land/flotant/water map where no flotant species were present in the existing conditions vegetation map remained unchanged over the 50-year model run, while areas mapped as flotant that had flotant species present in the existing conditions vegetation map functioned as intended with flotant converting to open water as time progressed. ***This activity focused on improving the communication between the ICM-LAVegMod and ICM-Morph.***

BACKGROUND

Flotant is defined here as marsh, permanently underlain by an open water layer that moves up and down as water levels change. Other floating marsh types identified by Sasser et al. (1996) expand and contract with changing water levels and experience inundation. Sasser et al. (1996) noted that flotant dominated by *Panicum hemitomon* (known as thick mat) and *Eleocharis baldwinii* (known as thin mat) are the only dominant species that occur on mats floating on top of a water layer. The 2017 ICM assumed that no other species can establish as dominants if environmental conditions move away from those tolerated by *P. hemitomon* and *E. baldwinii*. This should have led to the demise of flotant as salinity increased over time.

APPROACHES/METHODS

IMPROVE FLOTANT REPRESENTATION IN THE EXISTING CONDITIONS VEGETATION MAP

To determine the initial condition of flotant, two maps were prepared. The first one was a dominant species map that was used in ICM-LAVegMod (see Activity 5). The second was a map that indicates the probability of flotant occurring. Possible flotant areas can be delineated using a series of remotely sensed indices, the Normalized Difference Vegetation Index (NDVI) and the modified Normalized Difference Water Index (mNDWI). The NDVI (Carlson & Ripley, 1997) is an estimate of primary production, and the mNDWI is used to map the land/water interface (Xu, 2006). The intra-annual variability in all cloud-free images during year 2018 with respect to these two indices was examined. Sites with variable values with respect to these indices are more likely to contain either floating aquatic vegetation species or flotant marsh species in coastal Louisiana (Couvillion, personal observation). The combination of the potential of floating vegetation and knowledge of which species are dominant in the area can then be used to determine the area of flotant marsh.

The area of flotant was determined by the following rules to be applied in the order they are listed:

1. *Panicum hemitomon* (maidencane) or *Eleocharis baldwinii* (spikerush) occurring in areas that are not fresh marsh should be classified as bareground/land to allow the model to establish the appropriate non-fresh species. *Eleocharis* spp. are not easily separated into the individual species and *E. baldwinii* is easily confused with *E. parvula*, which is common in non-fresh areas of the coast, but not one of the modeled species. Classifying these areas as bareground will allow the ICM-LAVegMod to allow establishment of the appropriate species in the first year.
2. Potentially floating marsh in areas that do NOT contain: *P. hemitomon* or *E. baldwinii* should be classified as land with the non-flotant species that dominates it.
3. Remaining potentially floating marsh areas dominated by *E. baldwinii* should be classified as ELBA2_Flt
4. Remaining potentially floating marsh areas dominated by *P. hemitomon* should be classified as PAHE2_Flt
5. Remaining areas of attached marsh dominated by *P. hemitomon* should be classified as PAHE2

REVISIT TRANSITION/LOSS MECHANISMS USED IN THE ICM

Floating mats in *P. hemitomon* marshes are thicker than *E. baldwinii* floating marshes. Sasser et al. (1996) notes these are ~50 cm thick and available data from CRMS stations indicates that mat thickness in *P. hemitomon*-dominated marshes varied from 30 cm to > 2 m at site establishment. Consistent with the concept of gradual transition (see Activity 1) these mats should be assumed to survive at least one year following vegetation mortality before the peat deteriorates using the land cover type of *bareground_flt*. If

conditions allow for flotant marsh to re-establish the next year, these flotant remain as flotant (Figure 23). If the *bareground_flt* is not colonized by the following year (no new roots with aerenchyma to provide buoyancy) then the mat disintegrates or sinks and the area converts to open water. This open water is assumed to be 1 m deep based on the observations of depth to consolidated sediment under flotant at CRMS flotant sites. *Bareground_flt* isconsidered flotant and follows the ICM-Morph rules that no organic matter and mineral sediment deposition accumulates.
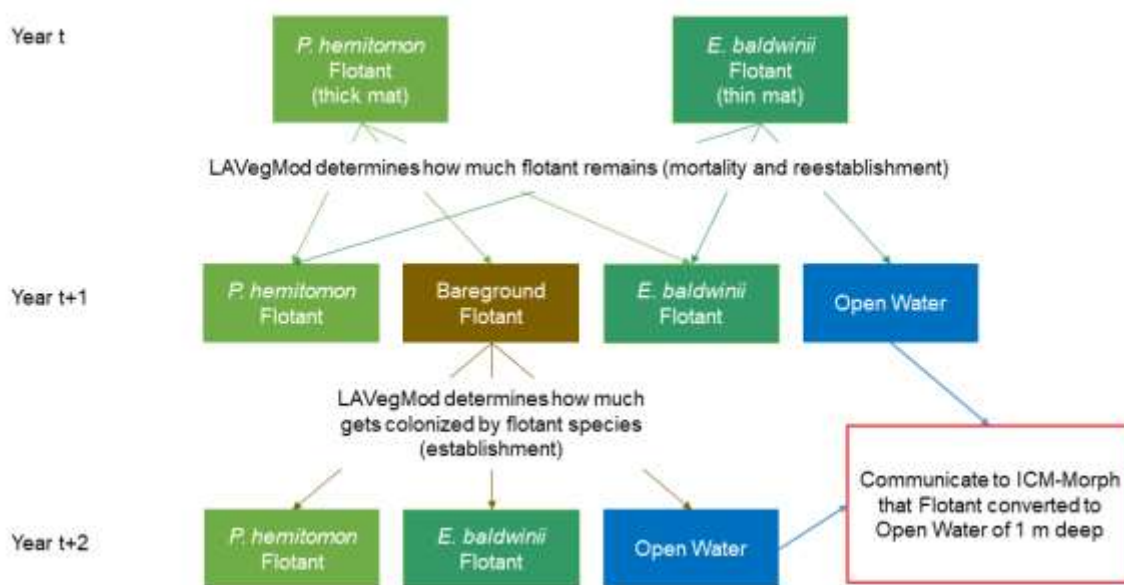
Figure 23. Proposed transitions among flotant thick and thin mats in ICM-LAVegMod.

In contrast, Sasser et al. (1996) observed that flotant dominated by *E. baldwinii* were < 30 cm thick. Consequently, when ICM-LAVegMod determines that the conditions are unsuitable for *E. baldwinii* to persist and no flotant species can establish, the area converts to open water.

RECOMMENDATIONS AND NEXT STEPS

The team recommends updating the existing conditions vegetation map based on suggested ordered rules to improve representation of flotant on the landscape and to improve communication between ICM-LAVegMod and ICM-Morph subroutines, and update ICM-LAVegMod code to accommodate the flotant types and transitions outlined in Figure 23.

2.5 ACTIVITY 4B: EXPLORE AND RECOMMEND OPTIONS TO IMPROVE FORESTED WETLAND ALGORITHMS

ISSUE

In the 2017 ICM output, areas of forested wetlands tended to convert to marshes more rapidly than observed in the field. This is likely because the ICM-Hydro under-predicted water level variability compared to CRMS observations because of large compartments and lack of wind-induced water movement. Herbaceous vegetation was thus able to replace forested wetlands because low water level variability favored herbaceous vegetation. Additionally, the collapse thresholds utilized in the 2017 ICM allowed for the transition of forested wetlands directly to open water.

The forested wetlands in the ICM are divided into two groups: bottomland hardwoods (BLH) and swamp forest (SWAMP). In ICM-LAVegMod, mortality for the BLH species was based on changes in elevation relative to MWL, while the SWAMP species mortality was determined similarly to the herbaceous marsh species (Appendix H). Establishment of all forested wetland species was based on germination and seedling survival (Appendix I). *This activity focused on hydrological recommendations to improve forested wetland representation in the 2023 ICM.*

Table 14. Wetland vegetation species that make up the two groups of the fresh forested wetland habitat types (see Table 4) in the 2017 ICM.

Habitat Type	Species
Bottomland Hardwood Forest	*Quercus lyrata, Quercus texana, Quercus laurifolia, Ulmus americana, Quercus nigra, Quercus virginiana*
Swamp Forest	*Salix nigra, Taxodium distichum, Nyssa aquatic*

APPROACHES/METHODS

In a post-2017 Coastal Master Plan study, water level variability output from 2017 ICM-Hydro was multiplied by a correction factor for the Lake Maurepas compartments before being passed to ICM-LAVegMod in an attempt to maintain forested wetlands for longer in model simulations. With this adjustment, a decline in fresh forested wetlands over time was still observed, but the decline was slower than for simulations without the adjustment (Baustian et al., 2018a). One of the improvements proposed for ICM-Hydro is to refine the resolution in parts of the domain presently covered with forested wetlands and to move the ICM-LAVegMod boundary upslope to accommodate expected sea level rise. These improvements will change water level variability in the forested wetland areas. However, most of the water-level variability in the swamp areas are likely driven by wind patterns and will not be fully captured by ICM-Hydro, so an adjustment to the hydrology outputs (e.g., water levels used to calculate water level variability) may still be necessary as described above for the Lake Maurepas compartments. It is also important to note that bottomland hardwood species in the northern portions of basins might experience

modeled hydrological conditions, e.g., annual MWL, that could also be influenced by high water events from rivers and that improvements to ICM-Hydro for the 2023 ICM will impact this effect.

RECOMMENDATIONS AND NEXT STEPS

The team makes the following recommendations:

1. Refine the resolution of the ICM-Hydro compartments to test differences in water level variability between observed and predicted in the forested wetland dominated areas and check how quickly the forested wetlands transition to marshes; assess need to include a correction factor.

2. Test the removal of the collapse threshold for forested wetlands in ICM-Morph and allow for transition to herbaceous wetlands (Activity 1).

2.6 ACTIVITY 5: COORDINATE WITH MODEL INPUT TEAM AS NEEDED TO CREATE EXISTING CONDITIONS VEGETATION MAP

ISSUE

A new existing conditions vegetation map was needed to represent current conditions (year 2018 for the 2023 ICM). The flotant habitat must be mapped consistently for both ICM-Morph and ICM-LAVegMod, and the grouping of species into habitats needs to be considered (details in Appendix H). *This activity involves support for the development of a new existing conditions vegetation map.*

BACKGROUND

ICM-LAVegMod starts from an existing conditions vegetation map that shows the most current distribution (year 2018 for 2023 ICM) of the dominant species included in the subroutine. Because other subroutines in the ICM use habitat type as an input, each grid cell in the subroutine needs to be assigned to one habitat type.

APPROACHES/METHODS

The existing conditions vegetation map requires a list of species. The 2001, 2007, and 2013 coastwide vegetation surveys (Sasser et al., 2014) and the 2018 CRMS vegetation plot data (Table 15) were used to revisit the list dominant species used in the 2017 ICM. All of these surveys use the Braun-Blanquet ocular estimate of species cover (Kent, 2011). To determine the dominant vegetation at each plot, first the species that had a cover greater than 50% of the plot (Braun-Blanquet classes 4 and 5) were assigned as dominant. If no species at the plot was assigned, it was then determined how many species had a cover of 25 to 50% (Braun-Blanquet class 3). If there was only one species that qualified, then this species was assigned as the dominant. Otherwise the plot was assigned to the no clear dominant group.

Year	Number of plots	Sample Size (m²)	Origin
2001	3790	150	Coastwide survey
2007	3912	150	Coastwide survey
2013	4039	150	Coastwide survey
2018	3185	4	CRMS

To rank the dominant species in order of importance, the percentage of the plots that were assigned to that species in each year was first determined. Then, the average percentage was calculated based on the dominance over the four years, and the species were ranked from most common dominant to least common dominant.

The species recommended for inclusion as well as the classification of the 2013 coastwide vegetation survey and the 2018 CRMS vegetation plots were used as training and validation data to create a 2018 existing conditions map for use in the 2023 Coastal Master Plan. Multiple Sentinel-2 images acquired throughout 2018 are the basis for a classification conducted at 10-meter spatial resolution. The 2013 sites observed to have experienced a change between the 2013 survey and the 2018 imagery, as assessed via remotely sensed imagery in a methodology known as "change-vector analysis", were excluded from the training set. The remaining data points were used as training data for a remotely sensed classification.

Decision tree classifiers including Classification and Regression Tree (CART) and Random Forest classification algorithms were used to develop a classification using stratified random samples from the training set. At these training sites, the values of the independent or predictor variables (i.e., remotely sensed reflectance values and indices) are recorded and sets of decision trees are automatically generated and pruned until a comprehensive ruleset was developed that most accurately reflects the training data. These rulesets are then applied throughout the remotely sensed imagery to create a complete classification of the wetland vegetation community types throughout the coast. Nine iterations of this classification procedure were conducted, and the mode was then taken as the final vegetation classification. The resulting land cover dataset was processed by using a neighborhood filter to remove changes smaller than 1.4 ha. The filtering removed some of the noise caused by environmental variance and classification error.

RESULTS

A total of 147 species were identified that dominated at least one plot in the four years (Table 16). First, all species were evaluated that are modeled in 2017 ICM-LAVegMod. It is recommended to keep most of these, except HYDRO (*Hydrocotyle umbellata*) and BAHA (*Baccharis halimifolia*) because they have less than 0.5% average occurrence. A few others that have less than 0.5% occurrence were recommended to remain on the list. The first group of these are shrubs (MOCE2 *Morella cerifera* and IVFR *Iva frutescens*)

that are under sampled in the surveys because the surveys are focused on herbaceous marshes. Of the three shrubs (BAHA, IVFR, and MOCE), BAHA is the least common (Table 16) and occurs under similar water level variability and salinity conditions to MOCE. Therefore, BAHA was removed from the model. The second group are species that are common in deltaic environments (SALA2 *Sagittaria latifolia* and COES *Colocasia esculenta*), that are expected to increase with proposed sediment diversion projects. AVGE *Avicennia germinans* was left in the subroutine because it is increasing in occurrence along the coast (Comeaux et al., 2012).

A few notable species were recommended to be added to the subroutine because they had greater than 0.4% of average occurrence and could be used for classifying to other vegetation communities (Appendix I) and they include: SCAM6, *Schoenoplectus americanus*; POPU5, *Polygonum punctatum*; ELCE, *Eleocharis cellulose;* SPCY, *Spartina cynosuroides*; and SCRO5, S*choenoplectus robustus.* Not recommended for addition was VILU3 *Vigna luteola* because it is a vine that covers underlying vegetation and contributes a relatively small amount to the total biomass in areas where it was dominant. Others not included are from CRMS sites without a clear dominant and ELEOC (*Eleocharis* spp) which includes many species of *Eleocharis* that can only be identified to the species level based on microscopic characteristics of their achenes. These species have different environmental requirements and therefore should not be included in ICM-LAVegMod. Mortality matrices and establishment matrices were developed for the added vegetation species for use in ICM-LAVegMod.

Table 16. Ranking of the dominant species (mainly marsh species) in the last 20 years as determined from the average percentage occurrence and recommendations for inclusion. 2001, 2007, and 2013 observations were from helicopter surveys. 2018 was from CRMS. Included are species that were in ICM-LAVegMod for the 2017 Coastal Master Plan analysis, species that were recommended to be added to ICM-LAVegMod, and species that had greater than 0.4% occurrence but were not recommended for inclusion.

Rank	Dominant	2017 ICM	2001	2007	2013	2018	Average	Recommendation for 2023 ICM
1	SPPA	Yes	36.3%	25.9%	25.4%	25.1%	28.2%	Keep
2	No clear dominant	No	16.7%	15.9%	15.6%	14.9%	15.8%	DO Not include
3	SPAL	Yes	11.3%	16.3%	15.5%	11.4%	13.6%	Keep
4	PAHE2	Yes	10.4%	6.3%	5.3%	4.1%	6.5%	Keep
5	SALA	Yes	6.5%	3.4%	6.3%	3.8%	5.0%	Keep
6	PHAU7	Yes	3.3%	4.0%	5.3%	4.9%	4.4%	Keep
7	TYDO	Yes	0.4%	3.4%	6.1%	1.5%	2.8%	Keep
8	VILU3	No	0.8%	3.2%	0.7%	6.1%	2.7%	DO Not include
9	SCAM6	No	1.3%	2.2%	3.2%	2.3%	2.3%	Add

Rank	Dominant	2017 ICM	2001	2007	2013	2018	Average	Recommendation for 2023 ICM
10	DISP	Yes	1.3%	2.3%	2.1%	1.7%	1.8%	Keep
11	JURO	Yes	0.6%	1.2%	1.9%	2.7%	1.6%	Keep
12	ELEOC	No	0.0%	1.4%	1.6%	1.0%	1.0%	DO Not include
13	SCCA11	Yes	0.7%	1.3%	1.3%	0.7%	1.0%	Keep
14	PAVA	Yes	1.3%	1.4%	0.8%	0.3%	1.0%	Keep
15	CLMA10	Yes	0.4%	1.0%	1.1%	0.8%	0.8%	Keep
16	ELBA2	Yes	0.7%	1.4%	0.8%	0.1%	0.7%	Keep
17	POPU5	No	0.2%	0.9%	0.5%	1.1%	0.7%	Add
18	ELCE	No	1.8%	0.1%	0.1%	0.1%	0.5%	Add
19	ZIMI	Yes	0.1%	0.4%	0.5%	1.0%	0.5%	Keep
20	SPCY	No	0.3%	0.6%	0.6%	0.4%	0.5%	Add
22	MOCE2	Yes	0.1%	0.3%	0.5%	0.8%	0.4%	Keep
24	SALA2	Yes	0.8%	0.3%	0.1%	0.3%	0.4%	Keep
26	SCRO5	No	0.1%	0.3%	0.5%	0.6%	0.4%	Add
28	HYDRO	Yes	1.0%	0.1%	0.1%	0.0%	0.3%	Drop
29	COES	No	0.2%	0.1%	0.2%	0.6%	0.3%	Add
30	IVFR	Yes	0.0%	0.4%	0.5%	0.2%	0.3%	Keep
36	AVGE	Yes	0.0%	0.2%	0.3%	0.2%	0.2%	Keep
39	BAHA	Yes	0.0%	0.0%	0.1%	0.4%	0.1%	Drop

The grouping of species into habitats was also considered. In the 2017 ICM, a grid cell in ICM-LAVegMod was assigned a habitat type based on the species with the greatest cover. It was proposed for 2023 ICM that the habitat type be assigned based on the cover weighted average score assigned to each species (Table 17). The weighted average score, developed by Visser et al. (2002), was assigned based on the abundance (or cover) of each species in each habitat type as reported by Chabreck (1970). Plants primarily occurring in fresh areas are assigned a score of 0.25. Plants that occur almost equally in both fresh and intermediate marshes are assigned a score of 1.5. Plants primarily occurring in intermediate are assigned a score of 2.75. Plants that occur almost equally in both intermediate and brackish marshes are assigned a score of 7.15. Plants primarily occurring in brackish marshes are assigned a score of 11.5. Plants that occur almost equally in both brackish and saline marshes are assigned a score of 17.5. Plants primarily occurring in saline areas are assigned a score of 24. Then a grid cell of ICM-LAVegMod could be assigned a marsh class based on weighted average score (Table 18).

Table 17. Habitat types and weighted average scores assigned to all species recommended to be included in ICM-LAVegMod for the 2023 Coastal Master Plan analysis.

Habitat Types based on 2017 ICM	Species	Weighted Average Score
Bottomland Hardwood Forest	*Quercus lyrata, Quercus texana, Quercus laurifolia, Ulmus americana, Quercus nigra, Quercus virginiana*	0.25
Swamp Forest	*Salix nigra, Taxodium distichum, Nyssa aquatica*	0.25
Fresh Flotant	*Panicum hemitomon, Eleocharis baldwinii*	0.25
Fresh Attached Marsh	*Morella cerifera, Panicum hemitomon, Sagittaria latifolia, Zizaniopsis miliacea, Colocasia esculenta*	0.25
Intermediate Marsh	*Cladium mariscus, Sagittaria lancifolia, Polygonum punctatum, Eleocharis cellulosa*	1.50
	Iva frutescens, Paspalum vaginatum, Phragmites australis, Schoenoplectus californicus, Typha domingensis	2.75
Brackish Marsh	*Spartina patens, Schoenoplectus americanus*	7.15
	Spartina cynusuroides, Schoenoplectus robustus	11.50
Saline Marsh	*Juncus roemerianus, Distichlis spicata*	17.50
	Spartina alterniflora, Avicennia germinans	24.00

Table 18. Assignment of an ICM-LAVegMod grid cell to a marsh class (FIBS) based on the weighted average score of the different species present.

Marsh Class	Weighted Average Score
Fresh	≤ 2
Intermediate	$2 < x \leq 5$
Brackish	$5 < x \leq 18$
Saline	> 18

MODEL IMPROVEMENT TESTING

A model test (G025) was performed to check how changing the way that FIBS class was assigned may alter the distribution of habitat types. In the 2017 ICM-LAVegMod (G400) the marsh class was assigned by first determining which species had the greatest cover in the grid cell and then using the marsh class to which that species was assigned to determine the overall marsh class for that grid cell. The proposed 2023 ICM-LAVegMod approach uses a weighted average: the marsh class score of a species was multiplied by its cover and the sum of these multiplications was divided by the total vegetative cover. The marsh class was then determined based on this weighted average (Table 18). Open water was classified in ICM-Morph and was not affected. Because rules for elevation change and collapse handled by ICM-Morph are based on FIBS categories, changes to FIBS classification can affect land area in the 2017 ICM framework.

Test results of G025 were compared to 2017 ICM output of future with action and medium scenario (G400, SO4). It was hypothesized that the largest difference between G025 and the G400 method would be in the classification of fresh and intermediate marshes. This hypothesis was based on the assignment of *S. lancifolia* to the intermediate marsh in G400, while in G025 it depends on the cover of the other species. In addition, there are more species in the fresh and intermediate marsh classes in G025. It was also expected that the G025 approach will smooth the gradients in the FIBS classes and will avoid the occurrence of fresh marshes immediately adjacent to saline marshes. In addition, it was expected that changes in classification will lead to changes in land loss patterns, but it was hypothesized that these would be relatively minor.

The proposed FIBS classification system, that uses the weighted average score (from G025), shows a more consistent estuarine gradient and seems to represent a distribution more consistent with patterns that have been observed in the Louisiana coastal zone (see Appendix H). It was also suggested that if more categories of vegetation are desired then the self-organizing map approach by Snedden (2019) should be utilized for the eleven vegetation communities. Appendix I provides a method of how to use the 34 vegetation species (Table 17) from ICM-LAVegMod output to classify into 11 types (Figure 4).

RECOMMENDATIONS AND NEXT STEPS

The team recommends the following:

- Include a total of 34 vegetation species (including SAV, Table 17) in the existing conditions vegetation map in ICM-LAVegMod
- Utilize the weighted average score approach to classify habitat types

2.7 ACTIVITY 6: COORDINATE WITH ICM-INTEGRATION AND CODING TEAM ON ADJUSTING MODEL CODE

This activity is ongoing. Refinement of improvements recommended by the team will continue as the improvements are tested and integrated into the ICM framework. Details will be documented in a report from the ICM-Integration and Coding Team.

2.8 ACTIVITY 7: SUBMERGED AQUATIC VEGETATION (SAV) MODULE UPDATES

ISSUE

Most of the habitat suitability indices (HSIs) utilized in the 2023 Coastal Master Plan depend on SAV output, and previous (2012 and 2017) ICM output seemed to underestimate the SAV spatial distribution. The SAV module in 2017 ICM-LAVegMod (Visser & Duke-Sylvester, 2017; Visser et al., 2013) needs to be validated and potentially calibrated given the validation results. Other models and data describing SAV likelihood of occurrence (SLOO) (DeMarco, 2018; DeMarco et al., 2018) are available that can inform the SAV component of ICM-LAVegMod and potentially be used to adapt the modeling approach following evaluation of the 2017 approach. *This activity is focused on improving SAV representation in the 2023 Coastal Master Plan modeling efforts.* As this work is still ongoing, so only the approach is described here.

APPROACHES/METHODS

To improve the SAV module component for the 2023 ICM efforts, a strategic approach was necessary. Initially, a quantitative assessment of the accuracy of the existing 2017 ICM-LAVegMod will occur by comparing the model results with existing data over the same time period. These results will inform the team as to next steps, specifically to determine if the 2017 ICM-LAVegMod SAV module was 1) still applicable as is, 2) applicable following calibration, or 3) inaccurate and in need of being replaced. These steps are described below, and further detail will be documented in a future report.

TASK 1. VALIDATE EXISTING SAV MODULE

To assess the accuracy and precision of the existing SAV module output from the 2017 ICM efforts, available data describing SAV presence, biomass, and cover across coastal Louisiana will be compared to the existing SAV output from the 2017 ICM. Observed SAV data (nearly 500 field observations) are available for years 2013 – 2015 (DeMarco et al., 2018), corresponding with 2017 ICM-LAVegMod output for the existing SAV module from calibration years run. The two datasets will be spatially overlaid to visualize areas of disagreement (error) between the field observations and model runs over the landscape. Additionally, a tabular dataset describing the 2017 ICM-LAVegMod SAV module accuracy will be generated, including a confusion matrix to describe patterns of error (predicted presence when there was absence and predicated absence when there was presence), as well as other statistics describing model accuracy

and performance. A potential challenge with this activity will be in comparing the cell size (max 0.5 km^2) of the SAV module output to the actual observed SAV data (0.25 m^2 sampling quadrat), which may require some conversion.

TASK 2. DEVELOP AN APPROACH FOR A NEW SAV MODULE

While the validation of the 2017 ICM-LAVegMod is ongoing, development of an approach to adjust, improve, or replace the existing model with a new SAV module will be considered. This approach will evaluate key outputs from the 2023 ICM-Hydro and ICM-Morph to drive the SAV module, including but not limited to total suspended sediments (TSS), exposure to wave action/currents, depth, and salinity, as well as environmental and SAV data collected over the coast from other sources (i.e., CRMS, remotely sensed imagery).

TASK 3. MODULE CALIBRATION

If the existing SAV module performs adequately and is deemed suitable following team evaluation, then calibration of the existing model may occur by using newly available SAV data. This effort will incorporate both SAV field data and coastal environmental data from multiple sources (i.e., CRMS) to more precisely quantify the current parameters used to drive the SAV module in 2017 ICM-LAVegMod. Additionally, a robust method will be developed for converting presence of SAV to percent cover for use in the HSI models where appropriate and needed.

TASK 4. IMPLEMENTATION OF NEW SAV MODULE

If the SAV module in 2017 ICM-LAVegMod is found to be inaccurate or otherwise unfit for use in the 2023 ICM effort, a new SAV module will be implemented within 2023 ICM-LAVegMod. The 2023 SAV module would incorporate identified parameters of significance and quantify the likelihood of SAV occurrence and assumed coverage based on model outputs from other relevant output from 2023 ICM. Following the development of the preferred approach, coordination with the team will allow for testing of the 2023 SAV module and adjusting accordingly on the updated outputs.

3.0 SUMMARY OF RECOMMENDATIONS, NEXT STEPS, AND FURTHER NEEDS

The following summarize what the team recommends as the next steps needed from each of the activities to update the ICM for the 2023 Coastal Master Plan.

3.1 ACTIVITY 1: PROVIDE RECOMMENDATION FOR ADJUSTING COLLAPSE THRESHOLDS

- Remove the two-week salinity collapse threshold for swamps as there was no evidence of such sudden loss occurring in fresh forested wetlands in Louisiana.
- Land change aspects of the ICM should be modified to reflect:
  - Gradual Transitions
    - Consider the approach to bareground lowering described in this memo and determine the rate of lowering based on model tests (proposed tests at 0 cm and 5 cm per year).
    - Modify ICM-LAVegMod to include a two-week salinity mortality component for fresh marsh species to reflect acute effects of salinity on vegetation. Areas would convert to bareground, assuming no other species establish, and would be available for vegetation establishment the following year.
  - Water Depth Limitation
    - Replace collapse thresholds for FIBS with the water depth limitation by salinity for vegetation occurrence.
    - Apply the water depth limitation based on two consecutive years.
    - Calculate depth at the scale of the 30 m x 30 m pixel.
    - Explore the effects of water depth limitation using a curve based on the 99.5th quantile of the CRMS data.
  - Elevation for Vegetation Establishment
    - Use an elevation for vegetation establishment of MWL+10 cm (G022) and retest with the updated dispersal rates.
- Further model testing:
  - Bareground lowering 1 (G###). Remove collapse thresholds for forested wetlands and FIBS. Retain collapse threshold for bareground and land gain threshold. Add distinction between *bareground_new* and *bareground_old*, and lower elevation of *bareground_old* by 5 cm yr^{-1}.
  - Bareground lowering 2 (G###). Same as for Bareground lowering 1 but do not lower elevation of bareground, i.e., test of lowering = 0 cm yr^{-1}.

New dispersal (G###). Replace existing dispersal distance (1 grid cell) with three dispersal classes (by species). See Table 7.

- Further research needs or data gaps:
  - Field or laboratory experiments that test the water depth limitations of vegetation species and how these vary with salinity
  - Direct observations of elevation loss from changes in % total cover of vegetation or other metrics of marsh deterioration
  - Observations of the inundation characteristics (depth and duration of flooding) of emerging substrates where new vegetation is establishing.

3.2 ACTIVITY 2: REFINE THE ORGANIC MATTER ACCRETION APPROACH

- A new look-up table based on Q_{org} (OMAR) by habitat type (GO27 test run) and Q_{sed} (MMAR) produced by ICM-Hydro as inputs to the ideal mixing model should be the path forward for modeling organic matter accumulation and organic and mineral components of vertical accretion in 2023 ICM.
- The GO24 approach or another approach that considers inundation impacts to organic soil formation and subsequent accretion should be implemented if inundation outputs from ICM-Hydro are sufficiently reliable. The GO24 approach should also be further developed to reflect possible differences in OMAR between Chenier and Delta Plain settings, and efforts should be made to ensure that refractory organic soil components are appropriate for the taxa modeled in subtropical and microtidal settings such as the northern Gulf of Mexico.
- Further research needs or data gaps:
  - Field or laboratory experiments that test the response of soil organic matter accumulation responses to potential future conditions (e.g., increased carbon dioxide concentrations, temperatures, nutrient and water levels)
  - Improve parameterization of belowground biomass response to inundation for *S. patens* and *S. alterniflora* taking into account nutrient enrichment and decomposition
  - Additional marsh organ studies that examine belowground biomass response to *S. lancifolia* and *P. hemitomon*
  - The GO24 approach should be further investigated to reflect possible differences in OMAR between Chenier Plain and Delta Plain settings
  - Observational and modeling studies are needed to better understand how fine-grained mineral sediments infiltrate downward into the soil profile of highly porous wetland soils given that porosity in most Louisiana coastal wetland soils exceeds 0.8.
  - Evaluate the use of short-term and long-term accretion rates for representation of annual time steps and at 50-year estimates of OMAR.

3.3 ACTIVITY 3: COORDINATE WITH ICM-INTEGRATION AND CODING TEAM ON DEVELOPMENT OF UNSTRUCTURED GRID FOR LAVEGMOD V2

The ICM-Integration and Coding Team will develop and test approaches to adjust the ICM-LAVegMod grid to restrict the ICM-LAVegMod domain to areas where wetland vegetation is expected to change.

3.4 ACTIVITY 4: EXPLORE AND RECOMMEND OPTIONS TO IMPROVE FLOTANT MARSH AND FORESTED WETLAND ALGORITHMS

- Update existing conditions vegetation map based on suggested ordered rules to improve representation of flotant on the landscape and to improve communication between ICM-LAVegMod and ICM-Morph subroutines.
- Refine the resolution of the ICM-Hydro compartments to test differences in water level variability between observed and predicted in the forested wetland dominated areas and check how quickly the forested wetlands transition to marshes.
- Test the removal of the collapse threshold for forested wetlands in ICM-Morph and allow for transition to herbaceous wetlands (Activity 1).
- Further research needs: consider adding wind to the ICM-Hydro to better represent water level patterns in the wetlands including the fresh forested wetland areas.

3.5 ACTIVITY 5: COORDINATE WITH MODEL INPUT TEAM AS NEEDED TO CREATE EXISTING CONDITIONS VEGETATION MAP

- Include a total of 34 vegetation species (including SAV, Table 17) in the existing conditions vegetation map in ICM-LAVegMod
- Utilize the weighted average score approach to classify habitat types
- The work on the existing conditions vegetation map is continuing and will be documented in more detail in a separate report from the Model Inputs Team
- Further research needs:
    - Perform a coastwide vegetation survey to improve spatial cover of more recent vegetation. This can also assist with QA/QC of the existing conditions vegetation map and model output.
    - Research applicability of new survey techniques for coastwide habitat mapping (e.g., drones, stratified random design vs grid sampling, multispectral imagery, and combinations thereof).

3.6 ACTIVITY 6: COORDINATE WITH ICM-INTEGRATION AND CODING TEAM ON ADJUSTING MODEL CODE

The work by ICM-Integration and Coding Team will continue by testing, refining, and integrating the model improvements recommended in this report into the ICM framework as part of the model development process.

3.7 ACTIVITY 7: SAV MODULE UPDATES

Work will continue with the SAV module updates beyond what has been initially reported.

4.0 REFERENCES

Acharya, C. N. (1935). Studies on the anaerobic decomposition of plant materials. *Biochemical Journal*, *29*(5), 1116–1120.

Adams, W. A. (1973). The Effect of Organic Matter on the Bulk and True Densities of Some Uncultivated Podzolic Soils. *Journal of Soil Science*, *24*(1), 10–17.

Baustian, J. J., Mendelssohn, I. A., & Hester, M. W. (2012). Vegetation's importance in regulating surface elevation in a coastal salt marsh facing elevated rates of sea level rise. *Global Change Biology*, *18*(11), 3377–3382.

Baustian, M. M., Clark, F. R., Jerabek, A. S., Wang, Y., Bienn, H. C., & White, E. D. (2018a). Modeling current and future freshwater inflow needs of a subtropical estuary to manage and maintain forested wetland ecological conditions. *Ecological Indicators*, *85*, 791–807.

Baustian, M. M., Meselhe, E., Jung, H., Sadid, K., Duke-Sylvester, S. M., Visser, J. M., Allison, M. A., Moss, L. C., Ramatchandirane, C., Sebastiaan van Maren, D., Jeuken, M., & Bargu, S. (2018b). Development of an Integrated Biophysical Model to represent morphological and ecological processes in a changing deltaic and coastal ecosystem. *Environmental Modelling & Software*, *109*, 402–419.

Baustian, M. M., Stagg, C. L., Perry, C. L., Moss, L. C., Carruthers, T. J. B., & Allison, M. (2017). Relationships Between Salinity and Short-Term Soil Carbon Accumulation Rates from Marsh Types Across a Landscape in the Mississippi River Delta. *Wetlands*, *37*(2), 313–324.

Baustian, M. M., Stagg, C. L., Perry, C. L., Moss, L., & Carruthers, T. (In review). Long-term carbon sinks in marsh soils of the Mississippi River Deltaic Plain are at risk to wetland loss. *JGR-Biogeosciences*.

Blum, L. K. (1993). Spartina alterniflora root dynamics in a Virginia marsh. *MARINE ECOLOGY-PROGRESS SERIES*, *102*, 169–178.

Brown, S., Couvillion, B. R., Dong, Z., Meselhe, E., Visser, J. M., Wang, Y., & White, E. D. (2017). *2017 Coastal Master Plan: Attachment C3-23: ICM Calibration, Validation, and Performance Assessment* (p. 95). Baton Rouge, LA: Coastal Protection and Restoration Authority.

Cahoon, D. R., Ford, M. A., & Hensel, P. F. (2004). Ecogeomorphology of *Spartina Patens* -dominated tidal marshes: Soil organic matter accumulation, marsh elevation dynamics, and disturbance. In S. Fagherazzi, M. Marani, & L. K. Blum (Eds.), *Coastal and Estuarine Studies* (pp. 247–266). Washington, D. C.: American Geophysical Union.

Cahoon, D. R., & Reed, D. J. (1995). Relationships among Marsh Surface Topography, Hydroperiod, and Soil Accretion in a Deteriorating Louisiana Salt Marsh. *Journal of Coastal Research*, *11*(2), 357–369.

Callaway, J. C., DeLaune, R. D., & Patrick Jr., W. H. (1997). Sediment accretion rates from four coastal wetlands along the Gulf of Mexico. *Journal of Coastal Research*, *13*(1), 181–191.

Carle, M. V., Sasser, C. E., & Roberts, H. H. (2013). Accretion and vegetation dommunity dhange in the Wax Lake Delta following the historic 2011 Mississippi River flood. *Journal of Coastal Research*, 569–587.

Carlson, T. N., & Ripley, D. A. (1997). On the relation between NDVI, fractional vegetation cover, and leaf area index. *Remote Sensing of Environment*, *62*(3), 241–252.

Chabreck, R. H. (1970). *Marsh zones and vegetative types in the Louisiana coastal marshes* (Doctor of Philosophy). Louisiana State University, Baton Rouge, LA.

Chambers, L. G., Steinmuller, H. E., & Breithaupt, J. L. (2019). Toward a mechanistic understanding of "peat collapse" and its potential contribution to coastal wetland loss. *Ecology*, *0*(ja), 15.

Charles, S. P., Kominoski, J. S., Troxler, T. G., Gaiser, E. E., Servais, S., Wilson, B. J., Davis, S. E., Sklar, F. H., Coronado-Molina, C., Madden, C. J., Kelly, S., & Rudnick, D. T. (2019). Experimental saltwater intrusion drives rapid soil elevation and carbon loss in freshwater and brackish Everglades marshes. *Estuaries and Coasts*.

Comeaux, R. S., Allison, M. A., & Bianchi, T. S. (2012). Mangrove expansion in the Gulf of Mexico with climate change: Implications for wetland health and resistance to rising sea levels. *Estuarine, Coastal and Shelf Science*, *96*, 81–95.

Conner, W. H. (1994). The Effect of salinity and waterlogging on growth and survival of baldcypress and Chinese tallow seedlings. *Journal of Coastal Research*, *10*(4), 1045–1049.

Couvillion, B. R., & Beck, H. (2013). Marsh collapse thresholds for coastal Louisiana estimated using elevation and vegetation index data. *Journal of Coastal Research*, *63*, 58–67.

Day, F. P., & Megonigal, J. P. (1993). The relationship between variable hydroperiod, production allocation, and belowground organic turnover in forested wetlands. *Wetlands*, *13*(2), 115–121.

Delaune, R. D., Nyman, J. A., & Patrick, W. H. (1994). Peat collapse, ponding and wetland loss in a rapidly submerging coastal marsh. *Journal of Coastal Research*, *10*(4), 1021–1030.

DeLaune, R. D., White, J. R., Elsey-Quirk, T., Roberts, H. H., & Wang, D. Q. (2018). Differences in long-term vs short-term carbon and nitrogen sequestration in a coastal river delta wetland: Implications for global budgets. *Organic Geochemistry*, *123*, 67–73.

DeMarco, K. (2018). *Shifting niche space in coastal landscapes: spatio-temporal patterns driving submerged aquatic vegetation across the northern Gulf of Mexico.* (Dissertation). Louisiana State University, School of Renewable Natural Resources. Retrieved from https://digitalcommons.lsu.edu/gradschool_dissertations/4603/

DeMarco, K., Couvillion, B., Brown, S., & La Peyre, M. (2018). Submerged aquatic vegetation mapping in coastal Louisiana through development of a spatial likelihood occurrence (SLOO) model. *Aquatic Botany*, *151*, 87–97.

Hackney, C. T. (1987). Factors Affecting Accumulation or Loss of Macroorganic Matter in Salt Marsh Sediments. *Ecology*, *68*(4), 1109–1113.

Hackney, C. T., & De La Cruz, A. A. (1980). In Situ Decomposition of Roots and Rhizomes of Two Tidal Marsh Plants. *Ecology*, *61*(2), 226–231.

Hatton, R. S., DeLaune, R. D., & Patrick, W. H. (1983). Sedimentation, accretion, and subsidence in marshes of Barataria Basin, Louisiana. *Limnology and Oceanography*, *28*(3), 494–502.

Hoeppner, S. S., Shaffer, G. P., & Perkins, T. E. (2008). Through droughts and hurricanes: Tree mortality, forest structure, and biomass production in a coastal swamp targeted for restoration in the Mississippi River Deltaic Plain. *Forest Ecology and Management*, *256*, 937–948.

Holmquist, J. R., Windham-Myers, L., Bliss, N., Crooks, S., Morris, J. T., Megonigal, J. P., Troxler, T., Weller, D., Callaway, J., Drexler, J., Ferner, M. C., Gonneea, M. E., Kroeger, K. D., Schile-Beers, L., Woo, I., Buffington, K., Breithaupt, J., Boyd, B. M., Brown, L. N., Dix, N., Hice, L., Horton, B. P., MacDonald, G. M., Moyer, R. P., Reay, W., Shaw, T., Smith, E., Smoak, J. M., Sommerfield, C., Thorne, K., Velinsky, D., Watson, E., Grimes, K. W., & Woodrey, M. (2018). Accuracy and Precision of Tidal Wetland Soil Carbon Mapping in the Conterminous United States. *Scientific Reports*, *8*(1).

Janousek, C., Buffington, K., Guntenspergen, G., Thorne, K., Dugger, B., & Takekawa, J. (2017). Decomposition of plant litter in Pacific coast tidal marshes, 2014-2015. U.S. Geological Survey data release, https://doi.org/10.5066/F70P0X6C

Janousek, C., Buffington, K., Thorne, K., Guntenspergen, G., Takekawa, J., & Dugger, B. (2016). Potential effects of sea-level rise on plant productivity: species-specific responses in northeast Pacific tidal marshes. *Marine Ecology Progress Series*, *548*, 111–125.

Kairis, P. A., & Rybczyk, J. M. (2010). Sea level rise and eelgrass (*Zostera marina*) production: A spatially explicit relative elevation model for Padilla Bay, WA. *Ecological Modelling*, *221*(7), 1005–1016.

Keddy, P. A., & Ellis, T. H. (1985). Seedling recruitment of 11 wetland plant species along a water level gradient: shared or distinct responses? *Canadian Journal of Botany*, *63*(10), 1876–1879.

Kent, M. (2011). *Vegetation description and data analysis: a practical approach*. Wiley-Blackwell.

Kirwan, M. L., & Guntenspergen, G. R. (2015). Response of plant productivity to experimental flooding in a stable and a submerging marsh. *Ecosystems*, *18*(5), 903–913.

Kirwan, M. L., Langley, J. A., Guntenspergen, G. R., & Megonigal, J. P. (2013). The impact of sea-level rise on organic matter decay rates in Chesapeake Bay brackish tidal marshes. *Biogeosciences*, *10*(3), 1869–1876.

Lane, R. R., Mack, S. K., Day, J. W., DeLaune, R. D., Madison, M. J., & Precht, P. R. (2016). Fate of soil organic carbon during wetland loss. *Wetlands*, *36*(6), 1167–1181.

Langley, J. A., Mozdzer, T. J., Shepard, K. A., Hagerty, S. B., & Megonigal, P. J. (2013). Tidal marsh plant responses to elevated CO_2, nitrogen fertilization, and sea level rise. *Global Change Biology*, *19*(5), 1495–1503.

Li, F., & Pennings, S. C. (2019). Response and recovery of low-salinity marsh plant communities to presses and pulses of elevated salinity. *Estuaries and Coasts*, *42*(3), 708–718.

Mariotti, G., Elsey-Quirk, T., Bruno, G., & Valentine, K. (2020). Mud-associated organic matter and its direct and indirect role in marsh organic matter accumulation and vertical accretion. *Limnology and Oceanography*, *65*(11), 2627-2641

McKee, K. L., & Grace, J. B. (2012). *Effects of Prescribed Burning on Marsh-Elevation Change and the Risk of Wetland Loss* (Open-File Report No. 2012–1031) (p. 51). Reston, VA: U.S. Geological Survey.

McKee, K. L., & Vervaeke, W. C. (2018). Will fluctuations in salt marsh–mangrove dominance alter vulnerability of a subtropical wetland to sea-level rise? *Global Change Biology*, *24*(3), 1224–1238.

Meselhe, E., White, E. D., & Wang, Y. (2017). *2017 Coastal Master Plan: Attachment C3-24: Integrated Compartment Model Uncertainty Analysis* (p. 68). Baton Rouge, LA: Coastal Protection and Restoration Authority.

Morris, J., Sundberg, K., & Hopkinson, C. (2013). Salt marsh primary production and its responses to relative sea level and nutrients in estuaries at Plum Island, Massachusetts, and North Inlet, South Carolina, USA. *Oceanography*, *26*(3), 78–84.

Morris, J. T., Barber, D. C., Callaway, J. C., Chambers, R., Hagen, S. C., Hopkinson, C. S., Johnson, B. J., Megonigal, P., Neubauer, S. C., Troxler, T., & Wigand, C. (2016). Contributions of organic and inorganic matter to sediment volume and accretion in tidal wetlands at steady state. *Earth's Future*, *4*(4), 110–121.

Morton, R. A., & Barras, J. A. (2011). Hurricane Impacts on Coastal Wetlands: A Half-Century Record of Storm-Generated Features from Southern Louisiana. *Journal of Coastal Research*, *275*, 27–43.

Mozdzer, T. J., Langley, J. A., Mueller, P., & Megonigal, J. P. (2016). Deep rooting and global change facilitate spread of invasive grass. *Biological Invasions*, *18*(9), 2619–2631.

Naidoo, G., McKee, K. L., & Mendelssohn, I. A. (1992). Anatomical and metabolic responses to waterlogging and salinity in *Spartina alterniflora* and *S. patens* (Poaceae). *American Journal of Botany*, *79*(7), 765–770.

Neubauer, S. C. (2008). Contributions of mineral and organic components to tidal freshwater marsh accretion. *Estuarine, Coastal and Shelf Science*, *78*(1), 78–88.

Nyman, J. A., DeLaune, R. D., & Patrick, W. H. (1990). Wetland soil formation in the rapidly subsiding Mississippi River Deltaic Plain: Mineral and organic matter relationships. *Estuarine, Coastal and Shelf Science*, *31*(1), 57–69.

Nyman, J. A., Walters, R. J., Delaune, R. D., & Patrick Jr, W. H. (2006). Marsh vertical accretion via vegetative growth. *Estuarine, Coastal and Shelf Science*, *69*, 370–380.

Nyman, J., DeLaune, R., Roberts, H., & Patrick, W., Jr. (1993). Relationship between vegetation and soil formation in a rapidly submerging coastal marsh. *Marine Ecology Progress Series*, *96*, 269–279.

Olliver, E. A., & Edmonds, D. A. (2017). Defining the ecogeomorphic succession of land building for freshwater, intertidal wetlands in Wax Lake Delta, Louisiana. *Estuarine, Coastal and Shelf Science*, *196*, 45–57.

O'Neil, T. (1949). *The muskrat in the Louisiana coastal marshes*. Louisiana Department of Wildlife and Fisheries.

Ouyang, X., & Lee, S. Y. (2014). Updated estimates of carbon accumulation rates in coastal marsh sediments. *Biogeosciences*, *11*(18), 5057–5071.

Penfound, Wm. T., & Hathaway, E. S. (1938). Plant communities in the marshlands of southeastern Louisiana. *Ecological Monographs*, *8*(1), 1–56.

Peng, D., Chen, L., Pennings, S. C., & Zhang, Y. (2018). Using a marsh organ to predict future plant communities in a Chinese estuary invaded by an exotic grass and mangrove: Multiple plant invasions in a Chinese estuary. *Limnology and Oceanography*, *63*(6), 2595–2605.

Pezeshki, S. R., & DeLaune, R. D. (1996). Responses of *Spartina alterniflora* and *Spartina patens* to rhizosphere oxygen deficiency. *Acta Oecologica*, *17*(5), 365–378.

Sasser, C. E., Gosselink, J. G., Swenson, E. M., Swarzenski, C. M., & Leibowitz, N. C. (1996). Vegetation, substrate and hydrology in floating marshes in the Mississippi river delta plain wetlands, USA. *Vegetatio*, *122*(2), 129–142.

Sasser, C. E., Visser, J. M., Mouton, E., Linscombe, J., & Hartley, S. B. (2014). Vegetation types in coastal Louisiana in 2013. 1 sheet, US Geological Survey Scientific Investigations Map 3290.

Schile, L. M., Callaway, J. C., Suding, K. N., & Kelly, N. M. (2017). Can community structure track sea-level rise? Stress and competitive controls in tidal wetlands. *Ecology and Evolution*, *7*(4), 1276–1285.

Shaffer, G., Sasser, C., Gosselink, J., & Rejmanek, M. (1992). Vegetation Dynamics in the Emerging Atchafalaya Delta, Louisiana, USA. *Journal of Ecology, 80*(4), 677-687. doi:10.2307/2260859

Shaffer, G. P., Wood, W. B., Hoeppner, S. S., Perkins, T. E., Zoller, J., & Kandalepas, D. (2009). Degradation of baldcypress–water tupelo swamp to marsh and open water in Southeastern Louisiana, U.S.A.: An irreversible trajectory? *Journal of Coastal Research*, *10054*, 152–165.

Slocum, M. G., & Mendelssohn, I. A. (2008). Use of experimental disturbances to assess resilience along a known stress gradient. *Ecological Indicators*, *8*(3), 181–190.

Snedden, G. A. (2019). Patterning emergent marsh vegetation assemblages in coastal Louisiana, USA, with unsupervised artificial neural networks. *Applied Vegetation Science*, *22*, 213–229.

Snedden, G.A. (2021). Soil properties and radioisotope activity across Breton Sound basin wetlands (2008-2013).   U.S. Geological Survey data release, https://doi.org/10.5066/P9XWAXOT (release date 02/17/2021)

Snedden, G. A., Cretini, K., & Patton, B. (2015). Inundation and salinity impacts to above- and belowground productivity in *Spartina patens* and *Spartina alterniflora*in the Mississippi River Deltaic Plain: Implications for using river diversions as restoration tools. *Ecological Engineering*, *81*, 133–139.

Snedden, G. A., & Steyer, G. D. (2013). Predictive occurrence models for coastal wetland plant communities: Delineating hydrologic response surfaces with multinomial logistic regression. *Estuarine, Coastal and Shelf Science*, *118*, 11–23.

Spalding, E. A., & Hester, M. W. (2007). Interactive effects of hydrology and salinity on oligohaline plant species productivity: Implications of relative sea-level rise. *Estuaries and Coasts*, *30*(2), 214–225.

Stagg, C. L., Schoolmaster, D. R., Krauss, K. W., Cormier, N., & Conner, W. H. (2017). Causal mechanisms of soil organic matter decomposition: deconstructing salinity and flooding impacts in coastal wetlands. *Ecology*, *98*(8), 2003–2018.

Stagg, C. L., Schoolmaster, D. R., Piazza, S. C., Snedden, G., Steyer, G. D., Fischenich, C. J., & McComas, R. W. (2016). A landscape-scale assessment of above- and belowground primary production in coastal wetlands: implications for climate change-induced community shifts. *Estuaries and Coasts*.

Steyer, G. D., Couvillion, B., Wang, H., Sleavin, B., Rybczyk, J., Trahan, N., Beck, H., Fischenich, C. J., Boustany, R., & Allen, Y. (2012). *Appendix D-2 Wetland Morphology Model Technical Report* (No. Appendix D-2) (p. 108). Baton Rouge, LA: Coastal Protection and Restoration Authority.

Tate, R. L. I. (1979). Effect of flooding on microbial activities in organic soils: carbon metabolism. *Soil Science*, *128*(5), 267–273.

Tenney, F. G., & Waksman, S. A. (1930). Composition of natural organic materials and their decomposition in the soil: V. Decomposition of various chemical constituents in plant materials under an-aerobic conditions. *Soil Science*, *30*(2), 143.

Visser, J., & Duke-Sylvester, S. (2017). LaVegMod v2: Modeling coastal vegetation dynamics in response to proposed coastal restoration and protection projects in Louisiana, USA. *Sustainability*, *9*(9), 1625.

Visser, J. M., Duke-Sylvester, S. M., Carter, J., & Broussard, W. P. (2013). A computer model to forecast wetland vegetation changes resulting from restoration and protection in coastal Louisiana. *Journal of Coastal Research*, *67*, 51–59.

Visser, J. M., & Peterson, J. K. (2015). The Effects of Flooding Duration and Salinity on Three Common Upper Estuary Plants. *Wetlands*, *35*(3), 625–631.

Visser, J. M., Sasser, C. E., & Cade, B. S. (2006). The effect of multiple stressors on salt marsh end-of-season biomass. *Estuaries and Coasts*, *29*(2), 328–339.

Visser, J. M., Sasser, C. E., Chabreck, R. H., & Linscombe, R. G. (1998). Marsh vegetation types of the Mississippi River deltaic plain. *Estuaries*, *21*(4B), 818–828.

Visser, J. M., Sasser, C. E., Chabreck, R. H., & Linscombe, R. G. (2002). The impact of a severe drought on the vegetation of a subtropical estuary. *Estuaries*, *25*(6,), 1184–1195.

Visser, J. M., Sasser, C. E., Linscombe, R. G., & Chabreck, R. H. (2000). Marsh vegetation types of the Chenier Plain, Louisiana, USA. *Estuaries and Coasts*, *23*(3), 318–327.

Visser, J., & Sandy, E. (2009). The effects of flooding on four common Louisiana marsh plants. *Gulf of Mexico Science*, *27*(1), 21–29.

Voss, C. M., Christian, R. R., & Morris, J. T. (2013). Marsh macrophyte responses to inundation anticipate impacts of sea-level rise and indicate ongoing drowning of North Carolina marshes. *Marine Biology*, *160*(1), 181–194.

Watson, E. B., Wigand, C., Davey, E. W., Andrews, H. M., Bishop, J., & Raposa, K. B. (2017). Wetland loss patterns and inundation-productivity relationships prognosticate widespread salt marsh loss for southern New England. *Estuaries and Coasts*, *40*(3), 662–681.

Watson, E. B., Wigand, C., Oczkowski, A. J., Sundberg, K., Vendettuoli, D., Jayaraman, S., Saliba, K., & Morris, J. T. (2015). *Ulva* additions alter soil biogeochemistry and negatively impact *Spartina alterniflora* growth. *Marine Ecology Progress Series*, *532*, 59–72.

White, D.A. (1993). Vascular plant community development on mudflats in the Mississippi River delta, Louisiana, USA. *Aquatic Botany*, 45(2-3), 171-194.

Wigand, C., Sundberg, K., Hanson, A., Davey, E., Johnson, R., Watson, E., & Morris, J. (2016). Varying inundation regimes differentially affect natural and sand-amended marsh sediments. *PLOS ONE*, *11*(10), e0164956.

Willis, J. M., & Hester, M. W. (2004). Interactive effects of salinity, flooding, and soil type on Panicum hemitomon. *Wetlands*, *24*(1), 43–50.

Xu, H. (2006). Modification of normalised difference water index (NDWI) to enhance open water features in remotely sensed imagery. *International Journal of Remote Sensing*, *27*(14), 3025–3033.

APPENDIX A: CRMS ANALYSIS (ACTIVITY 1)

1. INTRODUCTION

Existing CRMS data was evaluated in Activity 1 to test the 2017 ICM collapse thresholds (Table 2) by evaluating wetland vegetation occurrence that included assessing 1) change in vegetation cover (% total cover) if environmental data (e.g., salinity, water level) showed that collapse thresholds were exceeded for marshes, 2) the extent and frequency of wetland collapse, 3) occurrence of forested wetlands experiencing the collapse threshold, and 4) water depth limitation for vegetation occurrence. The main results are summarized in the report and details about the data analyses are discussed below.

2. CHANGE IN VEGETATION COVER

The CRMS vegetation data collection which includes observations of total % cover and species-level cover from ten 2 m x 2 m vegetation stations within the CRMS site (defined here as the 200 m x 200 m data collection area) began in 2006 with most sites reporting by 2007 (Figure A1, Folse et al. 2018).
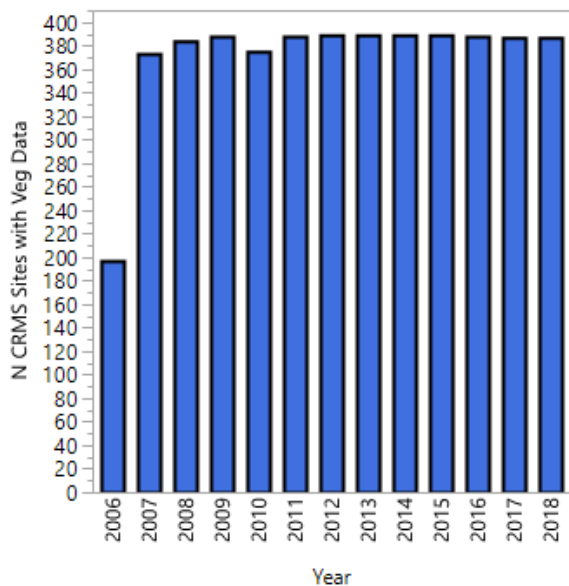
Figure A1. The number of CRMS sites per year from 2006 through 2018 that had vegetation data collected.

For each 2 m x 2 m vegetation station, the % total cover change was assessed relative to a five-year moving window beginning with 2007-2011 and continuing through 2014-2018. In each five-year window, the difference between % total cover at year five (e.g., Y5) and % total cover in every other year was calculated (e.g., Y5-Y4; Y5-Y3; Y5-Y2; Y5-Y1) along with the percent difference in % total cover over the interval.

A threshold for change in % total cover that represented vegetation collapse had to be defined. A coarse collapse threshold of 50% change in % total cover within a five-year window was initially proposed. Data were examined and a more precise definition was extracted from the distribution of change at stations (Figure A2). Stations that had experienced change > -2 standard deviations from the mean (-46.2%) were considered to collapse. 3,002 instances (out of 100,687) met the 46.2% change definition representing wetland collapse from 943 stations at 254 CRMS sites (Figure A2). Those 3,002 instances were explored further to determine whether the conditions previously predicted to cause wetland collapse (excessive flooding and salinity) were associated with the change in % total vegetation cover.
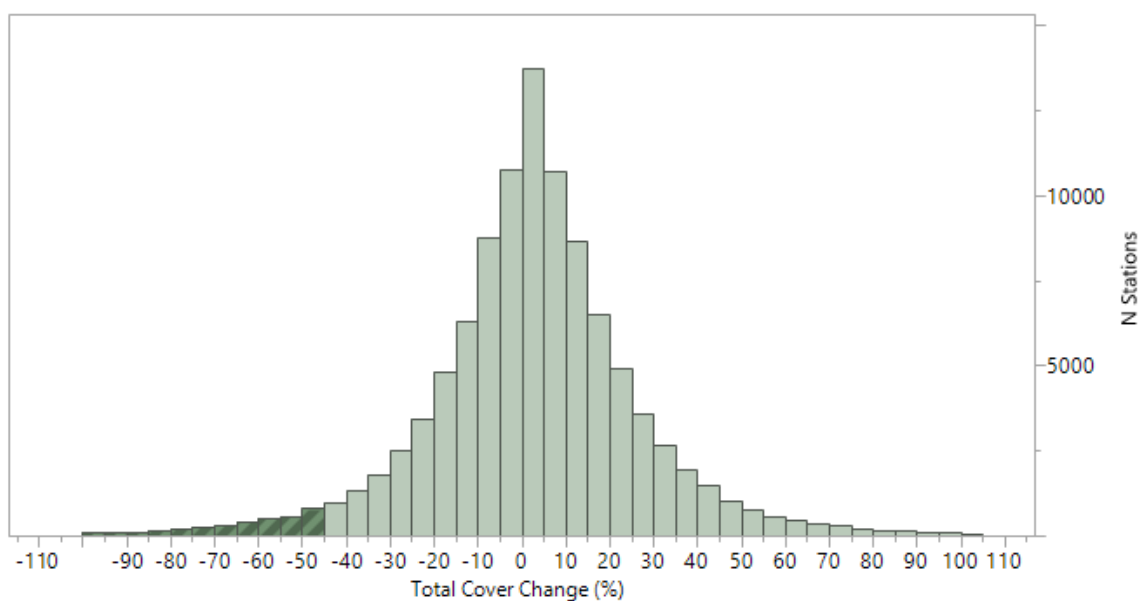
MEAN	0.09
STD DEV	23.13
STD ERR MEAN	0.07
UPPER 95% MEAN	0.23
LOWER 95% MEAN	-0.05
N	100687

Figure A2. The distribution of change in % total cover from stations at CRMS sites (top) and the related statistics (bottom).

Permanent vegetation loss (where total cover approached 0% and remained near 0% (< 5%) through 2018) did occur at 83 stations from 49 different sites (Figure A3). However, many of the sites that produced this result were known to be actively eroding into adjacent water bodies. The process in that case is not wetland collapse due to flooding or salt stress but rather physical removal of marsh soils and vegetation. That these stations are eroding can be verified by examining elevation change and accretion data which reveals an acceleration in elevation gain and very high accretion rates as the berm that is created on the edge of the eroding marsh moves through the site (Figure A4). Fifty-three stations from 22 sites were classified as converting to open water due to erosion while 30 stations from 19 sites were thought to be converting to open water due to some other process like flood or salt stress (Figure A5).
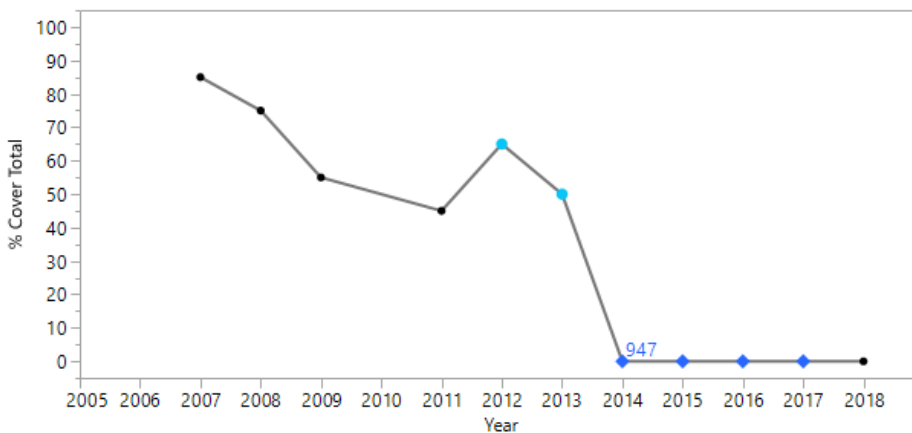
Plot for Station ID=CRMS0176-V23

Figure A3. Example of a CRMS Site (CRMS0176) that had a station (-V23) that experienced permanent vegetation loss.
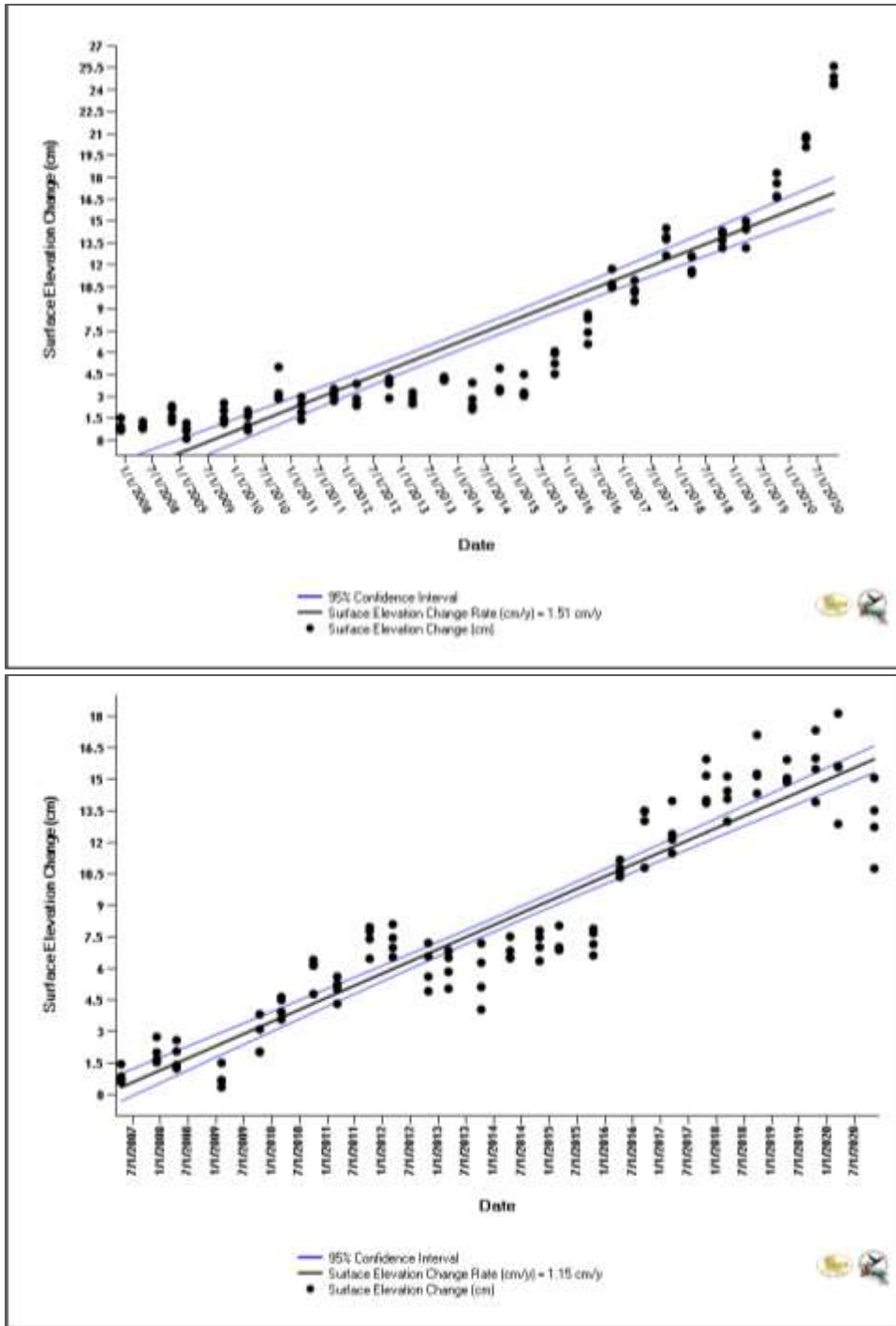
Figure A4. Examples of CRMS sites (CRMS0341 and 0178) that likely saw an acceleration in elevation gain and accretion associated with erosion into adjacent water bodies.
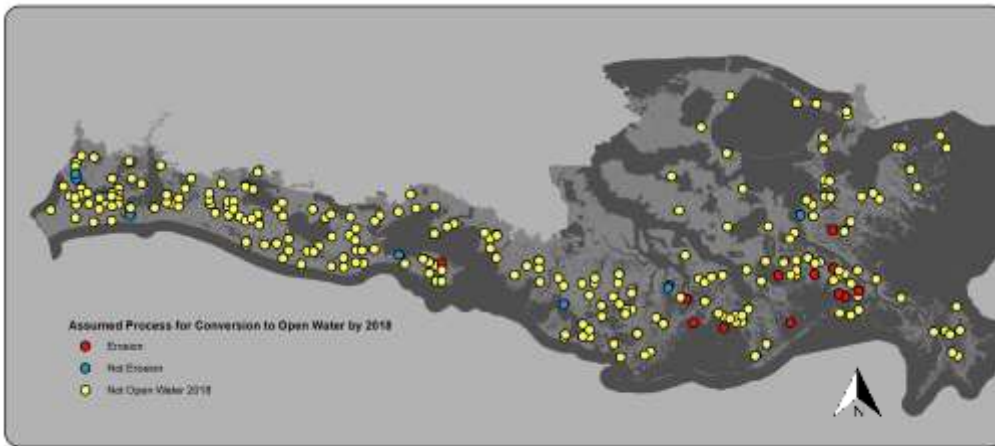
Figure A5. CRMS sites assessed for this exercise with an indication of whether permanent vegetation loss occurred prior to 2018 and which of those are thought to be due to erosion.

A small percentage of vegetation loss was permanent (9% stations including erosion; 3% stations excluding erosion). Based on CRMS vegetation surveys conducted during late summer each year, most sites that lost vegetation recovered prior to 2018; see examples from marsh habitat types in Figure A6. The sites that permanently lost vegetation and the sites that met the vegetation loss threshold but saw vegetation recover prior to 2018 were all assessed to determine whether the vegetation loss was precipitated by flood stress or salt stress as defined in 2017 ICM. The results are described in the next section.
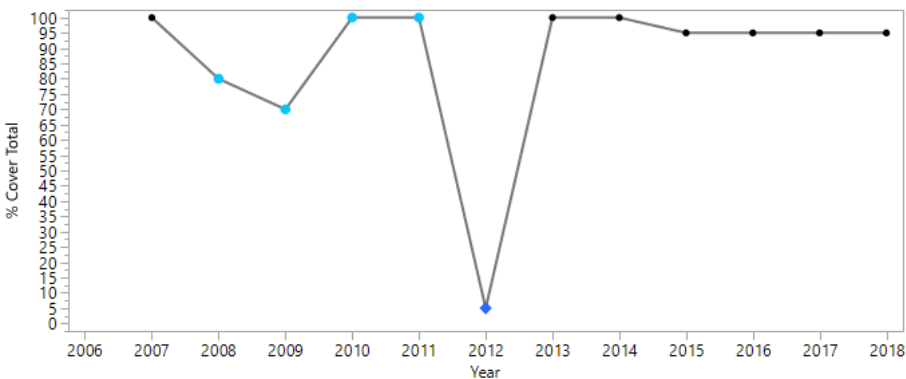
Plot for Station ID=CRMS0120-V26
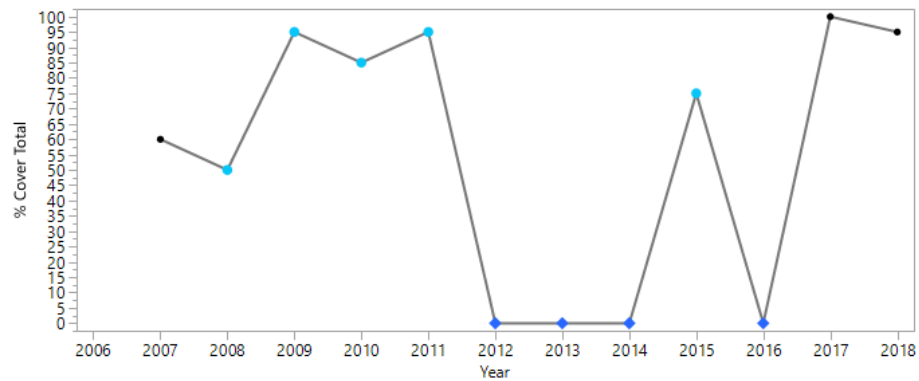
Plot for Station ID=CRMS0120-V81
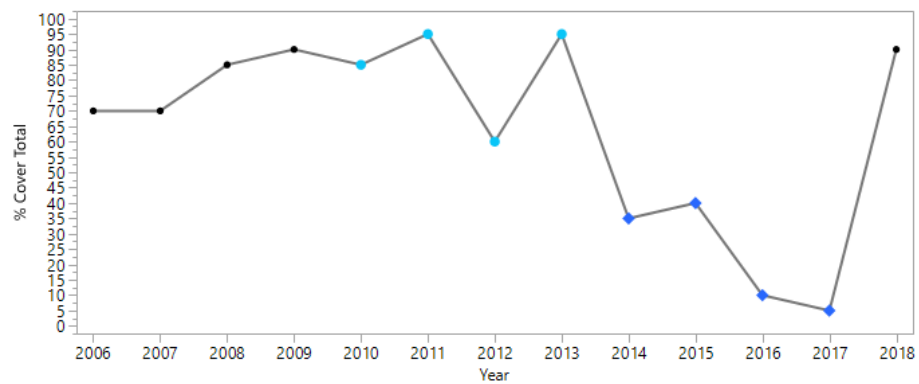
Plot for Station ID=CRMS0225-V28
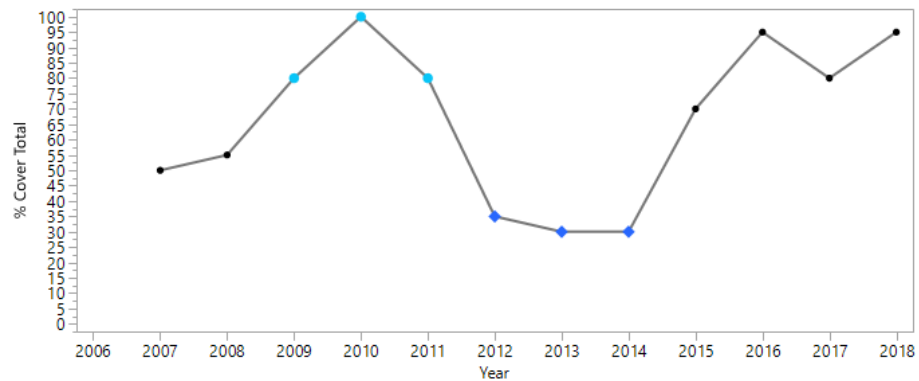
Plot for Station ID=CRMS1743-V01

Figure A6. Examples of CRMS sites from 2018 habitat types of fresh marsh (CRMS0120), intermediate marsh (CRMS0225), and brackish marsh (CRMS1743) with their respective stations (noted by -V##) that experienced a decrease and increase in % total cover over time.

3. EXTENT AND FREQUENCY OF WETLAND COLLAPSE

Hydrologic conditions assumed to cause wetland collapse in the 2017 ICM have been observed during the CRMS monitoring timeframe. Elevation data of each vegetation station is not measured with which flood depths at the station scale were calculated from the water elevation data available for each site. Salinity does not vary by vegetation station as one hydrology station represents the entire CRMS site.

Annual mean water depth > 0.36 m in intermediate marsh, > 0.26 m in brackish marsh, or > 0.24 m in saline marsh (Table 2) has been observed at 144/2426 stations (6%) from 17 sites. Maximum salinity thresholds of > 7 ppt in fresh marsh and > 5.5 ppt in swamps has been observed at 68 of 177 (38%) of fresh marsh sites and 6 of 59 (10%) of swamp sites (Figure A7). Therefore, some sites for multiple years did experience the environmental conditions that would trigger the 2017 ICM collapse thresholds.

Figure A7. Map of CRMS sites with the number of years in which the station exceeded inundation (top) and saline (bottom) thresholds from the 2017 ICM by habitat type (FIBS plus swamp).

Flooding above collapse thresholds did not necessarily cause vegetation collapse (Figure A8). Less than 5% of intermediate and brackish marsh sites that had vegetation loss also experienced flooding conditions above the 2017 ICM collapse thresholds. Saline marsh sites that lost vegetation crossed the flood stress threshold more frequently, but flood stress is not thought to be the major vegetation loss mechanism because erosion has been observed at those sites. Fresh marsh that exceeded the salinity threshold did elicit the predicted response in some cases (Figure A8). No swamp sites that experienced salinity above the threshold also lost canopy cover.
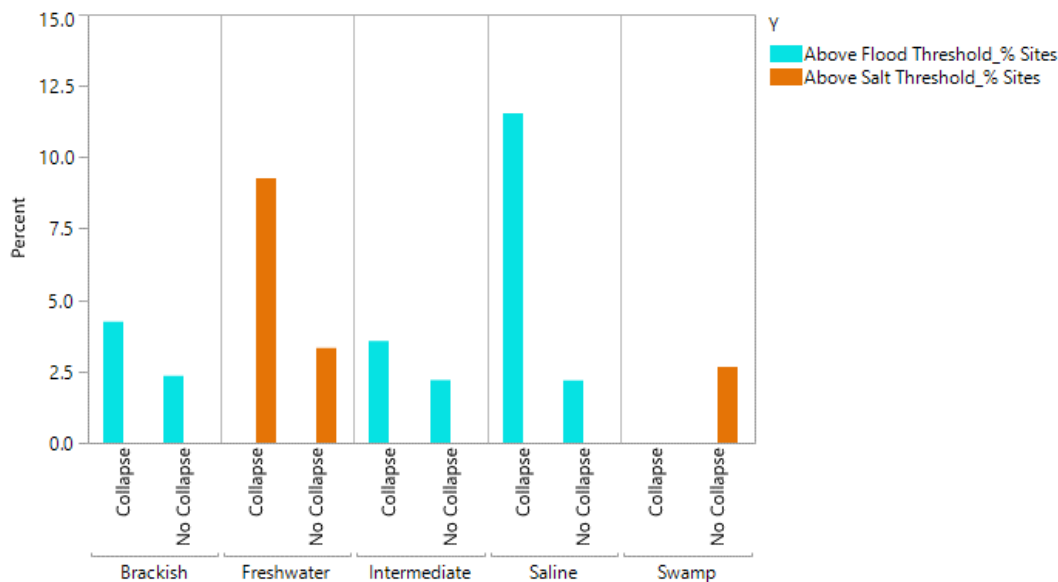
Figure A8. Collapse within Habitat Types. Percent of CRMS sites that experienced vegetation loss >46.2% in a five-year period that were above the flooding and salinity thresholds for wetland collapse as used in the 2017 ICM by habitat type.

By examining where on the coastal landscape there is vegetation loss and where there is elevated flood or salinity values, it becomes clear that they are probably not related (Figure A9). Most of the permanent vegetation loss on the deltaic plain is associated with erosion. The permanent loss that is not necessarily erosion is related to hurricanes and herbivory. Increased salinity in freshwater marshes occurred repeatedly and caused temporary vegetation impacts. No permanent vegetation loss was associated with increased salinity in fresh marsh.
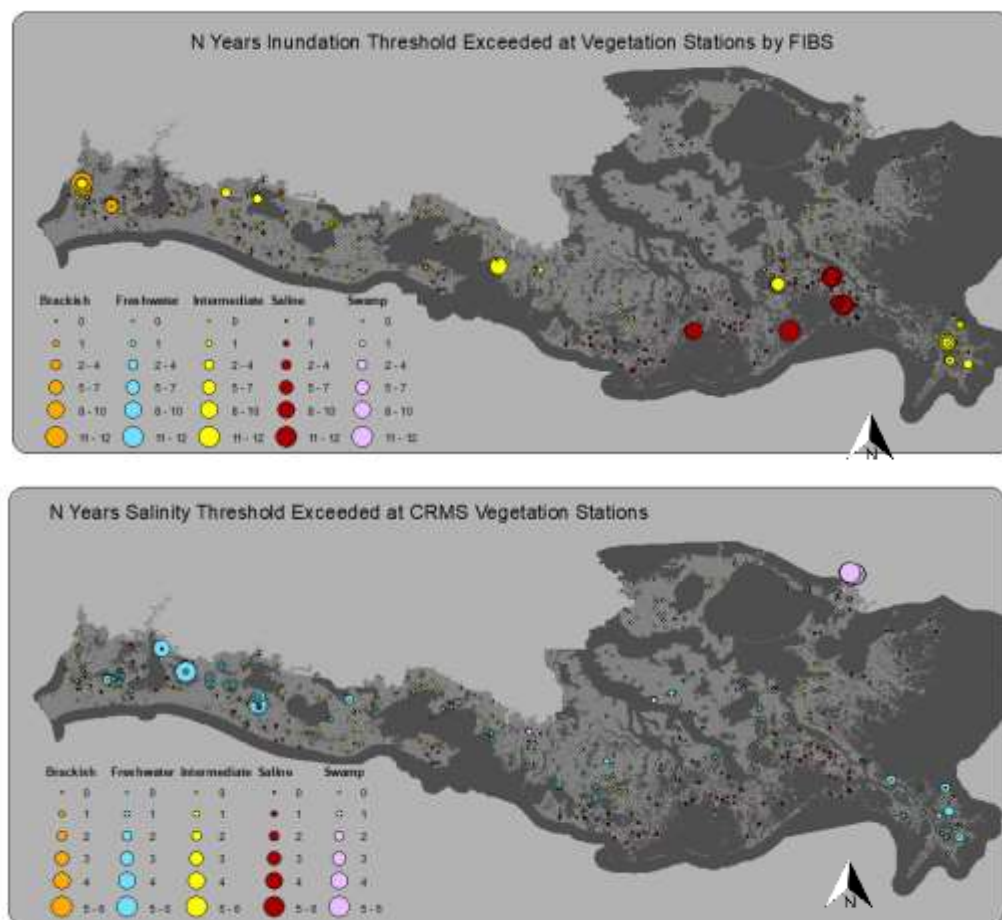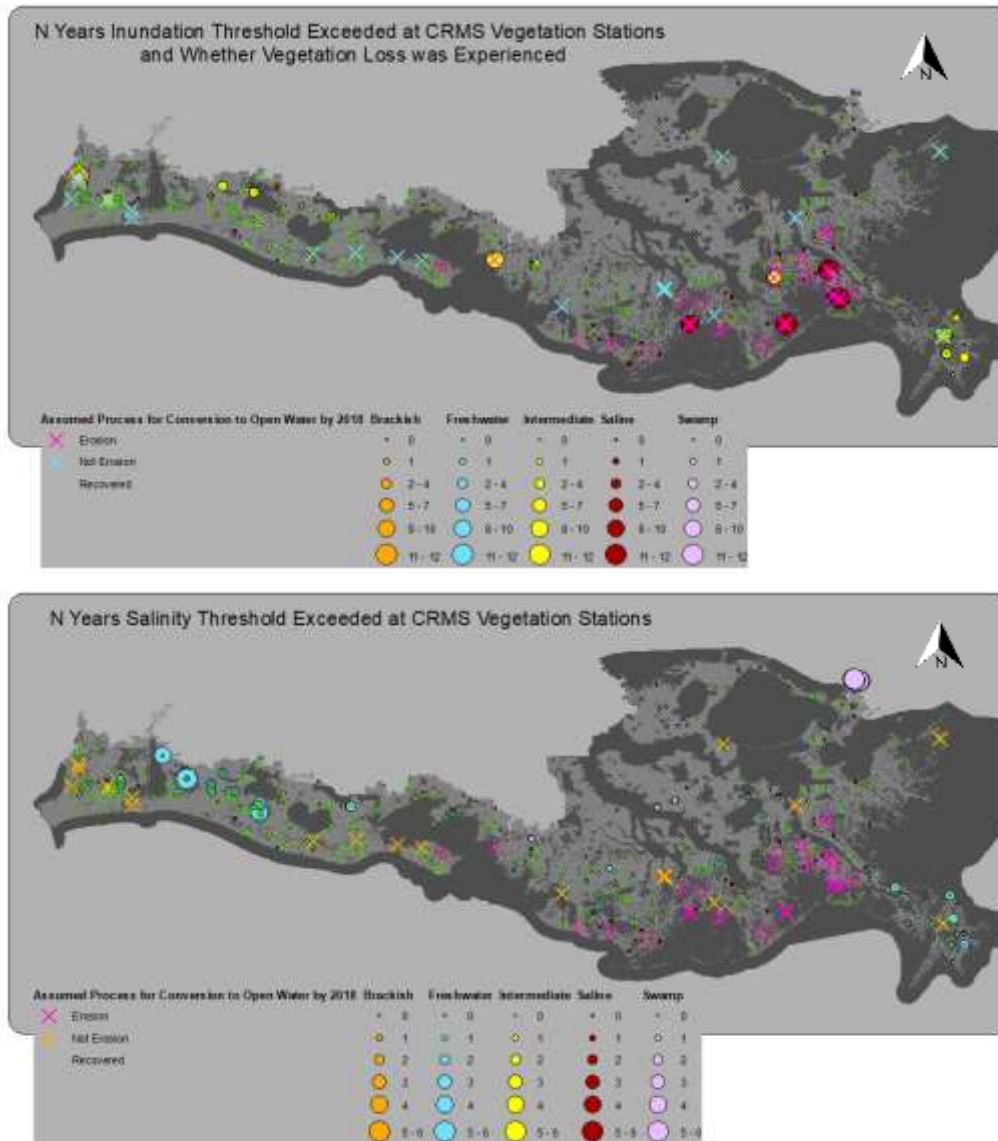
Figure A9. Map of CRMS sites with the number of years in which the station exceeded inundation (top) and salinity (bottom) thresholds from the 2017 ICM and where on the landscape permanent (X) and temporary (dot) vegetation loss was observed.

4. OCCURRENCE OF FORESTED WETLANDS EXPERIENCING COLLAPSE THRESHOLD

Canopy cover values in forested wetlands vary (Figure A10). Maurepas swamp sites and emerging Atchafalaya swamp sites have similar canopy cover values. Pontchartrain basin swamp sites have seen a loss of canopy cover while Atchafalaya and upper Barataria/Terrebonne swamp sites have seen an increase in cover. The observations of high salinity in swamps during the timeframe observed were all in the Pearl River swamp (Figure A9). Those sites have seen a decrease in canopy cover.
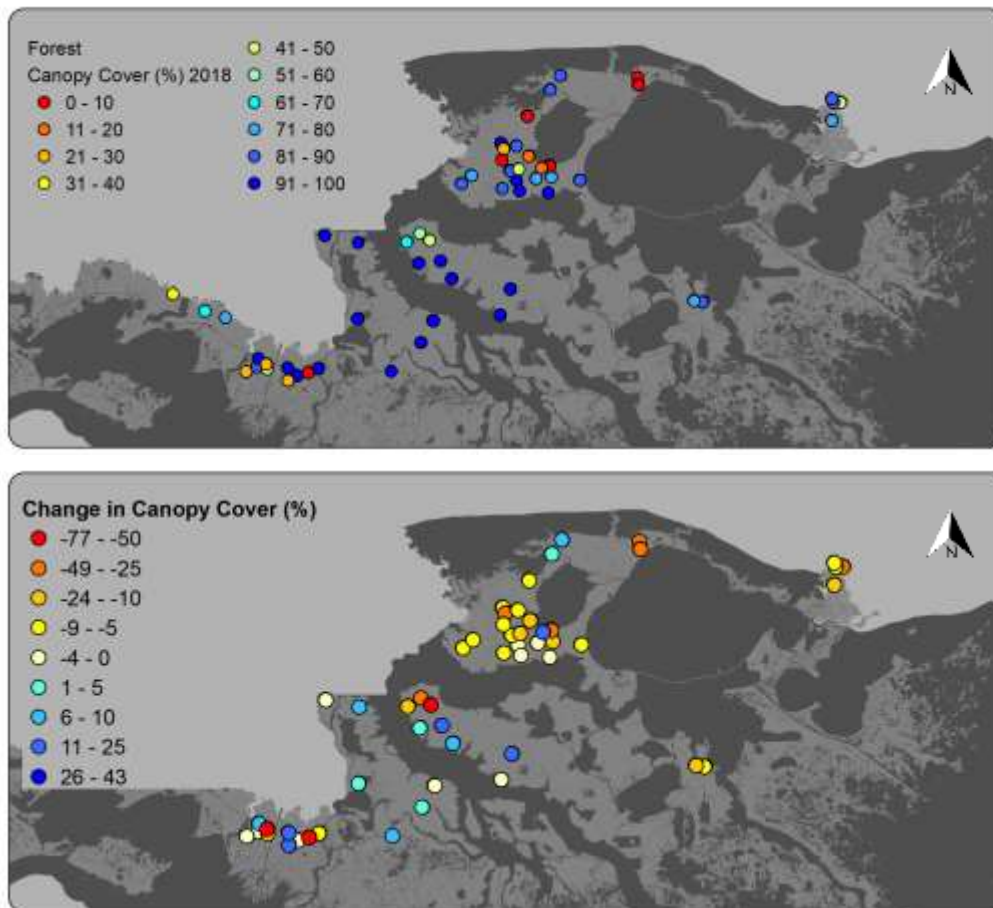
Figure A10. Canopy cover in 2018 at CRMS forested wetland sites (top) and change in canopy cover from 2007 to 2018 (bottom).

5. WATER DEPTH LIMIT FOR VEGETATION

The upper limit for vegetation occurrence can be defined as occurring at the upper bound of the 95th or 99th percentile confidence interval of the observed inundation depths, which varies as a function of the observed salinity at the same location over the same time frame. More specifically, this is the 97.5th and

99.5th quantile, respectively of the annual mean depth-salinity data pairs in CRMS from 2010 through 2017 and was calculated from a quantile regression analysis (Bolker, 2008) using the R statistical software (R Core Team, 2019). The 99.5th quantile of the data set was recommended as the water depth limitation which varies by salinity for vegetation occurrence.

The depth limit, *DL*, at a given salinity, S, is:

$$DL_S = \mu_{depth,S} + Z * \sigma_{depth,S} \qquad \text{Eq. A1}$$

where a quantile regression was used to determine the mean and standard deviation of inundation depths as a function of salinity, $\mu_{depth,S}$ and $\sigma_{depth,S}$, respectively. The upper bounds on the 95th and 99th percentile confidence intervals are calculated with Z = 1.96 and Z = 2.576, respectively.

$$\mu_{depth,S} = \beta_0 + \beta_1 * S \qquad \text{Eq. A2}$$

$$\sigma_{depth,S} = \beta_2 + \beta_3 e^{\beta_4 * S} \qquad \text{Eq. A3}$$

The coefficients determined from the quantile regression are:

β_0 = 0.0058

β_1 = -0.00207

β_2 = 0.0809

β_3 = 0.0892

β_4 = -0.19

The data tables and R code, and a readme document are available at https://github.com/CPRA-MP/ICM_LAVegMod/tree/master/inundation-salinity-quantiles.

Within ICM-Morph, the collapse algorithms can be updated to remove the collapse thresholds by habitat type previously used in the 2012 and 2017 master plans. The land change function in ICM-Morph can be updated to utilize raster datasets representing both annual mean salinity and annual mean inundation depth. For every raster pixel within the model domain classified as vegetated wetland, the annual mean salinity value can be used with Equations C1-C3 to calculate a pixel-specific annual mean inundation depth. This calculated value can be compared to the water depth limitation for vegetation survival (Figure 7), and if the output is greater than, or equal to, the water depth limitation for vegetation occurrence, the vegetated pixel can be converted directly to open water.

6. REFERENCES

Bolker, B., (2008). Ecological Models and Data In R. Princeton University Press.

R Core Team (2019). R: A language and environment for statistical computing. R Foundation for Statistical Computing, Vienna, Austria. URL https://www.R-project.org/.

APPENDIX B: FORESTED WETLANDS (ACTIVITY 1)

1. LITERATURE REVIEW

A literature review of published studies was examined for evidence of thresholds or collapse for forested wetlands to help inform the 2023 ICM.

Allen, Pezeshki, & Chambers, 1996		Key Points
System	Review	Baldcypress is highly susceptible to the combined stress of flooding and salinity
Species	Cypress	
Approach	Review	
Summary: Seedlings generally recover from the stress due to continuous shallow flooding, can grow rapidly as seedlings subjected to moist soil or periodic flooding. Pezeshki (1990) found no significant effects on height growth, net photosynthesis or stomatal conductance of bald cypress seedlings (60 days at 5 ppt). Detrimental effects combined flooding and salinity increase with increasing salinity. Davis et al. (1981) note that bald cypress is limited to salinity <2 ppt for more than 50% of the time that trees were flooded. But Myers et al. (1995) found seedlings planted in a frequently flooded marsh grew well for 1-4 years with groundwater salinity of 2.8 ppt.		

Conner, 1994		Key Points
System	South Carolina	Baldcypress seedlings died within two weeks of 10 ppt
Species	Cypress	
Approach	Lab experiment	
Summary: Bald cypress and Chinese tallow seeds raised for 4 months. July – October lab experiment. Treatments: flooded with 0 ppt (FO), watered with 0 ppt (WO), flooded with 2 ppt (F2), watered with 2 ppt water (W2), flooded with 10 ppt (F10), watered with 10 ppt water (W10), flooded with a simulated storm surge of 32 ppt (FS), watered with a simulated storm surge. F10 seedlings died within two weeks. Plants survived storm surge treatment (21 ppt- 2.5 ppt over 7 days).		

Conner, McLeod, & McCarron, 1997		Key Points
System	South Carolina	Differences in survival at 1 ppt could be related to age, size or seasonality of stress
Species	Cypress	
Approach	Lab experiment	

Summary: Seeds collected and raised for 4 months. Plants were flooded with 0, 2, and 10 ppt saltwater (F0, F2, and F10) and water level ~ 5 cm above soil surface. Watered plants were watered to saturation daily (W0, W2, W10). Almost all watered seedlings survived 12 weeks of treatment. All F0, F2, and FS seedlings survived. F10 caused mortality of all bald cypress, water tupelo, and green ash seedlings within two weeks. The difference in survival could be a response of seedling age, size (Allen et al., 1994), or response to the time of flooding (onset of dormancy prior to flooding).

Hackney, Avery, Leonard, Posey, & Alphin, 2007		Key Points
System	North Carolina	Cypress survived but with lower growth at soil salinity of 5 ppt
Species	Multiple	
Approach	Field data	

Summary: Salinity effect on wetland community structure at some stations. Even low level of salt, < 10% seawater led to major community change in tidal freshwater swamps if salt effect was chronic. Resulted in a shift in vegetation from woody tree species to herbaceous species. Process of community change begin at ~ 2 ppt. In the upper CFR estuary, bald cypress survived, with lower growth, even after soil salinity increased above 5 ppt.

Hoeppner, 2008		Key Points
System	Maurepas	Salinity stress associated with drought. Tree mortality associated with soil salinity (mean annual)
Species	Multiple	
Approach	Field data	

Summary: Spring 2000, 40 study plots (25 m x 25 m) along southern part of Lake Maurepas. Salinity data from two 0.75 m deep PVC wells -averaged for annual mean soil salinity at each plot. Soil salinity was highest at the Lake plots (2.16 ppt), and lowest at the Hope Canal plots (0.81 ppt). Salinity decreased from 2000 (drought) to 2003, slight increase in 2004. Interior areas had lower salinity levels than the Lake plots. – greatest during drought years. The two most saline plots had cumulative mortalities of 75% and 61%. Saltwater intrusion into soils, especially during 2000 drought, impacted *A. rubrum*, *N. aquatica,* and *F. pennsylvanica*. *N. aquatica*, *F. pennsylvanica*, and *A. rubrum* may be stressed/reduced growth at 2 to 3 ppt. Due to the negative correlation of salinity and flooding, the negative effect of salinity on aboveground biomass production could not be shown due to relationship of salinity and flooding (which also varied over time).

Keim, Dean, & Chambers, 2013		Key Points
System	Atchafalaya Basin	Differences in flooding did not influence mortality
Species	Cypress-tupelo	
Approach	Field data	
Summary: *Taxodium* (and to a lesser extent *Nyssa*) are very long-lived and can persist when hydrological regime changes and limits regeneration. Study in the Atchafalaya River Basin Floodway. Found that flooding stress does not alter density-dependent stand development in cypress-tupelo. Little evidence that flooding stress itself is responsible for competitive advantage of bald cypress - water tupelo is decreasing in importance as more susceptible to crown breakage in storms.		

Langston, Kaplan, & Putz, 2017		Key Points
System	Big Bend, FL	Complete turnover of species composition in 20 years
Species	Multiple	
Approach	Field data	
Summary: *Sabal palmetto* (cabbage palm) and *Juniperus virginiana* (southern red cedar). Tidal flooding frequency (TFF) based on weekly inundation (or not). Census trees in 2014, annually from 1992 to 1998, and in 2000 and 2005. Understory survey in the fall and winter of 2014/ 2015. TFF increased 1992 to 2014. Strong relationship between 2014 *S. palmetto* mortality and TFF. The 2014 survey showed continued forest decline of species richness, regeneration, and density with TFF. Between 1994 and 2014, distinct transitions forest understory to salt marsh shrubs to salt marsh along an increased tidal flooding gradient. Complete turnover in species composition on relict forest islands in 20 years.		

Middleton, 2016		Key Points
System	Delmarva peninsula	Higher mortality with higher salinities (>10 ppt - duration unclear). Differential sensitivity of species to salinity.
Species	Multiple	
Approach	Field data	
Summary: Damage to forested swamps by saltwater intrusion and/or wind and water surge - Hurricane Sandy on the Delmarva Peninsula (MD and DE). During Hurricane Sandy, elevated salinity for Oct.29-30, 2012 (Pocomoke City vs. Shelltown: max. 13.1 and 18.6 ppt,), dropped to pre-storm levels by Nov. 2, 2015 (0.08 ppt). Hickory site had higher % recently dead standing trees vs. other sites (7.9 ± 4.6% vs. 3.3 ± 1.9%). The % standing dead trees was higher in plots with higher soil salinity. Trees of species intolerant of salinity were killed e.g., *A. rubrum, A. laevis, Ilex* spp., and *T. distichum*. Order of tree susceptibility from most to least: *A. rubrum, Magnolia virginiana, Q. pagoda, L. styraciflua, T. distichum*, and *P. taeda*.		

Shaffer et al., 2009		Key Points
System	Maurepas	Mortality varied by species. Soil salinity highest in drought years
Species	Multiple	
Approach	Field data	

Summary: 20 study sites with paired 625-m^2 plots in the southern wetlands of Lake Maurepas- 3 different hydrological regimes (relict, degraded, and throughput). Abiotic - soil salinity, light penetration, pH, bulk density, redox potential (Eh), sulfide, nitrate, ammonia, and phosphate concentrations. Used spectral signatures of stations to extrapolate areally over the Manchac– Maurepas. Based on salinity - throughput and degraded different, distinction between relict swamp and either throughput or degraded swamp was less clear. Highest soil salinities during drought of 1999–2000 (max 4-5 ppt) followed by 2006 (~3 ppt)- also drought. Over 7 years, nearly 20% of the original 1860 trees in study plots suffered mortality, Mortality highest for midstory species (mostly swamp red maple and green and pumpkin ash). Tree primary production higher at sites with higher bulk densities and lower salinities.

Thomas, Doyle, & Krauss, 2015		Key Points
System	South Carolina and Georgia	Growth negatively related the salinity, 1- 3 ppt.
Species	Cypress	
Approach	Field data	

Summary: Investigated the climate and growth relations of *T. distichum* influenced by flooding and salinity along two coastal rivers. Tree ring analysis used to relate growth rate and pattern to climate history, salinity exposure, hydroperiod, and anthropogenic perturbations. Correlations between site chronologies and early growing season (April–July) PDSI, precipitation, and temperature. Salinity correlated with mean monthly low tide and mean annual river discharge. Tree growth at Savannah Middle showed a negative correlation with river salinity while tree growth at Waccamaw Middle did not (due to higher salinity Savannah Middle 0.83 ppt). Both lower sites experience mean monthly salinity of >2 ppt. At both sites, very few living trees remain since 2004.

2. REFERENCES

Allen, J. A., Chambers, J. L., & McKinney, D. (1994). Intraspecific variation in the response of Taxodium distichum seedlings to salinity. Forest Ecology and Management, 70(1), 203–214.

Allen, J. A., Pezeshki, S. R., & Chambers, J. L. (1996). Interaction of flooding and salinity stress on baldcypress (Taxodium distichum). Tree Physiology, 16, 307–313.

Conner, W. H. (1994). The effect of salinity and waterlogging on growth and survival of baldcypress and Chinese tallow seedlings. Journal of Coastal Research, 10(4), 1045–1049.

Conner, W. H., McLeod, K. W., & McCarron, J. K. (1997). Flooding and salinity effects on growth and survival of four common forested wetland species. Wetlands Ecology and Management, 5, 99–109.

Davis, D., DeRouen, M., Roberts, D., & Wicker, K. (1981). Assessment of extent and impact of saltwater intrusion into the wetlands of Tangipahoa Parish, Louisiana. Coastal Environments, Inc.

Hackney, C. T., Avery, G. B., Leonard, L. A., Posey, M., & Alphin, T. (2007). Chapter 8 - Biological, Chemical, and Physical Characteristics of Tidal Freshwater Swamp Forests of the Lower Cape Fear River/Estuary, North Carolina, 39.

Hoeppner, S. S., Shaffer, G. P., & Perkins, T. E. (2008). Through droughts and hurricanes: Tree mortality, forest structure, and biomass production in a coastal swamp targeted for restoration in the Mississippi River Deltaic Plain. Forest Ecology and Management, 256, 937–948.

Keim, R. F., Dean, T. J., & Chambers, J. L. (2013). Flooding effects on stand development in cypress-tupelo. In: Guldin, James M., Ed. 2013. Proceedings of the 15th Biennial Southern Silvicultural Research Conference. e-Gen. Tech. Rep. SRS-GTR-175. Asheville, NC: U.S. Department of Agriculture, Forest Service, Southern Research Station. 431-437., 175, 431–437.

Langston, A. K., Kaplan, D. A., & Putz, F. E. (2017). A casualty of climate change? Loss of freshwater forest islands on Florida's Gulf Coast. Global Change Biology, 23(12), 5383–5397.

Middleton, B. A. (2016). Differences in impacts of Hurricane Sandy on freshwater swamps on the Delmarva Peninsula, Mid-Atlantic Coast, USA. Ecological Engineering, 87, 62–70.

Myers, R. S., Shaffer, G. P., & Llewellyn, D. W. (1995). Baldcypress (Taxodium distichum (L.) Rich.) restoration in southeast Louisiana: The relative effects of herbivory, flooding, competition, and macronutrients. Wetlands, 15(2), 141–148.

Pezeshki, S. R., Delaune, R. D., & Patrick, W. H. (1990). Flooding and saltwater intrusion: Potential effects on survival and productivity of wetland forests along the U.S. Gulf Coast. Forest Ecology and Management, 33–34, 287–301.

Shaffer, G. P., Wood, W. B., Hoeppner, S. S., Perkins, T. E., Zoller, J., & Kandalepas, D. (2009). Degradation of Baldcypress–Water Tupelo Swamp to Marsh and Open Water in Southeastern Louisiana, U.S.A.: An Irreversible Trajectory? Journal of Coastal Research, 152–165.

Thomas, B. L., Doyle, T., & Krauss, K. (2015). Annual Growth Patterns of Baldcypress (Taxodium distichum) Along Salinity Gradients. Wetlands, 35(4), 831–839.

APPENDIX C: TEST RUN G020 (ACTIVITY 1)

1. INTRODUCTION

A model test (G020) was undertaken to assess replacing the collapse thresholds used in previous coastal master plans with a depth limitation for vegetation occurrence which varies by salinity. The collapse thresholds were only removed for FIBS. No change was made for swamp and bareground, and all other aspects of 2017 ICM remain the same. The water depth limitation shown in Figure 3 was applied based on a single year of hydrology. The test run was compared to a future with coastal master plan projects run using the 2017 ICM output (G400).

There are several key differences between this proposed approach and the collapse threshold approach used in the 2017 ICM. While the curve applied imposes limiting depths similar to those previously used for intermediate, brackish, and saline marshes (Table 2), the 2017 ICM thresholds required exceedance for two consecutive years. In addition, previously fresh marshes were not subject to any depth limitation and were subject to a maximum two-week salinity in any year.

Prior to the model test runs, the effects were hypothesized:

- Trend of land loss over time will be smooth in ecoregions (except for project effects).
- Project effects which address salinity will be less pronounced.

2. TEST RESULTS

This examination of land-water patterns is based on comparison of G020 and G400 – the simulation that includes all the 2017 Coastal Master Plan projects. Two areas of the coast were explored – Mermentau and Breton Sound basins.

MERMENTAU

Figure C1 shows land loss at Year 40 for G400. The large area of loss in the Mermentau Basin has been diagnosed as the result of a sudden loss of fresh marsh occurring in a single year around year 33.

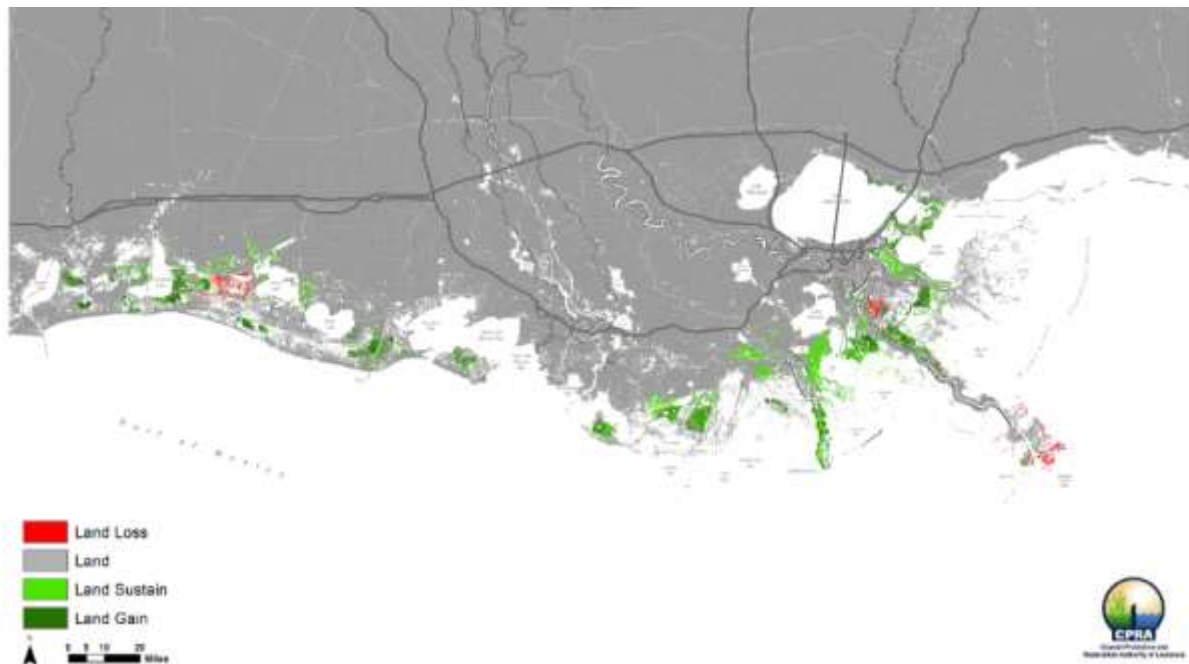Figure C1. Land loss map (vs. Future Without Action) for G400.

For G020 the difference map (vs. G400) shows gain in the area in Mermentau Basin (Figure C2). Thus, in G020 the mechanism that produced the loss in G400 has been removed.
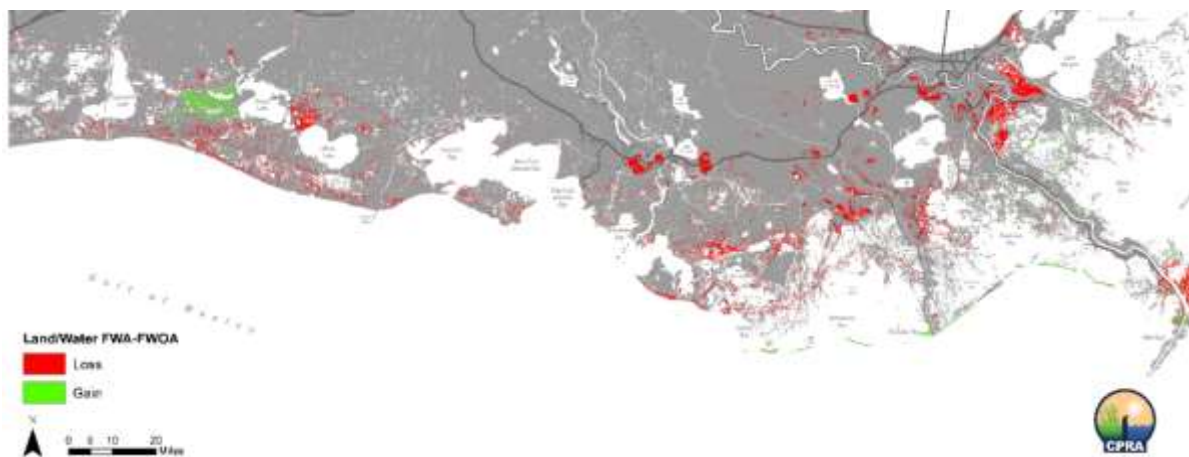

Figure C2. Comparison of G020 vs. G400 runs for year 40. Green indicates more land in G020 compared to G400. Red indicates G400 had land in an area which is not land in G020.

The plot of land change over time for G020 in the Mermentau/Lakes (MEL) ecoregion (Groves et al. 2017, Figure C3) shows no sudden change in land area in year 33. The offset between the land area curves is a result of alignment issues at the start of the simulation and is not considered a factor influencing the test of the depth limitation for vegetation occurrence. Figure C3 also shows greater land loss over time in MEL for G020. This is likely due to the loss of fresh marsh as a result of excessive flood depth – as fresh marshes would not have been subject to such loss in G400.
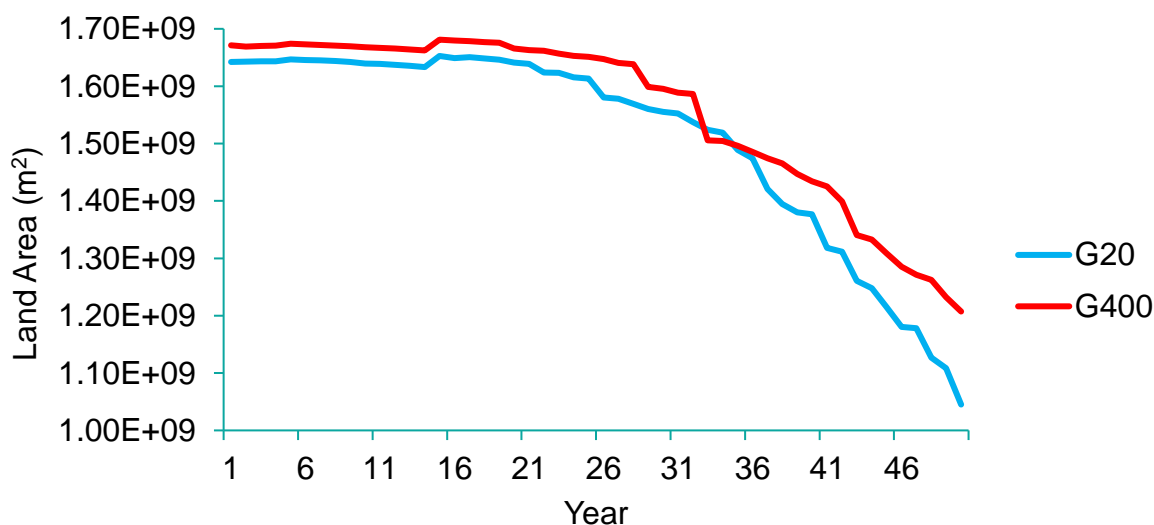
Figure C3. Land area over time for the Mermentau/Lakes ecoregion (MEL) for G020 and G400.

BRETON

Figure C2 also shows many areas where loss occurs in G020 but not in G400 (red areas) including large areas in Breton. The plot of land area over time for G020 for the Breton Sound ecoregion (BRT) shows greater land loss over the 50-year period for G020 (Figure C4). This is to be expected as much of the area is influenced by diversions in G400 leading to fresh marsh and also potentially high-water levels. The lines diverge over time starting at year seven, when the first diversion comes online, also supports this. G020 shows a sudden increase in land area in ~ year 15 probably associated with a marsh creation project. In G400, this increased land area appears to be sustained but is lost in G020.
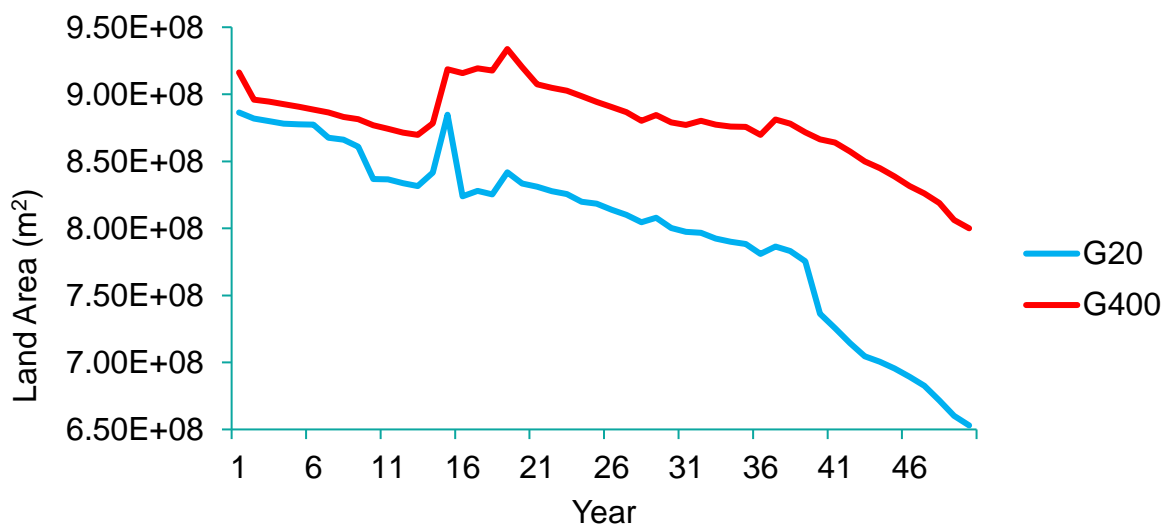
Figure C4. Land area over time for the Breton Sound ecoregion (BRT) for G020 and G400.

G020 also shows a sharp decrease in land area in ~Year 39. Inspection of the difference of G020-G400 land difference maps shows that much of the increased loss associated with G020 in the Central Wetlands occurs between year 35 and year 40. The vegetation map for year 35 (Figure C5) shows that much of the upper basin is fresh (presumably due to the influence of the diversions). This means that the G020 water depth limitation approach is causing loss in fresh marshes which are deeply flooded – an effect which did not occur in G400. Notably, many of the areas of additional loss in G020 in the year 40 difference map (Figure C2) also occur in areas of the coast which are likely to have been fresh at some point in the 40-year period. This effect was anticipated.
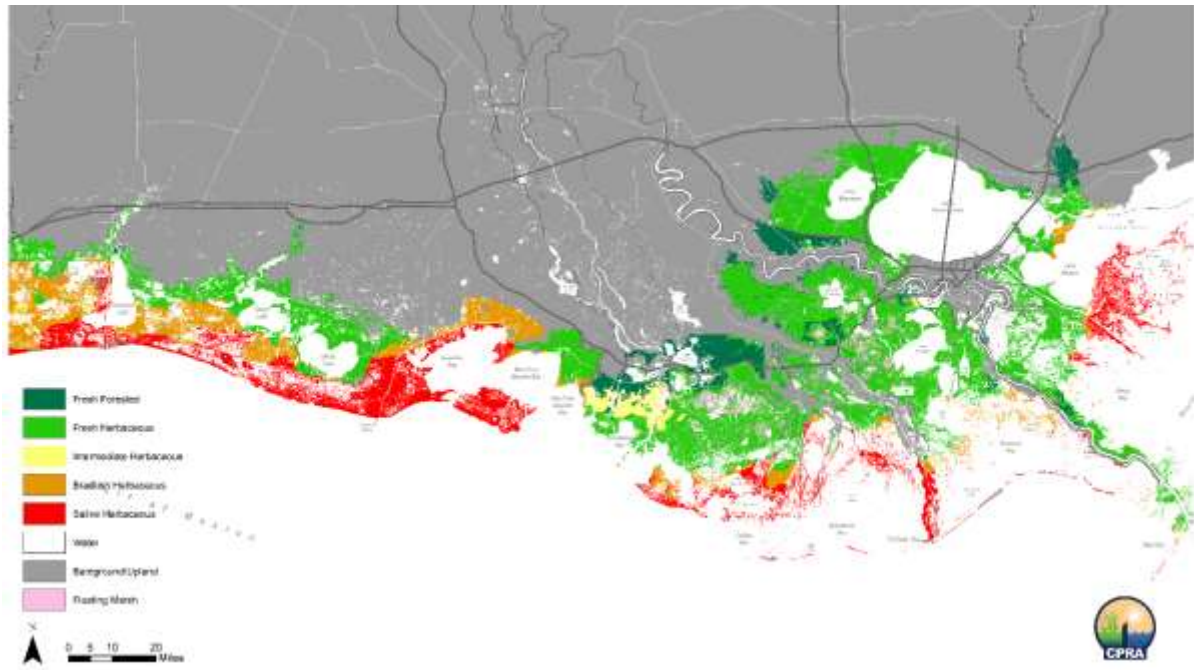
Figure C5. Vegetation cover for year 35 of G020 test run.

COASTWIDE

The year 50 land-water difference map (Figure C6) shows the net effect of the test over the complete 50-year run. Time series plots for the Eastern Chenier Ridges (ECR) ecoregion (Groves et al. 2017, Figure C3) indicate this loss occurs in the last decades (after year 26) of the simulation (Figure C7). This may be due to slight differences in the depth limitation imposed by the G020 approach compared to the fixed inundation depth for non-fresh marshes used in G400. These differences might be expected to be more manifest in the last decade of the simulation when the effects of sea level rise acceleration increase water depth more rapidly.
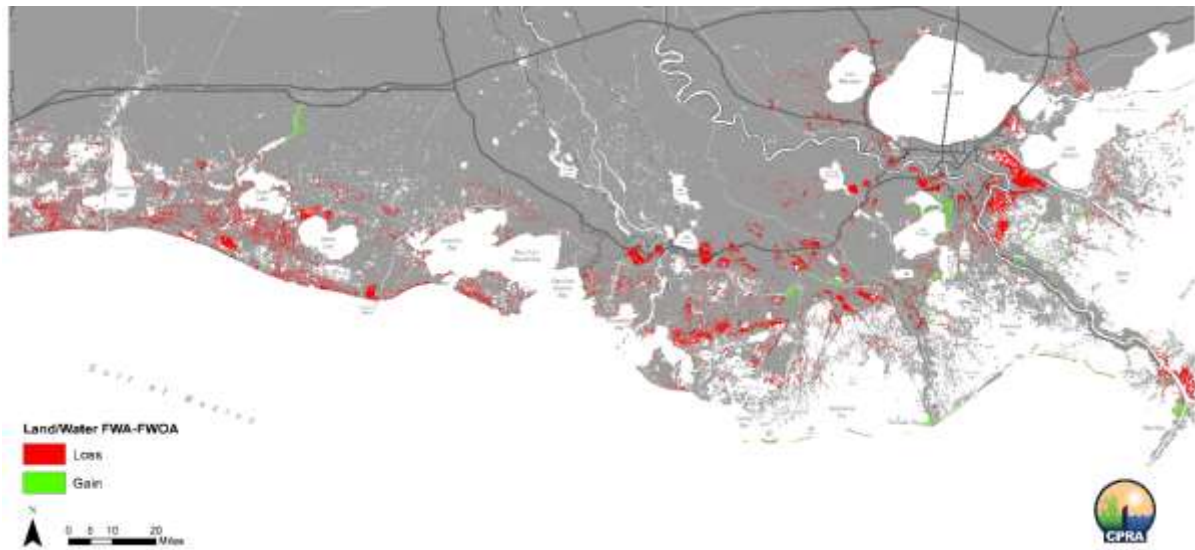
Figure C6. Land-water difference map for G020 vs. G400 at year 50.
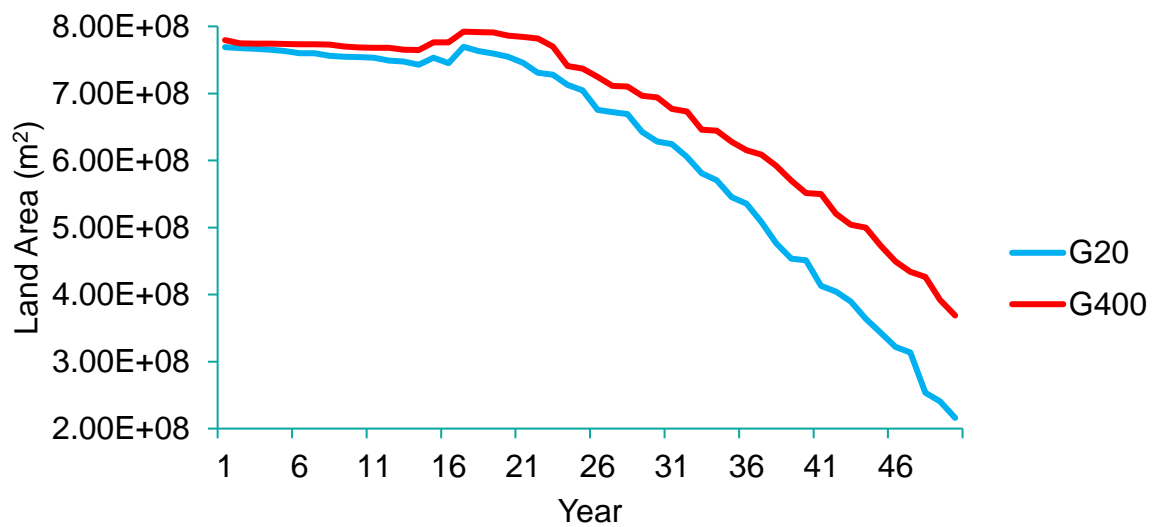
Figure C7. Land area over time for the Eastern Chenier Ridges ecoregion (ECR) for G020 and G400.

3. REFERENCES

Groves, D. G., Panis, T., & Sanchez, R. (2017). 2017 Coastal Master Plan: Appendix D: Planning Tool. Version Final. (p. 119). Baton Rouge, Louisiana: Coastal Protection and Restoration Authority.

APPENDIX D: TEST OF ELEVATIONS FOR VEGETATION ESTABLISHMENT (ACTIVITY 1)

1. INTRODUCTION

Two model tests (G021 and G022) were undertaken to explore the appropriate elevation relative to annual MWL at which vegetation can establish. Three runs were compared with different elevation thresholds:

- G021: Establishment elevation = MWL
- G022: Establishment elevation = MWL+10 cm
- G400: Establishment elevation = MWL+20 cm (base run reflecting the 2017 ICM approach)

In each run the elevation relative to MWL had to be met or exceeded for two consecutive years before the area becomes eligible for vegetation establishment. All other conditions in the 2017 ICM remain, so any new land resulting from the change in establishment elevation represents land that was lost due to the collapse thresholds used in the 2017 ICM.

The hypotheses included:

- Land gain in areas of active sediment deposition would be greater in G021 than in G022, and greater in G022 than in G400.
- Differences in new land gain will be spatially contiguous with existing land (i.e., deltas are growing as expected).
- No differences in areas without active subaqueous deposition (deltas and diversions).

2. RESULTS

LAND-WATER PATTERNS

Coastwide land change patterns at Year 25 for test runs G021 and G022 compared to the base run, G400, are shown in Figure D1. A closer look at land building in the Wax Lake Outlet for the same year and the same test runs is shown in Figure D2. There is a greater extent of new land relative to G400 from model test G021 than G022. For the most part the new land is contiguous with existing land, but there is some evidence of islands 'emerging' in open water and small irregular land areas. This may be a consequence of minor variations in the initial digital elevation map (DEM). There are also signs of interior ponds and some channels infilling. These effects seem to be greater in G021 than in G022 compared to the base run (G400).

Figure D1. Comparisons of land area at Year 25 for test runs G021 (top) and G022 (bottom) vs. the base run (G400). Green indicates more land in the test run than in the base run. Red indicates land in the base run in an area that is water in the test run. The Wax Lake area is circled in purple on both maps.

Figure D2. Zoomed in look at land area at Year 25 for test runs G021 (top) and G022 (bottom) vs. the base run, G400, for the Wax Lake area. Green indicates more land with the G021 than the G400. Red indicates the G400 model test run had land in an area which is not land in the test run. Refer to Figure D1 for scale.

Inspection of similar model results for areas further west in the Chenier Plain show minor variations in loss and gain with the test runs. These variations are thought to be due to variations in land-water mapping in early years of the simulation when the ICM is adjusting the initial conditions to be consistent with the ICM algorithms. These 'spin-up' patterns on the map are not relevant to the test of elevation for vegetation establishment and will be eliminated in the 2023 ICM simulations when this 'spin-up' will be conducted

prior to the start of the simulations. Patterns of loss/gain in interior wetlands occurring in later years of the simulation are likely be a consequence of slight adjustments in local hydrology due to the changing extent of land in the test run.

To the east, the test runs show similar patterns for Year 50 in terms of land gain in areas influenced by deltaic sedimentation (Figure D3). A closer look at land building along the Mississippi River for the same year and the same test runs is shown in Figure D4. For example, there is more land for both test runs near Fort St. Philip than in G400, and the effect may be slightly greater for G021. The model test G021 also shows more land gain by year 50 in the area of the Mid-Breton Sediment Diversion and in Barataria Basin, where some interior open water is shown to fill in (e.g., west of Bayou Perot).
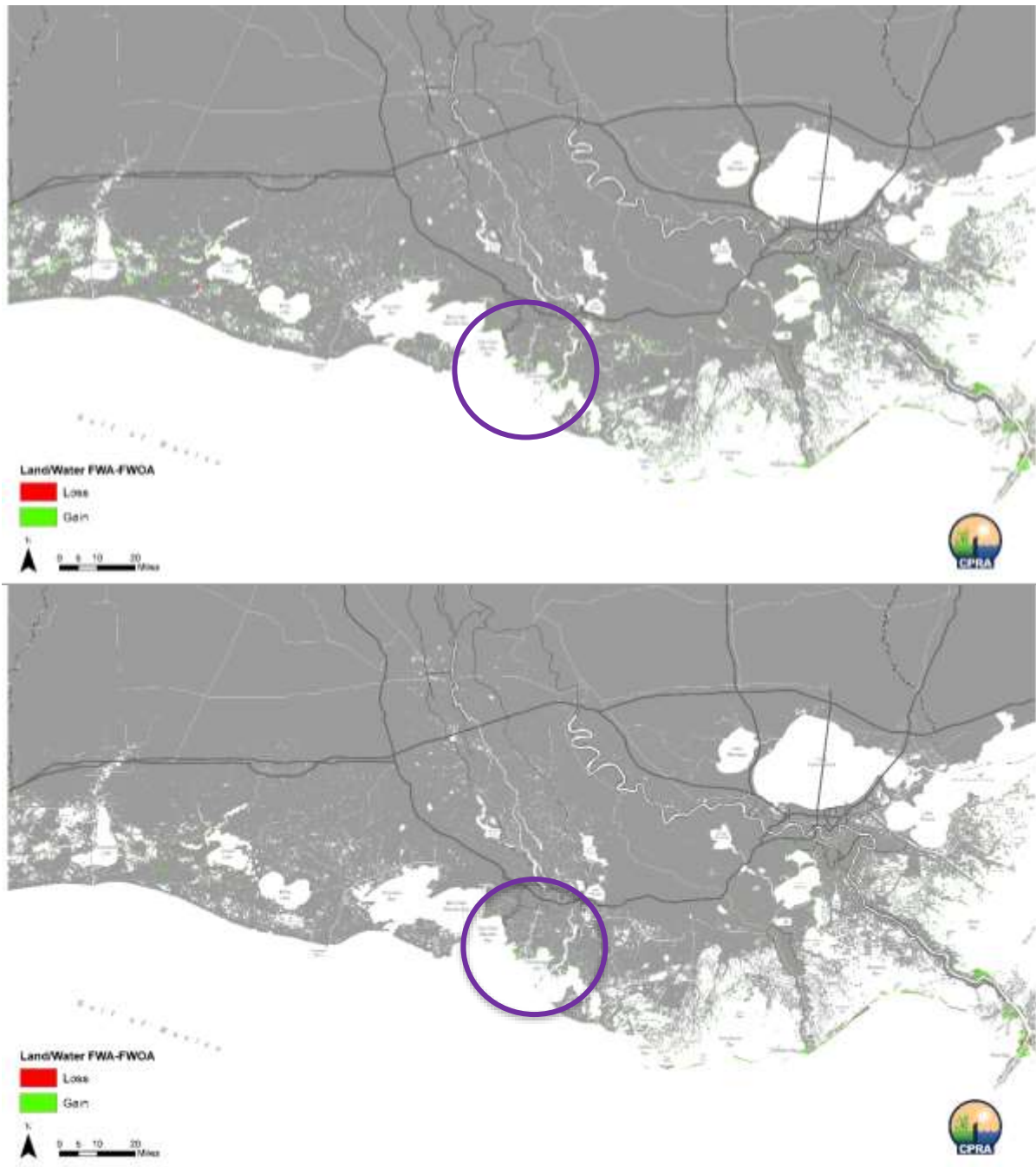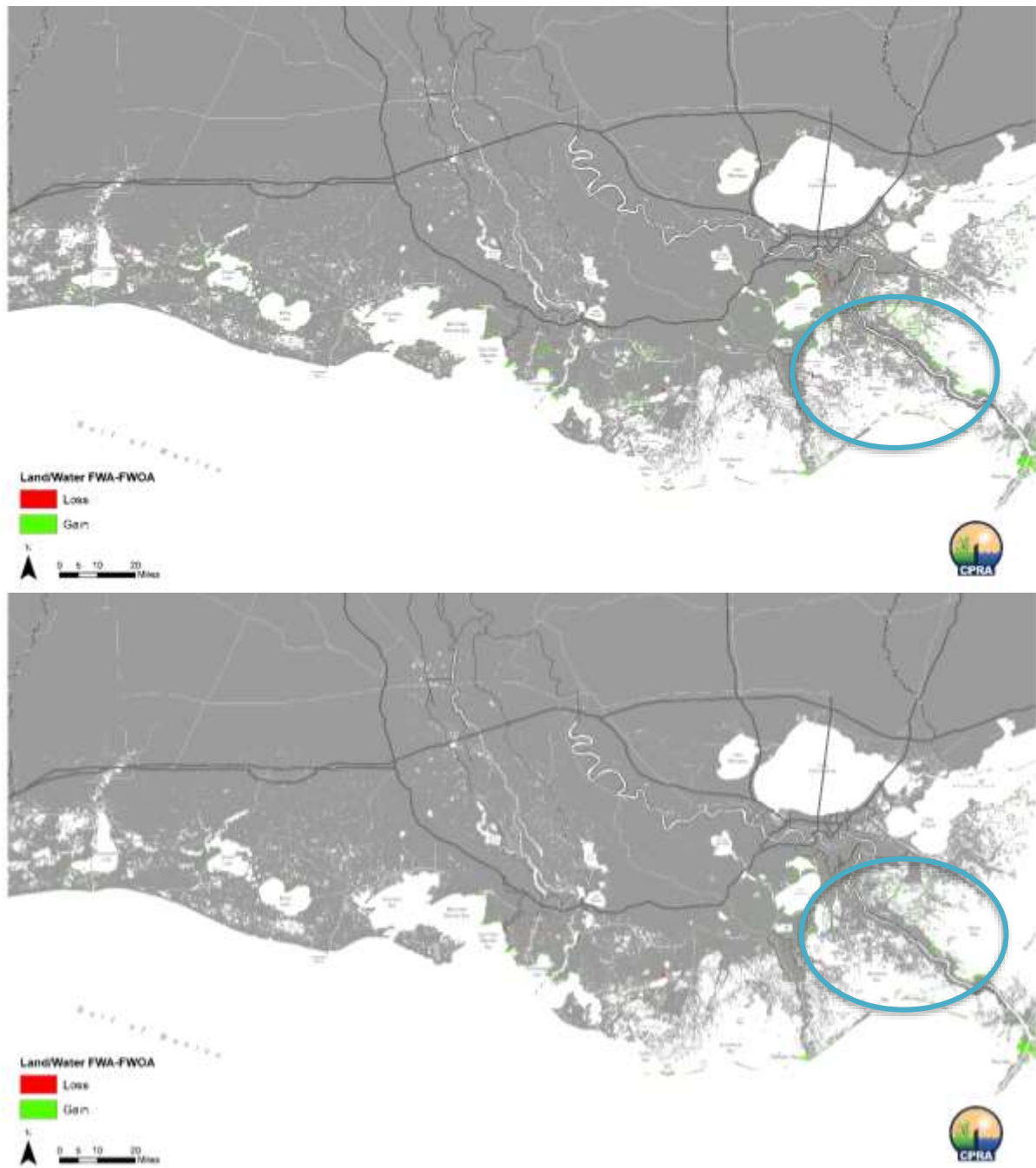
Figure D3. Comparisons of land area at Year 50 for test runs G021 (top) and G022 (bottom) vs. the base run (G400). Green indicates more land in the test run than in the base run. Red indicates land in the base run in an area that is water in the test run. The area is around the proposed locations for the mid-Breton and Mid-Barataria sediment diversions is circled in teal on both maps.
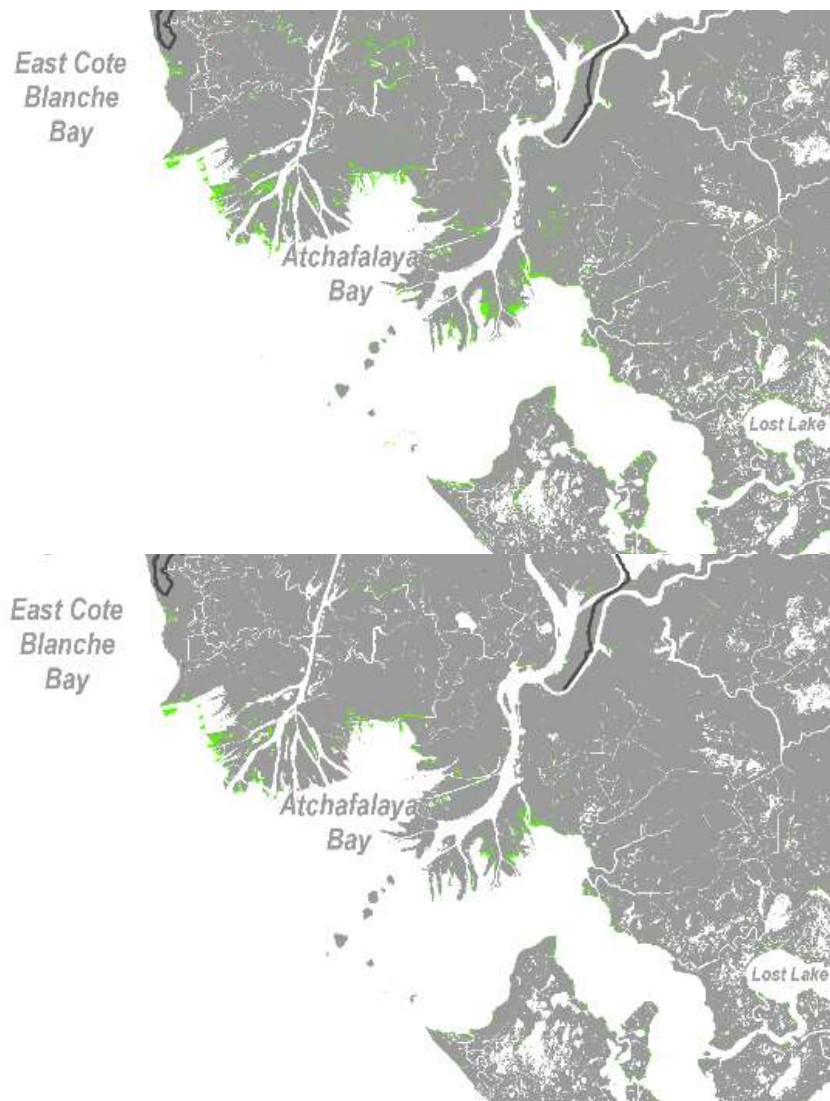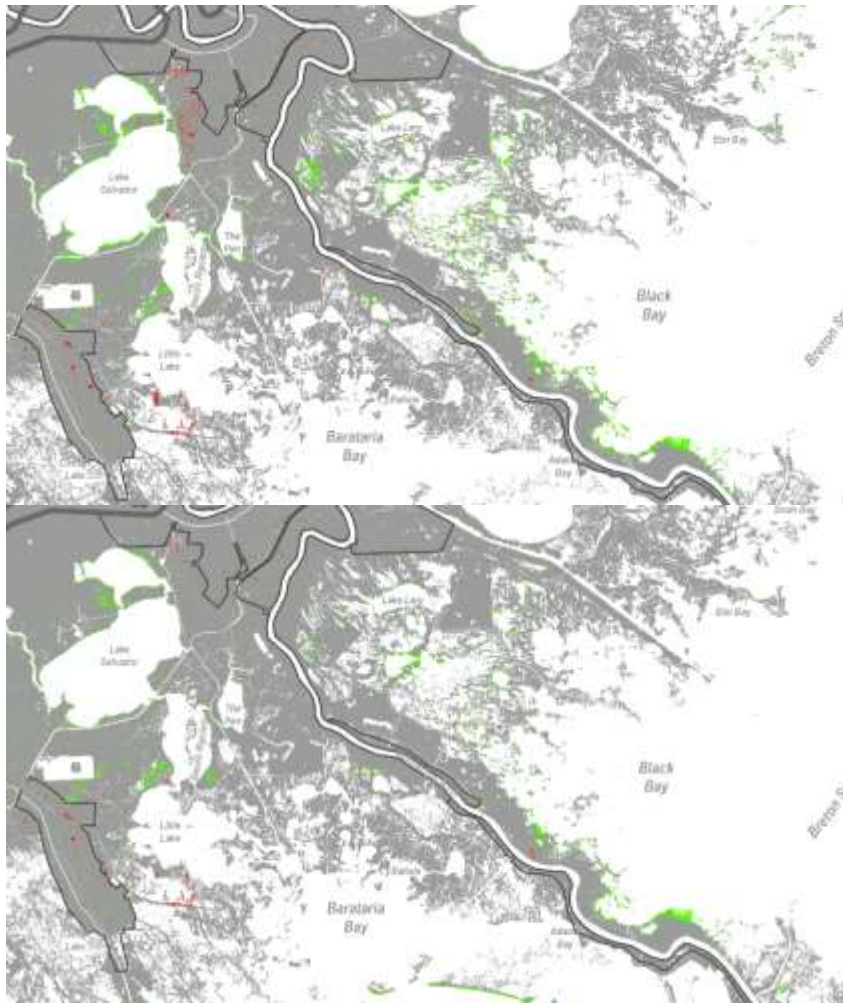
Figure D4. Zoomed in look at land area at Year 50 for test runs G01 (top) and G022 (bottom) vs. the base run, G400, for the area around the proposed locations for the Mid-Breton and Mid-Barataria sediment diversions. Green indicates more land with the G021 than the G400. Red indicates the G400 model test run had land in an area which is not land in the test run. Refer to Figure D3 for scale.

Areas of land gain around the margins of large water bodies (e.g., around the edge of Lake Salvador in Figure D4) are likely also associated with model spin-up and reconciliation of the initial land-water map with the initial DEM and ICM adjustments to both.

CHANGE OVER TIME

Plots of land area over time for all the 2017 ICM ecoregions (Groves et al., 2017) indicate that G021 has

the greatest land area, followed by G022 and then G400. However, the nature of the differences among the runs over time provides insight into the changes which are occurring with the test runs.

One of the hypotheses set forth in relation to the test was that areas of active sediment deposition would show greatest land for G021 followed by G022. Also, it was expected that the difference between test runs would increase over time, at least for the first few decades of the simulation where active sedimentation should outpace the effects of relative sea level rise.

Figure D5 shows land area over time for four ecoregions that include active deltas or the effects of sediment diversion operations. The Atchafalaya-Vermillion-Teche ecoregion (AVT) includes the Wax Lake Outlet and Atchafalaya Deltas. Over time, the model tests G022 and G400 separate (indicating that the effect is not simply a 'spin-up' issue). However, this is a large ecoregion and the differences among the runs are somewhat masked by other ancillary test run effects across the region. In the Upper Barataria ecoregion (UBA), the Breton Sound ecoregion (BRT), and the Bird's Foot Delta ecoregion (BFD), the three runs diverge over time for the first part of the simulation, suggesting that delta building is greater in model test runs G021 and G022 than in G400. In contrast, Figure D6 shows land area over time patterns for a few non-deltaic ecoregions, including Calcasieu/Sabine (CAS) and Mermentau/Lakes (MEL), for G021, G022, and G400. In these ecoregions, outputs from the test runs do not diverge over time from base run outputs.

The previous discussion of complex land loss/gain patterns attributed much of the difference to model spin-up issues and how changing the elevation for vegetation establishment interacted with adjustment of initial condition and land-water/DEM alignment. This effect would be expected to be manifest in the first few years of the simulation with little change in the following decades until different land loss processes begin to interact with the landscapes.

Figure D5. Land area over time for G021, G022, and the base run (G400) for ecoregions with active 'deltaic sedimentation' in the simulation (i.e., existing deltas and sediment diversions). AVT – Atchafalaya-Vermilion-Teche. UBA – Upper Barataria. BRT – Breton. BFD – Bird's Foot Delta.

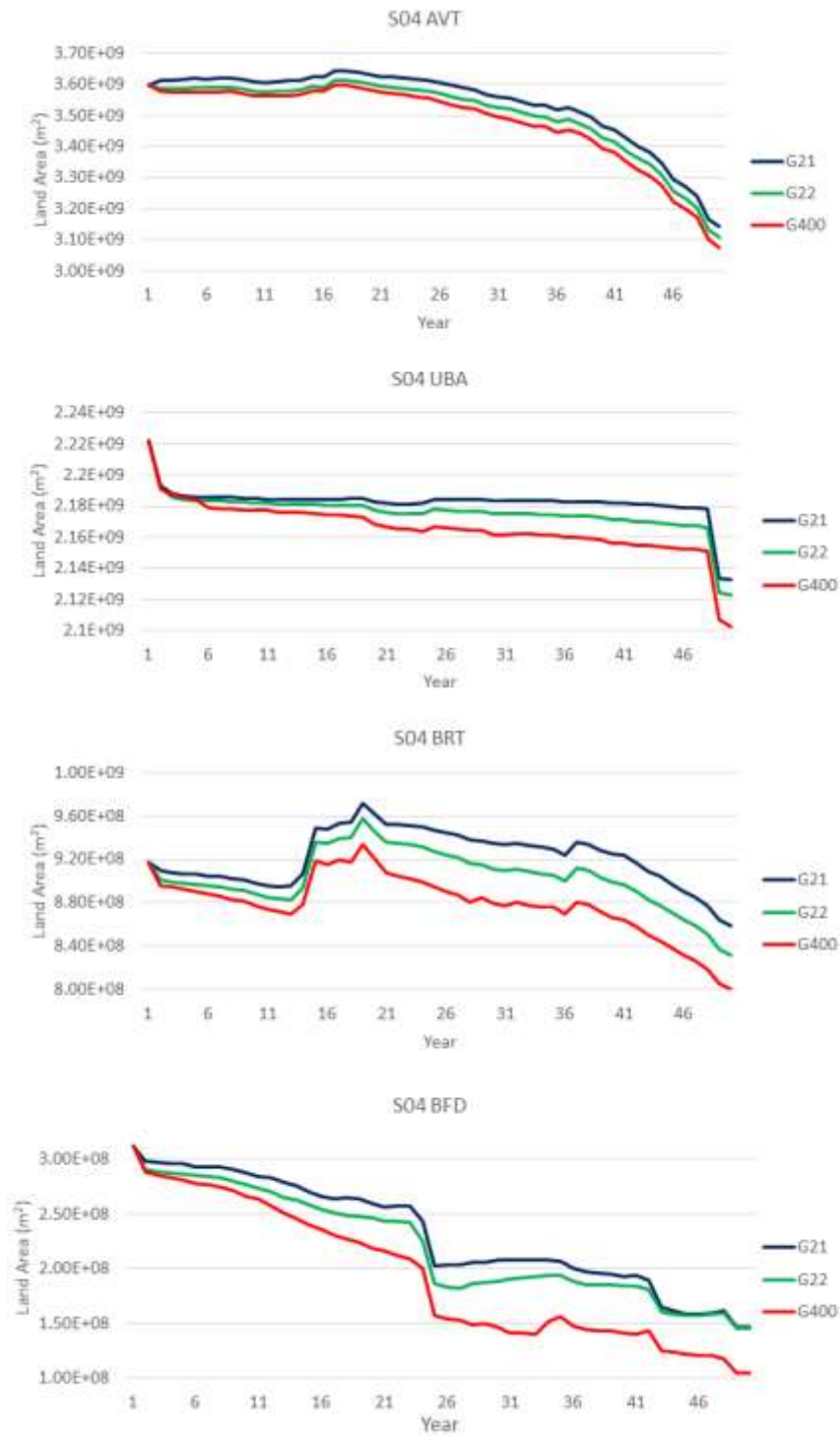Figure D6. Land area over time for G021, G022, and the base run (G400) for example ecoregions without active 'deltaic sedimentation'. CAS – Calcasieu/Sabine. MEL – Mermentau/Lakes.

3. REFERENCES

Groves, D. G., Panis, T., & Sanchez, R. (2017). *2017 Coastal Master Plan: Appendix D: Planning Tool*. Version Final. (p. 119). Baton Rouge, Louisiana: Coastal Protection and Restoration Authority.

APPENDIX E: ADJUSTMENTS TO ICM-MORPH (2017)

1. ADJUSTMENTS FROM THE WETLAND MORPHOLOGY MODEL (2012) TO ICM-MORPH (2017)

- Key citations: Couvillion and Beck, 2013; Brown et al., 2017a,b; White et al., 2017, 2019
- The 2012 Wetland Morphology model was integrated into the 2017 ICM as ICM-Morph. It was coupled with ICM-Hydro and ICM-LAVegMod at an annual time step in the 2017 ICM compared to a five-year time step for the 2012 models.
- Baseline data (elevation and land area) was updated from circa 2010 for the 2012 models to 2014 for the 2017 ICM.
- ICM-Morph traces elevation and land area change at 30 m x 30 m pixel resolution, increased from 500 m x 500 m pixel resolution in the 2012 Wetland Morphology Model.
- The upper limit of vertical accretion was assumed to be 2.26 cm yr^{-1} in the 2012 Wetland Morphology Model. In the 2017 ICM, the limit was 10 cm yr^{-1}.
- The collapse threshold approach uses 8-week growing season mean salinity in the 2012 Wetland Morphology Model rather than maximum of two-week mean salinity during a model year in ICM-Morph.
- Mineral sediment accumulation rates are provided by ICM-Hydro. Mineral sediment distribution and accumulation were calculated for three distinct zones (marsh edge, interior marsh, and open water) in the 2017 ICM compared to two zones (marsh and open water) in the 2012 models. Sediment accumulation is also calculated for sand, silt, and clay separately in the 2017 ICM.
- Mineral sediment in the 2012 Wetland Morphology model was redistributed within a compartment based on a sediment distribution probability surface, which was based upon the weighting of factors such as distance from sediment source, frequency of inundation, and distance from water bodies. In contrast, mineral sediment accumulation rates in ICM-Hydro were improved for the 2017 ICM with updated sediment distribution methodology incorporating sediment sources, sediment transport within the coastal area, sediment transfer to and from the marsh areas, and sedimentation processes within marsh areas.
- A constant 1,000 g m^{-2} yr^{-1} of sediment was assumed delivered to each hydrology compartment in the 2012 Wetland Morphology Model. In the 2017 ICM, sediment from tropical storms delivered from the offshore compartments to the marsh is re-

suspended from the bed due to higher wave energy, and the marsh is inundated due to higher water levels.

- A background change rate calculated from historical land change data for the 2012 models. In the 2017 ICM, spatially variable marsh erosion rates were calculated for all shorelines that experienced erosion during a 2004-2012 observation period by an updated algorithm in ICM-Morph.

- Q_{org} and BD were chosen for manipulation during the calibration of the accretion rates projected by ICM-Morph. Data related to these parameters were obtained for different combinations of hydrologic basins and vegetation types using soil data collected from CRMS and supplemented with Soil Survey Geographic Database (SSURGO) soil data where CRMS data were unavailable. The organic matter accumulation rates (OMAR), together with the mineral sediment accumulation rates and bulk density (BD) were used to estimate total vertical accretion (mm yr^{-1}) based on Couvillion et al. (2013).

- The underlying dataset used to derive the soil organic matter content and BD input data included mean values and standard deviations (SD) in ICM-Morph compared to mean values (also called "representative values") for the 2012 Wetlands Morphology Model. Mean and SD were calculated for each ecoregion and habitat type combination. For the ecoregion-habitat type groups in which data were unavailable, representative values were assigned from similar groups.

- Both BD and OMAR values were obtained for different ecoregion-habitat type groups through model calibration. Calibration of mean values for the 2017 ICM involved comparing modeled and observed vertical accretion from ^{137}Cs data (2006-2007) at 178 soil core locations across Louisiana coast. According to Brown et al. (2017b), if adjustments were needed during calibration for ICM-Morph in the 2017 ICM, BD and OMAR values were altered according to standard deviations from the mean of observed data. "For example, if modeled accretion values were, on average, lower than observed values, a new run was conducted with BD values 0.25 standard deviations lower than the mean. This process was repeated until values for BD and OMAR were obtained that resulted in an acceptable model performance" (Brown et al., 2017b).

- A background VAR of 2 mm yr^{-1} was also added to all accretion calculations of ICM-Morph to correct underestimation of observed VAR during calibration of BD and OMAR. It was found that mean BD and OMAR values for each ecoregion-habitat type group resulted in the best model performance.

2. REFERENCES

Brown, S., Couvillion, B. R, de Mutsert, K., Fischbach, J., Roberts, H., Rodrigue, M., Schindler, J., Thomson, G., Visser, J. M, & White, E. D (2017a). *2017 Coastal Master Plan: Appendix C:*

Modeling Chapter 3 - Modeling Components and Overview. Version Final. (p. 72). Baton Rouge, Louisiana: Coastal Protection and Restoration Authority.

Brown, S., Couvillion, B. R., Dong, Z., Meselhe, E., Visser, J. M., Wang, Y., & White, E. D. (2017b). *2017 Coastal Master Plan: Attachment C3-23: ICM Calibration, Validation, and Performance Assessment* (p. 95). Baton Rouge, LA: Coastal Protection and Restoration Authority.

Couvillion, B. R., & Beck, H. (2013). Marsh collapse thresholds for coastal Louisiana estimated using elevation and vegetation index data. *Journal of Coastal Research*, *63*, 58–67.

White, ED, E Meselhe, A McCorquodale, BR Couvillion, Z Dong, Scott Duke-Sylvester, and Y Wang. *2017 Coastal Master Plan: Attachment C3-22 – Integrated Compartment Model (ICM) Development* (p. 95). Baton Rouge, LA: Coastal Protection and Restoration Authority.

White, Eric D., Denise J. Reed, and Ehab A. Meselhe. (2019). Modeled sediment availability, deposition, and decadal land change in coastal Louisiana marshes under future relative sea level rise scenarios. *Wetlands*. https://doi.org/10.1007/s13157-019-01151-0.

APPENDIX F: IDEAL MIXING MODEL (ACTIVITY 2)

1. USING THE IDEAL MIXING MODEL TO BACK-CALCULATE VERTICAL ACCRETION RATES FROM MASS ACCUMULATION RATES

Once mineral and organic mass accumulation rates (MMAR, OMAR) are estimated, they will need to be converted to vertical accretion rates (VAR, cm yr^{-1}; see Figure 1). The ideal mixing model allows for the VAR (L T^{-1}) to be back-calculated from mineral and organic mass accumulation rates (M L^{-2} T^{-1}), based on Adams (1973) and recently applied to coastal wetland soils by Morris et al. (2016). In the 2012 and 2017 ICM, the MMAR and OMAR were additive, and once summed, this mass accumulation rate was divided by the bulk density (BD) to obtain an accretion rate.

An example is provided below to illustrate the application of the ideal mixing model and how it differs from the 2012 and 2017 ICM approach. Suppose an idealized site has a *LOI* value of 0.4 (idealized in the sense that it falls *exactly* on the mixing model curve). Suppose also that the site has a VAR of 0.5 cm yr^{-1}. The ideal mixing model indicates that it will have a corresponding bulk density value of 0.1796 g cm^{-3}. Taking the OMAR as BD × LOI × VAR, the value for OMAR is 0.0379 g cm^{-1} yr^{-1}. Similarly, MMAR is $BD \times (1 - LOI) \times VAR$, or 0.0569 g cm^{-1} yr^{-1}. The OMAR and MMAR can then be divided by their corresponding self-packing densities to obtain the mineral and organic components of vertical accretion (Table F1).

Table F1. Example of applying the ideal mixing model to derive vertical accretion rates from mass accumulation rates from an idealized site. Mass Accumulation Rate is divided by Self-Packing Density to calculate Vertical Accretion Rate (VAR) for soil components. The VAR of the soil components are summed for Total VAR.

Soil Component	Mass Accumulation Rate (g cm^{-2} yr^{-1})	Self- Packing Density (k_1 or k_2, g cm^{-3})	Vertical Accretion Rate (cm yr^{-1})
Organic	0.0379	0.0757	0.5007
Mineral	0.0569	2.1060	0.0270
Total	0.0948		0.5277

Notice that in the end the original total accretion rate was 0.5 (plus a rounding error). Also notice the volumetric leverage from organic accumulation can be calculated as VAR/OMAR, or 0.4745 cm yr^{-1} divided by 0.0359 g cm^{-2} yr^{-1}, giving a value of 13.21 cm^3 g^{-1} (this can also be calculated simply by taking the inverse of k_1). This volumetric leverage is similar to those obtained from soil coring studies

in northern Gulf of Mexico coastal wetlands where the VAR is regressed against OMAR, including 9.0 cm^3 g^{-1} from 18 cores collected across Breton Basin in 2008 (Snedden, 2021), 12.9 cm^3 g^{-1} in Terrebonne Basin (Nyman et al., 1993), 13.7 cm^3 g^{-1} in coastal LA (DeLaune et al., 1989), 8.0 cm^3 g^{-1} in coastal LA/TX (Turner et al., 2000), and 10.9 cm^3 g^{-1} in Barataria Basin (DeLaune et al., 2013).

2. EXAMPLE OF APPLYING THE IDEAL MIXING MODEL TO CRMS DATA

In reality, observed sites do not fit the curve exactly (r^2 for the ideal mixing model was 0.86). When a real site is used, CRMS0225 from the 2018 survey, with BD = 0.1561 g cm^{-3}, LOI = 0.3841, and vertical accretion = 1.11 cm yr^{-1}, the calculated VAR (Table F2) differs from the observed value by 0.1795 cm yr^{-1}, or about 20%. This error is due to the fact that the CRMS site does not fall exactly on the ideal mixing model curve.

Table F2. Example of applying the ideal mixing model to derive vertical accretion rates from mass accumulation rates from a CRMS site. Mass Accumulation Rate is divided by Self-Packing Density to calculate Vertical Accretion Rate (VAR) for soil components. The VAR of the soil components are summed for Total VAR.

Soil Component	Mass Accumulation Rate (g cm^{-2} yr^{-1})	Self- Packing Density (k_1 or k_2, g cm^{-3})	Vertical Accretion Rate (cm yr^{-1})
Organic	0.0666	0.0757	0.8798
Mineral	0.1067	2.1060	0.0507
Total	0.1733		0.9305

3. USING THE IDEAL MIXING MODEL TO ANTICIPATE ACCRETION RESPONSES TO PERTURBATIONS

In the examples above, a known accretion rate (from CRMS0225) was used to calculate mass accumulation rates. But the 2023 ICM will be obtaining mineral and organic mass accumulation rates from different subroutines of the model (mineral from ICM-Hydro and organic from ICM-LAVegMod), and those values will be used to estimate VAR. Under these circumstances, it is critical to have reliable values of k_1 and k_2. As an example, taking the values for mass accumulation rate at CRMS0225 (see Table F2), suppose a sediment diversion becomes operational and excessive inundation reduces organic matter accumulation but the diversion increases mineral matter accumulation. Those values would then need to be taken and translated into VAR to simulate the impact of the project on the receiving wetlands. In this example, the original OMAR (0.0666 g cm^{-2} yr^{-1}) is reduced 35% to 0.0433

g cm^{-2} yr^{-1}, and the original MMAR (0.1067 g cm^{-2} yr^{-1}) is increased tenfold to 1.0670 g cm^{-2} yr^{-1} (Table F3).

Table F3. Example of applying the ideal mixing model to derive vertical accretion rates from mass accumulation rates from a site with perturbations. Mass Accumulation Rate is divided by Self-Packing Density to calculate Vertical Accretion Rate (VAR) for soil components. The VAR of the soil components are summed for Total VAR.

Soil Component	Mass Accumulation Rate (g cm^{-2} yr^{-1})	Self- Packing Density (k$_1$ or k$_2$, g cm^{-3})	Vertical Accretion Rate (cm yr^{-1})
Organic	0.0433	0.0757	0.5720
Mineral	1.0670	2.1060	0.5067
Total	1.1103		1.0787

Under this hypothetical scenario, the model predicts a roughly 17% increase over the baseline VAR. The accretion component derived from organic matter accumulation would decrease, but that decrease would be offset by a coincident increase in mineral accumulation that resulted from increased sediment supply.

4. COMPARING IDEAL MIXING MODEL AND APPROACH OUTLINED IN CONCEPTUAL MODEL

Continuing the "sediment diversion into CRMS0225" example above, and applying the approach outlined in 2012 and 2017 ICM, whereby the TMAR is divided by BD to obtain the VAR, the new (post-sediment diversion) total mass accumulation rate of 1.1103 g cm^{-2} yr^{-1} is divided by the measured bulk density 0.1561 g cm^{-3}, giving 7.11 cm yr^{-1}. In reality, that bulk density would increase with the new mineral matter going in, decreasing the volume and accretion accordingly. Determining how *BD* would change is challenging; fortunately, the ideal mixing model gets around this issue (see Figure 10).

This new (post-sediment diversion) BD value from Equation 2 could be calculated as

$$BD = \frac{0.0433 + 1.067}{\frac{0.0433}{k_1} + \frac{1.067}{k_2}} \tag{F1}$$

which gives *BD* = 1.293 g cm^{-3} (compared to the measured pre-sediment diversion value of 0.1561 g cm^{-3}). Clearly in that example, *BD* would increase in response to the manipulation, and the ideal mixing model estimates the new value.

5. COMPARING OBSERVED VAR WITH VAR PREDICTED BY THE IDEAL MIXING MODEL AT CRMS SITES

The CRMS accretion data and the 2018 soil survey dataset were used to test the utility of the ideal mixing model approach. A depth-averaged value of soil properties matched the plot-set 1 (PS1) accretion values (accretion rates derived from the original feldspar marker horizons deployed from 2006 to 2009). The rates were assumed to be constant through time, not only during the measurement period, but also before (and after, in a few cases where the PS1 plots were abandoned). This assumption allowed for truncating soil property profiles to a depth of 24 cm that corresponded with the time of the PS1 marker horizon deployment as a coast-wide average to facilitate an expedient proof of concept analysis. A finalized analysis would include the matching of PS1 accretion depth and corresponding depth of soil properties on a site-by-site basis.

Using the CRMS data and assumptions described above, OMAR and MMAR were calculated from measured BD, LOI, and PS1 VARs. The OMAR and MMAR were then divided by k_1 and k_2, respectively, to provide modelled organic and mineral components of VAR, as well as TVAR (OMAR + MMAR). The modelled TVAR values were then regressed against the CRMS feldspar VARs (Figure F1).
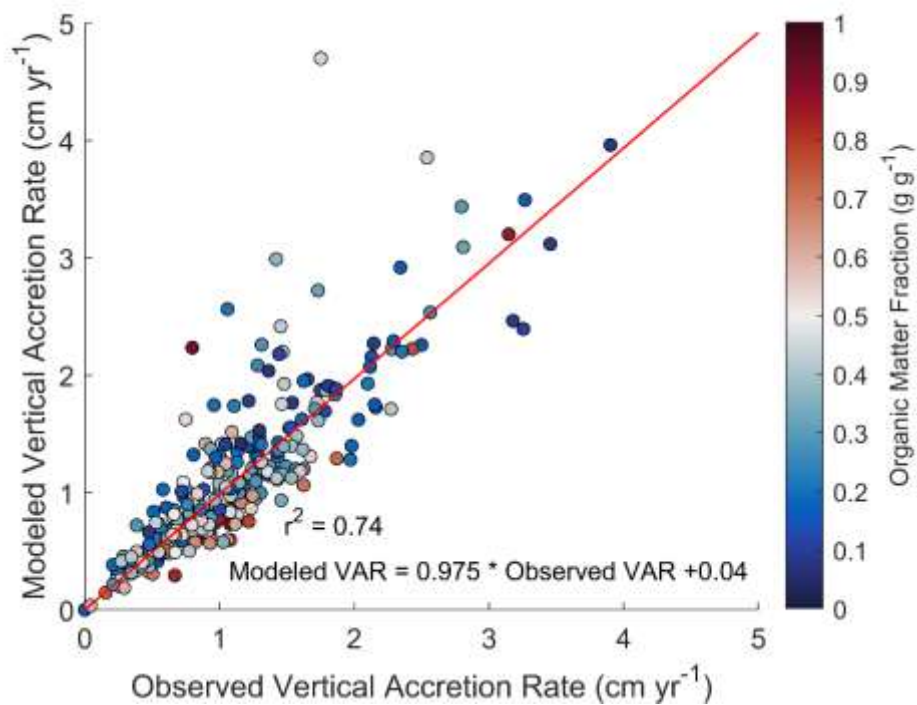
Figure F1. Modeled versus observed total vertical accretion rates from CRMS sites.

The dots are values used in the regression of modelled total VAR (left vertical axis) against the observed feldspar VAR (horizontal axis) (Figure F1). The color of the dot is an indication of the organic matter content (via loss on ignition) for the sample (color bar). The r^2 was 0.74, with a slope of 0.975, indicating that the model reliably predicts overall accretion, with a slight underestimate of around 2.5% (on average). There may be some explainable reasons for this underestimation such as compaction of soil properties, which would have the overall effect of increasing the density of the samples, and hence k_1 and k_2, thus decreasing the volumes/accretion rates.

The modeled accretion rates, along with the percent of modeled accretion that is mineral, were mapped across CRMS sites (Figure F2). The size of the dots indicates the accretion rate, and the color indicates the percent mineral accretion. High mineral accretion rates (dark-brown large circles) tend to be observed near river mouths.
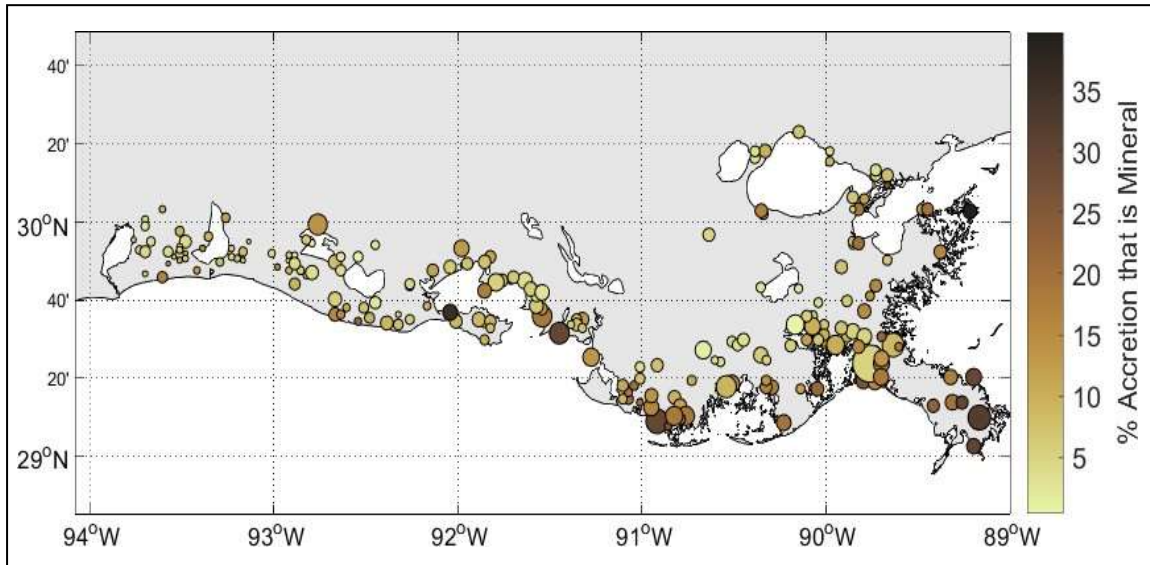

Figure F2. CRMS sites across the Louisiana coast with an estimate of the percent total vertical accretion that is derived from mineral sediment. Larger circles represent higher total vertical accretion rates.

6. REFERENCES

Adams, W. A. (1973). The Effect of Organic Matter on the Bulk and True Densities of Some Uncultivated Podzolic Soils. *Journal of Soil Science*, *24*(1), 10–17.

DeLaune, R. D., Kongchum, M., White, J. R., & Jugsujinda, A. (2013). Freshwater diversions as an ecosystem management tool for maintaining soil organic matter accretion in coastal marshes. *Catena*, *107*, 139–144.

DeLaune, R., Whitcomb, J. H., Patrick Jr., W. H., & Pezeshki, S. R. (1989). Accretion and canal impacts in a rapidly subsiding wetland, I. 137Cs and 210Pb techniques. *Estuaries*, *12*(4), 247–259.

Morris, J. T., Barber, D. C., Callaway, J. C., Chambers, R., Hagen, S. C., Hopkinson, C. S., Johnson, B. J., Megonigal, P., Neubauer, S. C., Troxler, T., & Wigand, C. (2016). Contributions of organic and inorganic matter to sediment volume and accretion in tidal wetlands at steady state. *Earth's Future*, *4*(4), 110–121.

Nyman, J., DeLaune, R., Roberts, H., & Patrick, W., Jr. (1993). Relationship between vegetation and soil formation in a rapidly submerging coastal marsh. *Marine Ecology Progress Series*, *96*, 269–279.

Turner, R. E., Swenson, E. M., & Milan, C. S. (2000). Organic and Inorganic Contributions to Vertical Accretion in Salt Marsh Sediments. In M. P. Weinstein & D. A. Kreeger (Eds.), *Concepts and Controversies in Tidal Marsh Ecology* (pp. 583–595). Springer Netherlands.

APPENDIX G: OMAR LOOK-UP TABLE TESTS (ACTIVITY 2)

1. TESTS OF LOOK-UP TABLES WITH OMAR AND OMAR-INUNDATION RESPONSE FUNCTIONS

Model tests (G027, G024, and G026) were conducted and compared to a run with the 2017 ICM (G400) that included all the projects included in the 2017 Coastal Master Plan to assess how the proposed approaches would influence ICM results. In the 2017 ICM, organic matter accretion is added to mineral matter accretion, which occurs in areas where wetlands are flooded. Organic matter and mineral matter accretion are added together in ICM-Morph, and together they impact the elevation of the marsh platform, inundation depth and thus land loss for non-fresh marshes (Table 2). Model tests included the following:

- **G027:** Test Approach 2 that utilized the OMAR look-up table based on 2014-2018 CRMS soil survey data and longer-term vertical accretion with the ideal mixing model by habitat type.
- **G024:** Test Approach 4 that used belowground production estimates that were adjusted to reflect inundation duration stress (e.g., % time flooded) to estimate OMAR by habitat type, after which the ideal mixing model was applied to translate mass accumulation rates to organic accretion.
- **G026**: Test feasibility of Approach 4 by assessing the characteristics of inundation duration conditions by habitat type.

Note that all runs were compared to G400, the future with action run from the 2017 ICM (i.e., with master plan projects in place), and all runs were conducted using the medium environmental scenario from 2017 (S04).

The following effects were hypothesized prior to the test runs, and then the results were examined for changes that included:

- **G027:** the total wetland area and elevation will be higher in G027 compared to G400 because the range of mean total VAR as inputs (0.9 to 1.4 cm yr^{-1}) was higher than the previous range of means for all basins used in the 2012 and 2017 ICM (0.3-1.6 cm yr^{-1}) (Steyer et al. 2012).
- **G024:** the total wetland area and elevation will likely be lower in G024 compared to G400 due to applying a response to inundation duration stress. Areas of wetland loss (red color) caused by inundation should be more apparent in G024 compared to

G400. Near the end of the simulation (year 40+) the acceleration of wetland loss and elevation loss will likely be evident in the time-series data and higher in G024 compared to G400 due to more rapid rises in eustatic sea level. The coastwide patterns of vegetation should not change much because it was assumed the accretion rates from G024 will not significantly alter the water-level variability that ICM-LAVegMod uses to establish vegetation.

- **G026**: the percent time flooded from the 2017 ICM output (G400) should have a similar distribution of % time flooded (e.g., most observations are near 60% of mean annual inundation) as observed in CRMS data for early years of the simulation. Later years should have higher % time flooded because of impacts of sea level rise and subsidence. A histogram of % time flooded for G400 could help inform where along the X axis of these plots (for an example see Figure 2) these marshes may fall.

2. GOVERNING EQUATIONS

G400 – 2017 ICM APPROACH:

$$VAR = \frac{Q_{sed} + Q_{org}}{BD} \tag{G1}$$

where VAR is vertical accretion rate, Q_{sed} (MMAR) is provided by ICM-Hydro, and Q_{org} (OMAR) is taken from a look-up table. Note that the original equations described for the 20192 and 2017 ICM used H to represent vertical accretion rate.

G024 – INUNDATION STRESS + IDEAL MIXING MODEL:

$$VAR = \frac{Q_{org}}{k_1} + \frac{Q_{sed}}{k_2} \tag{G2}$$

where Q_{org} = 0.089 and 0.107 g cm^{-2} yr-1 for fresh and swamp sites, respectively, and k_1 and k_2 are the self-packing densities of organic (0.076 g cm^{-3}) and mineral (2.106 g cm^{-3}) matter, respectively. For intermediate, brackish, and saline sites, Q_{org} is taken as

$$Q_{org} = 0.1 \times \left[Ae^{-\beta * flood}\right] \tag{G3}$$

where *A* is an intercept term taking a value of 0.8887, 6.371, and 1.772 g cm^{-2} yr^{-1} for intermediate, brackish, and saline sites, respectively; *β* is a decay coefficient taking a value of 0.01, 0.045, and 0.025 for intermediate, brackish, and saline sites, respectively; *flood* is % time flooded. The quantity

$Ae^{-\beta*flood}$ is the modeled belowground annual production, which is multiplied by 0.1 to retain only the refractory component of organic matter that contributes to long-term soil development (Figure 18). Q_{sed} (MMAR) is provided by ICM-Hydro.

G027 – OMAR FROM CRMS DATA BY HABITAT TYPE + IDEAL MIXING MODEL

The VAR is determined with Equation G2, with Q_{sed} (MMAR) provided by ICM-Hydro and Q_{org} values provided by a look-up table according to habitat type (Table G1).

Table G1. OMAR by habitat type applied for test run GO27.

Habitat Type	OMAR (or Q_{org}) g cm^{-2} yr^{-1}
Fresh	0.089
Intermediate	0.062
Brackish	0.063
Saline	0.093
Swamp	0.107

3. RESULTS

Test results (G0##) were compared to G400 and difference maps were made to determine how the approaches influenced the environmental conditions. For example, if there is a lower value in the new approach compared to G400 (G0## vs. G400) it will show up as a red color and if there is a higher value in the new approach compared to G400, it will be a green color.

Outputs that were available included:

- land/water difference map – every 5 years for 50 years
- elevation difference map – every 5 years for 50 years
- vegetation map – every 5 years for 50 years
- timeseries plots of land/water, elevation, and vegetation – for 50 years
- percent inundated – calculated hourly

The test runs are designed to evaluate changes in the wetland areas. Changes shown in the model outputs related to open water areas, e.g., increases or decreases in depth, reflect aspects of the model which were not modified in order that the tests could be expedited. These changes, as well as those shown in upland or forced drainage areas should be ignored.

G027: TEST APPROACH 2 THAT UTILIZES THE OMAR LOOK-UP TABLE OF CRMS DATA WITH THE IDEAL MIXING MODEL BY HABITAT TYPE.

Land/Water and elevation change differences (G027-G400) throughout much of the coast are positive (Figure G1). This is particularly evident throughout the Mermentau Basin.
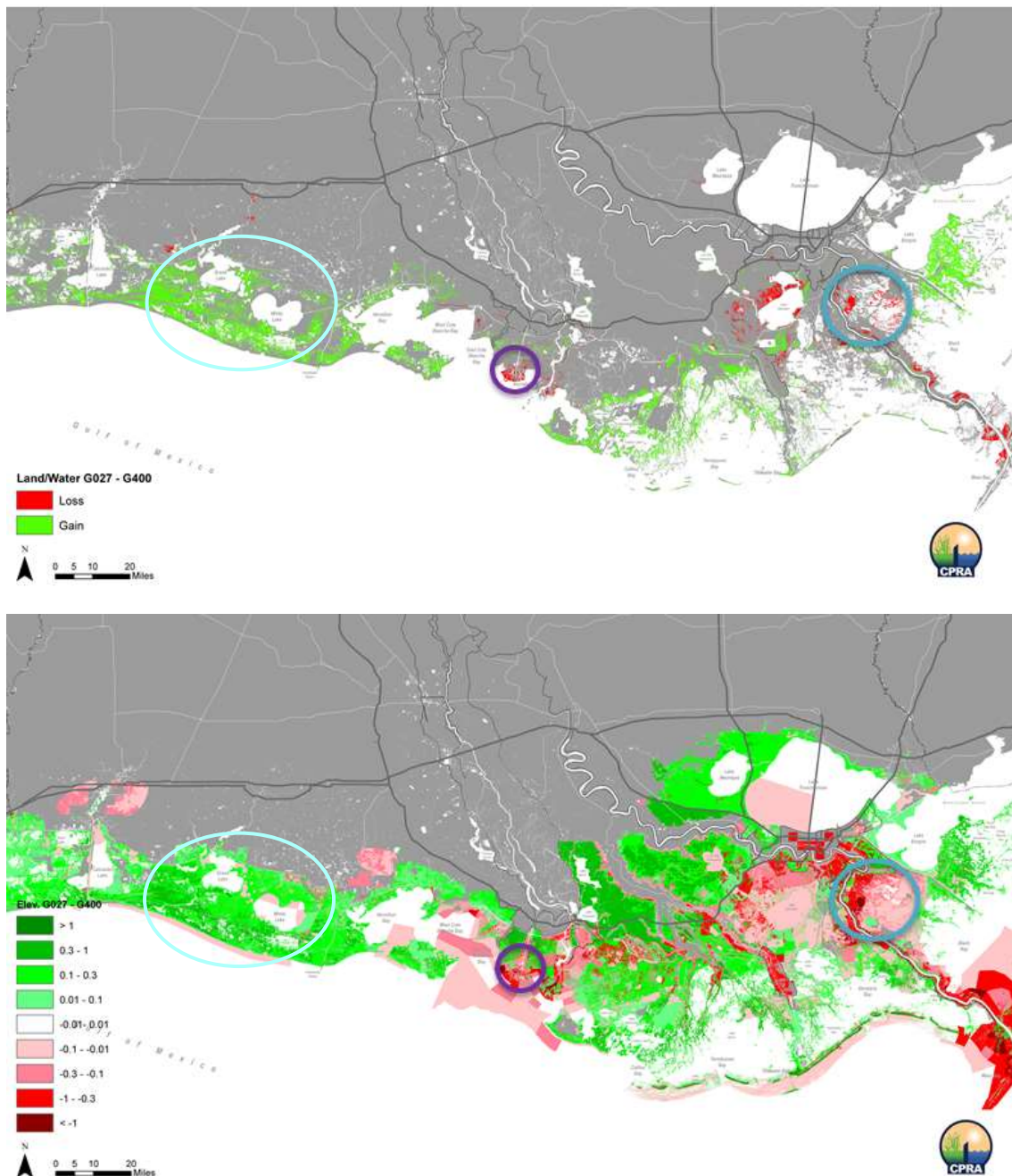
Figure G1. Land water (top) and elevation differences (bottom) between G027 and G400 at year 50. Green indicates G027>G400; red indicates G027<G400. Specific areas of interest are circled: Mermentau Basin in light blue, Wax Lake Delta in purple, and near the receiving areas for proposed Mid-Breton and Mid-Barataria sediment diversions in teal.

Land/water and elevation change differences (G027-G400) are negative near fluvially-dominated areas (river deltas, diversion receiving areas). For example, see Wax Lake Delta G027-G400, year 5 (below left) and G027-G400, year 50 (below right). Even by year 5, G027 has substantially less land and is lower than G400 (Figure G2).

Figure G2. Zoomed in look at land area change (top) and elevation differences (bottom) between G027 and G400 during year 5 (left) and year 50 (right) at Wax Lake delta. Refer to G1 for scale. Green indicates G027>G400; red indicates G027<G400.

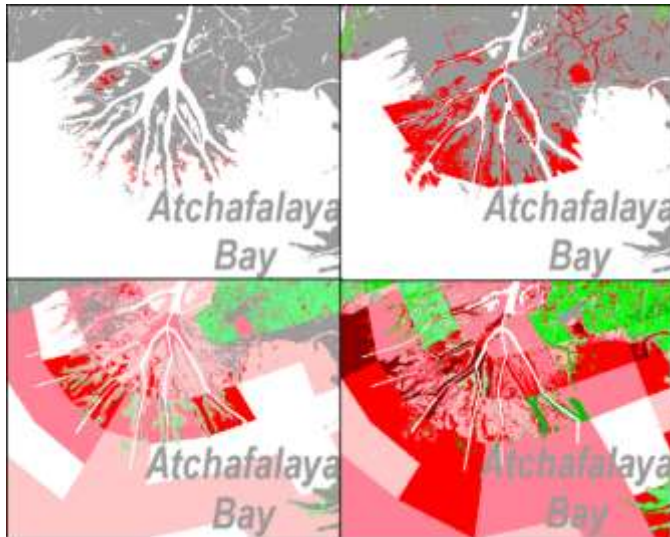Negative difference for G027-G400 also occur in Mid-Breton and Mid-Barataria regions (Figure G3).
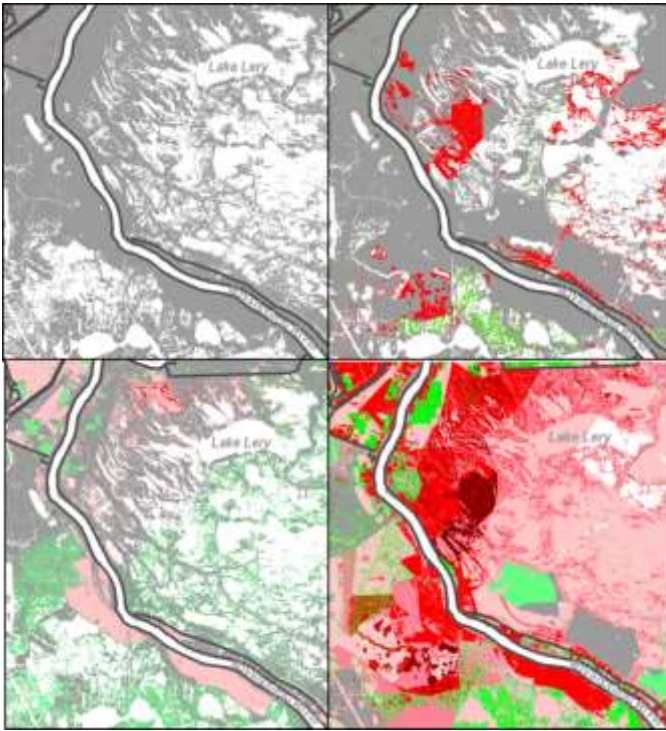
Figure G3. Zoomed in look at land area (top) and elevation differences (bottom) between G027 and G400 during year 5 (left) and year 50 (right) near receiving areas of proposed Mid-Breton and Mid-Barataria sediment diversions. Refer to G1 for scale. Green indicates G027>G400; red indicates G027<G400.

G024: TEST APPROACH 4 THAT USED BELOWGROUND PRODUCTION ESTIMATES THAT WERE ADJUSTED TO REFLECT INUNDATION STRESS TO ESTIMATE OMAR WITH THE IDEAL MIXING MODEL BY HABITAT TYPE.

Land/Water and elevation change differences (G024-G400) throughout much of the coast are positive. This is particularly evident throughout the Mermentau basin but also present in the lower delta plain (Figure G4).
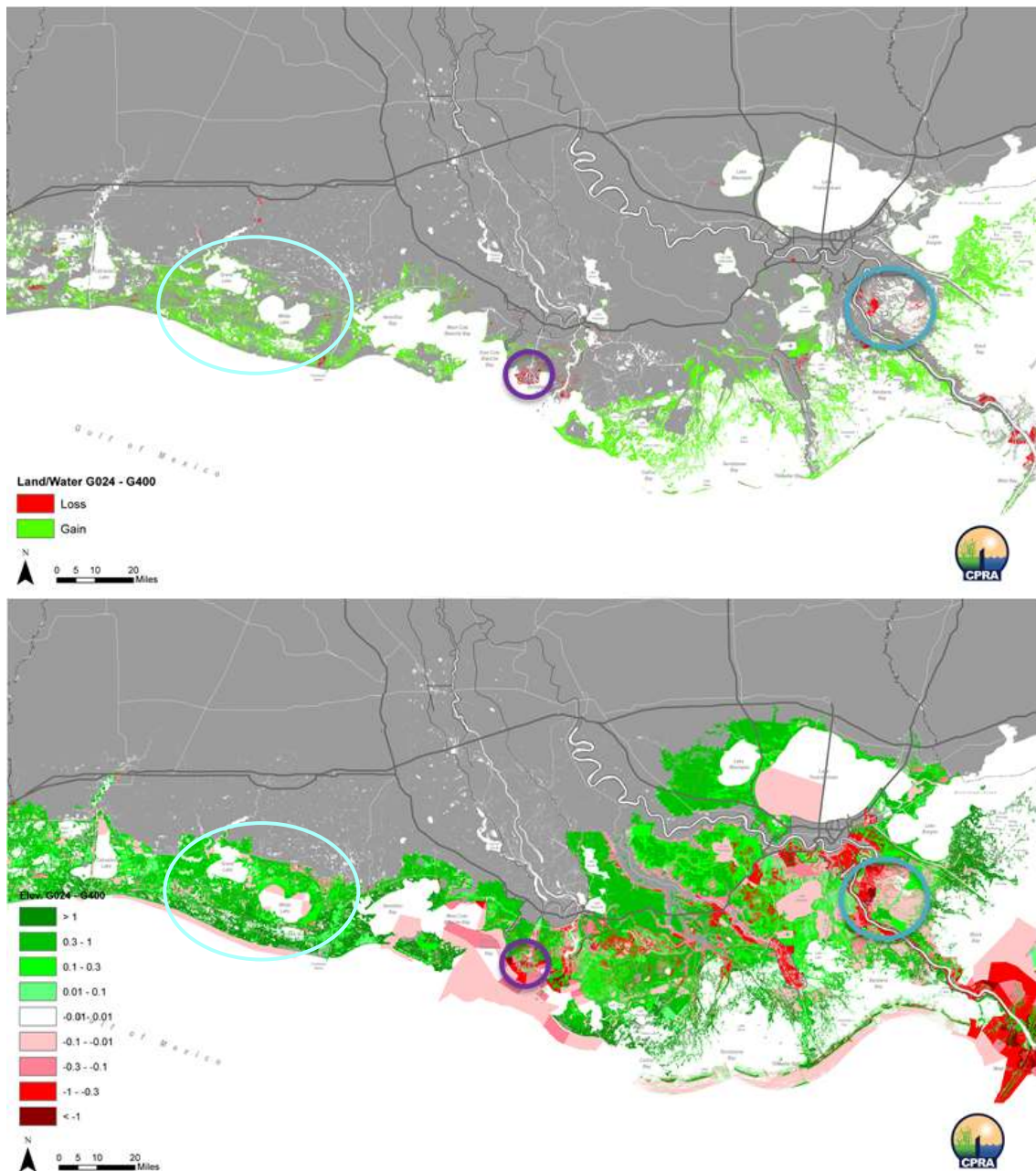
Figure G4. Land water (top) and elevation differences (bottom) between G024 and G400 at year 50. Green indicates G024>G400; red indicates G024<G400. Specific areas of interest are circled: Mermentau Basin in light blue, Wax Lake Delta in purple, and near the receiving areas for proposed Mid-Breton and Mid-Barataria sediment diversions in teal.

Land/water and elevation change differences (G024-G400) are negative near fluvially-dominated areas (river deltas, diversion receiving areas) (Figure G5). These trends are similar to those observed for the G027 test run described above.

Figure G5. Zoomed in look at land area change (top) and elevation differences (bottom) between G024 and G400 during year 5 (left) and year 50 (right) at Wax Lake delta. Refer to G4 for scale. Green indicates G027>G400; red indicates G027<G400.

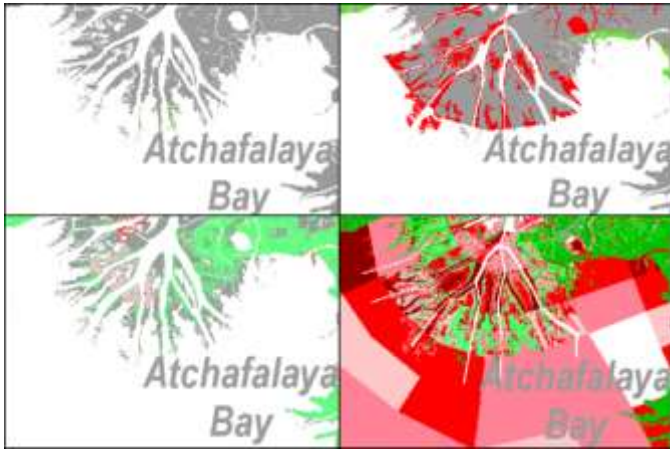The negative differences also occur in the Mid-Breton and Mid-Barataria regions (left is 5 years, right 50 years, Figure G6).
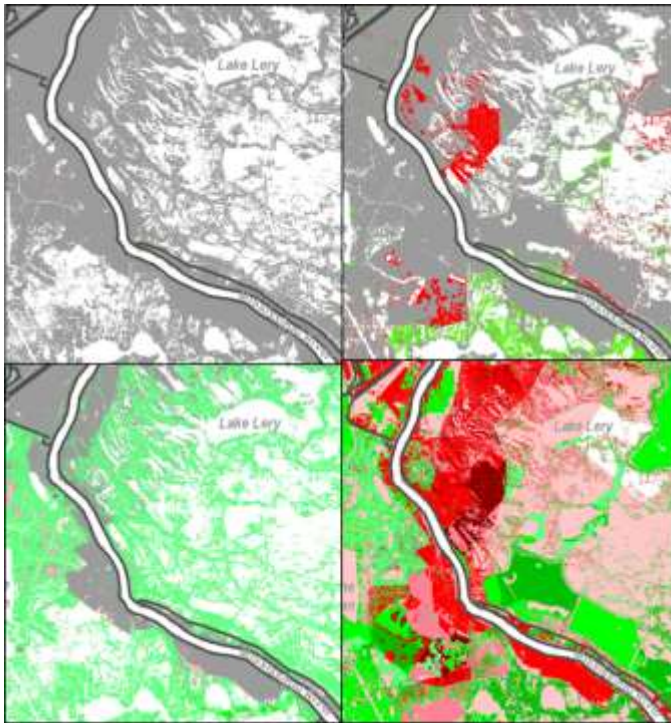
Figure G6. Zoomed in look at land area (top) and elevation differences (bottom) between G024 and G400 during year 5 (left) and year 50 (right) near receiving areas of proposed Mid-Breton and Mid-Barataria sediment diversions. Refer to G4 for scale. Green indicates G027>G400; red indicates G027<G400.

It is also important to note that the G024 approach should be further investigated to reflect possible differences in OMAR between Chenier Plain and Deltaic plain settings.

G026: TEST APPROACH 4 BY ASSESSING THE LIKELIHOOD OF INUNDATION STRESS CONDITIONS (E.G., % TIME FLOODED) FROM 2017 ICM OUTPUT INCLUDING BY HABITAT TYPE.

The inundation rates provided by G026 are quite low compared to recent (2010-2017) CRMS observations. For example, much of the lower delta plain was either gray (0% flooded) or red (0-10% flooded), which is less than the minimum value (17%) for 54 saline marsh sites in the CRMS database that meet inundation data completeness criteria (Figures G7 and G8).

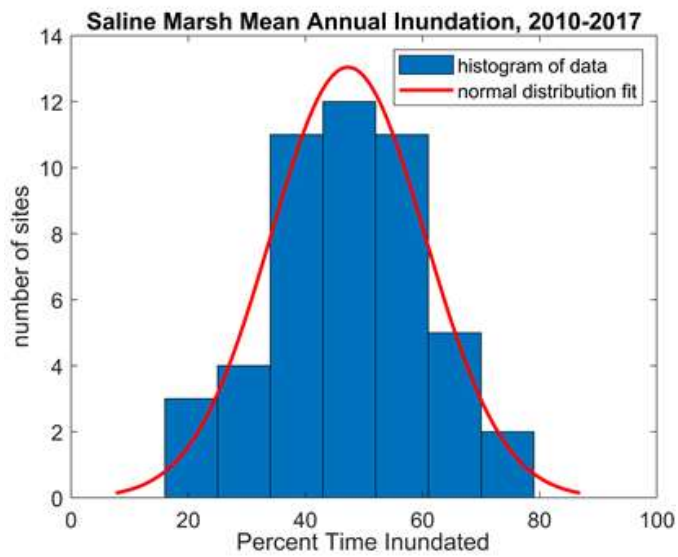Figure G7. Histogram and normal distribution fit of inundation rates for 54 saline marsh CRMS sites, 2010-2017.
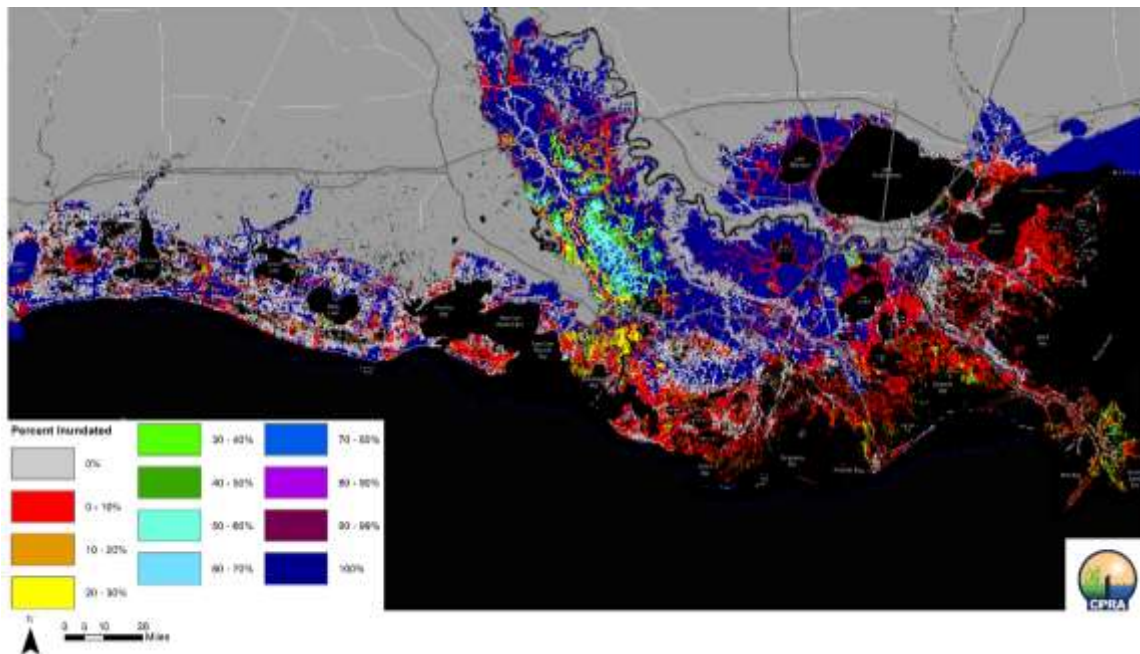
Figure G8. Spatial distribution of % time inundated from ICM-Hydro for G026 test run, year 10.

The distribution of inundation rates estimated by ICM-Hydro indicates that 19.4% of the model domain exhibits 0% inundation, and 63.0% of the domain exhibits 100% inundation (Figure G9).
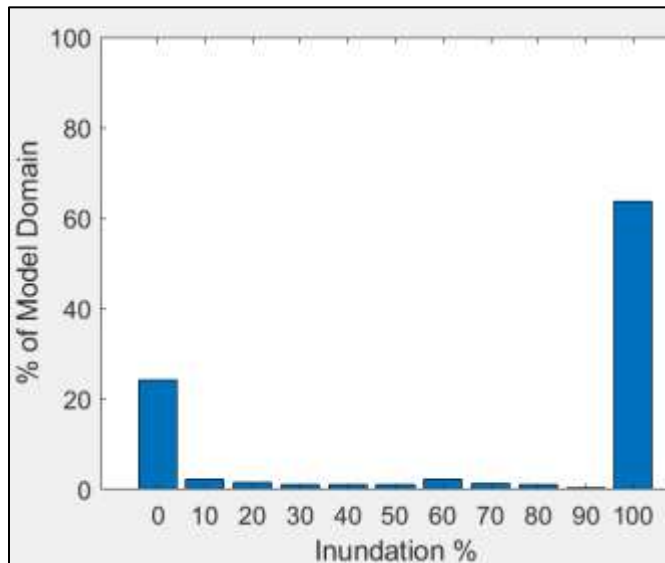
Figure G9. Distribution of inundation rates across ICM-Hydro model domain during year 10. Bar includes ± 5%.

It is possible that portions of the model domain that are upland habitats may comprise a large portion of the areas calculated as 0% inundated, and, likewise, regions that are permanent water bodies or areas of marsh loss prior to year 10 of the model run that result in calculations of permanent inundation. However, eliminating sites that are either never (0%) or permanently (100%) flooded still produce distributions that are strongly skewed compared to observed inundation rates at CRMS sites, with 40% of the remaining model domain exhibiting inundation rates less than 20% (Figure G10).
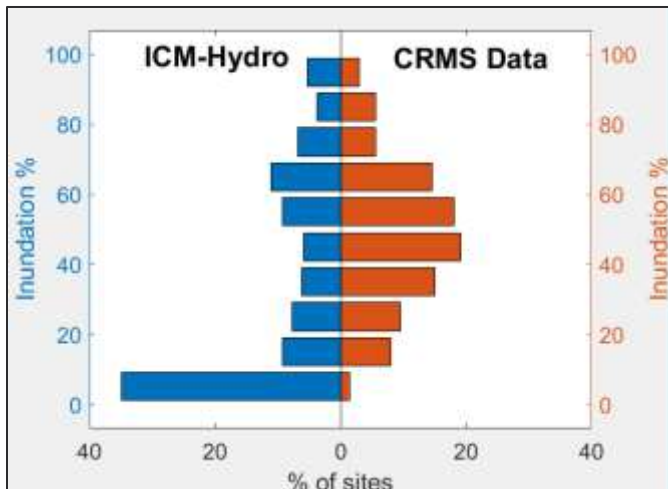
Figure G10. Distribution of inundation rates produced by ICM-Hydro during year 10, excluding model nodes that are either never (0%) or permanently (100%) flooded (blue); distribution of inundation rates observed at CRMS sites coastwide, 2010-2017 (orange).

4. SUMMARY FINDINGS

The method for modeling accretion in the 2012 and 2017 predictive models uses a look-up table that requires BD values to be determined *a priori* by basin/habitat types. In situations where the relative contributions of mineral and organic matter accumulation can change over time while the vegetation classification remains static, a single BD by habitat type by basin may be unresponsive to these temporal variations. For example, in situations where diversion operations change the marsh classification from brackish to fresh, the BD values under G400 actually decrease, as look-up table values for fresh marshes come from fresh peat marshes in the upper reaches of the basin (note that the 2017 ICM does not utilize the Deltaic category identified in Table 10 for the 2012 Coastal Master Plan). In reality, BD should increase due to increased input of mineral material. Because BD values are low for fresh marshes in Barataria and Breton Basins (0.05 g cm^{-3}) under the G400 model test run (Table 9), the volumetric leverage is inflated and accretion is overestimated. A transition to BD values nearly an order of magnitude higher in fresh marshes in deltaic settings and diversion outfall areas has been observed at CRMS3169 (Figure 21), which is situated in the immediate outfall of the Davis Pond freshwater diversion.

The ideal mixing model approach proposed here eliminates the need to designate a value for BD, as it solves for it through an equation based on the overall physical relationship between organic matter content and mineral matter content in soils at CRMS sites that uses the relative contributions of mineral and organic mass accumulation rates as input variables.

2012/2017 ICM APPROACH

The team started with a hypothetical Barataria brackish marsh site that carries (from the look-up table) the following BD and OM values (Table G2). For the example here, the team assumed the VAR was the mean value for brackish marshes in Barataria Basin (1.18 cm yr^{-1}).

Table G2. Assumed values for Organic Matter, Bulk Density, and Vertical Accretion for a hypothetical Barataria brackish marsh site.

Metric	Value
OM (g g^{-1})	0.49
BD (g cm^{-3})	0.15
VAR (cm yr^{-1})	1.18

From those numbers, the team calculated Q$_{sed}$ (MMAR) as

$$Q_{sed} = (1 - OM) * BD * VAR = 0.0903 \ g \ cm^{-2}yr^{-1} \tag{G4}$$

and Q$_{org}$ as

$$Q_{org} = OM * BD * VAR = 0.0867 \ g \ cm^{-2}yr^{-1} \tag{G5}$$

Now that the team had values for Q_{sed} (MMAR) and Q_{org} (OMAR), the team could use them to calculate VAR (cm yr^{-1})

$$VAR = \frac{Q_{sed}+Q_{org}}{BD} \tag{G6}$$

Notice here the "10,000" in the divisor on the right-hand side is omitted because the length units are in centimeter, so there was no need to convert from meters. If converting units from meters to centimeters, then multiply BD (divisor) by 10,000.

Inserting our values of Q_{sed} (MMAR) and Q_{org} (OMAR) gives

$$VAR = \frac{0.0903 \ g \ cm^{-2}yr^{-1}+0.0867 \ g \ cm^{-2}yr^{-1}}{0.15 \ g \ cm^{-3}} \tag{G7}$$

or, *VAR* = 1.18 cm yr^{-1}.

Notice the fraction can be algebraically split to partition the mineral and organic components such that

$$VAR_{mineral} = \frac{0.0903 \ g \ cm^{-2}yr^{-1}}{0.15 \ g \ cm^{-3}} = 0.60 \ cm \ yr^{-1} \qquad (G8)$$

and

$$VAR_{organic} = \frac{0.0867 \ g \ cm^{-2}yr^{-1}}{0.15 \ g \ cm^{-3}} = 0.58 \ cm \ yr^{-1} \qquad (G9)$$

Now suppose a river diversion into the basin becomes operational, causing Q_{sed} (MMAR) to increase ten-fold, to 0.903 g cm^{-2} yr^{-1}. Q_{org} (OMAR) remains constant (the team assumed that inundation does not impact production or decomposition), so it retains its value 0f 0.0867 g cm^{-3}.

The team then used the new value of Q_{sed} (MMAR, from the ICM-Hydro) and BD (from the look-up table, fresh marsh in Barataria; 0.05 g cm^{-3}) to calculate vertical accretion:

$$VAR = \frac{0.903 \ g \ cm^{-2}yr^{-1} + 0.0867 \ g \ cm^{-2}yr^{-1}}{0.05 \ g \ cm^{-3}} \qquad (G10)$$

or, VAR = 19.8 cm yr^{-1}, with $VAR_{mineral}$ and $VAR_{organic}$ components taking values of 18.1 and 1.7 cm yr^{-1}, respectively.

So the vertical accretion has increased from 1.18 cm yr^{-1} to 19.8 cm yr^{-1} as a result of the increased sediment input, or nearly a 20-fold increase. This remarkable increase largely results from using the low BD value from fresh marshes in Barataria Basin (0.05 g cm^{-3} in the look-up table), but also because the volumetric leverage of organic and mineral accumulation are treated equally, even though the ideal mixing model indicates that it is nearly 30 times less for mineral than organic, on a per mass basis.

PROPOSED 2023 APPROACH WITH IDEAL MIXING MODEL

Going back to the starting values, i.e., "pre-diversion" (Table G2),

Q_{sed} (MMAR) is calculated as

$$Q_{sed} = (1 - OM) * BD * VAR = 0.0903 \ g \ cm^{-2}yr^{-1} \qquad (G11)$$

Q_{org} (OMAR) is calculated as

$$Q_{org} = OM * BD * VAR = 0.0867 \ g \ cm^{-2}yr^{-1} \qquad (G12)$$

The team then divided these mass accumulation rates by their corresponding self-packing densities to partition the accretion to the mineral and organic contributions (Table G3).

Table G3. Calculated mass accumulation rates and vertical accretion rates with self-packing densities for organic and mineral soil pre-diversion.

Soil Component	Mass Accumulation Rate (g cm^{-2} yr^{-1})	Self-Packing Density (g cm^{-3})	Vertical Accretion Rate (cm yr^{-1})
Organic	0.0867	0.076	1.14
Mineral	0.0903	2.106	0.04
Total	0.1770		1.18

Notice the team obtained the same total accretion value (1.18 cm yr^{-1}) as in the G400 pre-diversion example above, but much less of the total accretion is attributed to mineral sedimentation under the ideal mixing model (0.04 cm yr^{-1}) compared with G400 (0.6 cm yr^{-1}). This discrepancy arises from the fact that under G400, the volumetric leverages of mineral and organic matter are treated equally, while the ideal mixing model approach recognizes the fact that they are, in fact, quite different. Then the diversion comes online and increases Q_{sed} (MMAR) tenfold. Q_{org} (OMAR) remains unchanged (Table G4).

Table G4. Calculated mass accumulation rates and vertical accretion rates with self-packing densities for organic and mineral soil components post-diversion.

Soil Component	Mass Accumulation Rate (g cm^{-2} yr^{-1})	Self-Packing Density (g cm^{-3})	Vertical Accretion Rate (cm y^{r-1})
Organic	0.0867	0.076	1.14
Mineral	0.9030	2.106	0.43
Total	0.9897		1.57

So using the same scenario with the ideal mixing model, the VAR is increased 33% over the original ("pre-diversion") rates.

The discrepancy between the two approaches arises from estimating the BD with a look-up table based on basin and habitat type, specifically from using values representative of highly organic inactive delta fresh marshes (BD = 0.05 g cm^{-3}) when in many cases (such as diversion receiving

areas) values should be more representative of high mineral-content active delta fresh marshes (BD = 0.5-0.6 g cm^{-3}). Even if representative values are used, the look-up table approach is based on correlations between basin/habitat type classification and soil properties rather than the causal mechanisms that drive them. In this case those causal mechanisms are the relative contributions of mineral and organic mass accumulation and their highly disparate volumetric conversion constants (self-packing densities). The ideal mixing model indicates that the resulting BD for organic and mineral mass accumulation rates of 0.0867 and 0.9030 g cm^{-2} yr^{-1}, respectively, would be 0.63 g cm^{-3}.

All of this suggests that in areas dominated by mineral matter accumulation, particularly (but not restricted to) those areas where mineral matter is increasing from initial conditions through time (e.g., diversions), the accretion response will be overestimated using the 2017 ICM approach (G400 test run). Thus, when comparing approaches utilizing the ideal mixing model (G027 and G024 model test runs) vs G400, fluvially-dominated regions such as deltas and diversion receiving areas should show less accretion with the G027/G024 approach than with the G400 approach, and hence the dominance of red in these regions on the difference maps (see Figures G1-7).

It was hypothesized that land area at the end of the model run for G024 would be less than that for either G400 or G027, given the fact that this model approach is sensitive to inundation and 0.63 m of eustatic sea level rise was applied over the course of these 50-year model runs. However, G024 showed the greatest overall land area at the end of the model run (despite the accretion deficits in deltaic/diversion receiving areas relative to G400 described above). This outcome is likely a result of the low inundation rates produced by ICM-Hydro compared to those observed in the CRMS dataset. With G026 output indicating that 40% of the model domain exhibits inundation rates under 15%, much of the model domain would exhibit unrealistically high organic accretion rates, as the belowground production rates that drive organic accretion would all fall on the far left of the inundation-production curves for intermediate, brackish, and saline marsh classifications (Figure 18).

5. REFERENCES

Steyer, G. D., Couvillion, B., Wang, H., Sleavin, B., Rybczyk, J., Trahan, N., Beck, H., Fischenich, C. J., Boustany, R., & Allen, Y. (2012). *Appendix D-2 Wetland Morphology Model Technical Report* (No. Appendix D-2) (p. 108). Baton Rouge, LA: Coastal Protection and Restoration Authority.

APPENDIX H: WEIGHTED AVERAGE FIBS SCORE

1. TEST OF WEIGHTED AVERAGE FIBS SCORE APPROACH

A model test (G025) was performed to check how changing the way that fresh, intermediate, brackish and saline (FIBS) classes were assigned may alter the distribution of habitat types. In the 2017 ICM (G400) the FIBS class was assigned by first determining which species had the greatest cover on land in the vegetation grid cell and then using the FIBS class of that species to determine the overall FIBS classification of the grid cell. The new method uses a weighted average: the FIBS score of a species was multiplied by its cover and the sum of these multiplications was divided by the total vegetative cover. FIBS class was then determined based on this weighted average (Table 18). Open water was classified in ICM-Morph and was not affected. Because rules for elevation change and collapse thresholds handled by ICM-Morph are based on FIBS classes in the 2017 ICM framework, changes to FIBS classification can affect land change.

Test results of G025 were compared to 2017 ICM output of future with action and with the medium scenario (G400). It was hypothesized that the largest difference between G025 and the G400 method would be in the classification of fresh and intermediate marshes. This hypothesis was based on the assignment of *Sagittaria lancifolia* to the intermediate marsh in G400, while in G025 it depended on the cover of the other species. In addition, there are more species assigned in the fresh and intermediate marsh classes. It was also expected that the G025 approach would smooth the gradients in the FIBS classes and avoid the occurrence of fresh marshes immediately adjacent to saline marshes. Lastly, it was expected that changes in classification will lead to changes in land loss patterns, but it was hypothesized that these will be relatively minor.

2. RESULTS

The model test G025 shows the improvement in capturing the gradient from fresh to saline marsh classes compared to model test G400, for example in the Barataria Basin (Figure H1). The largest difference observed is that in G400 all marshes dominated by *Spartina patens* are classified as brackish marshes. In the approach tested in G025, other species present distinguish these marshes into intermediate and brackish marshes. The second largest difference is that in G400 model test run all marshes dominated by *Spartina alterniflora* are classified as saline marshes, whereas in the new system other species present distinguish these marshes into saline and brackish marshes.
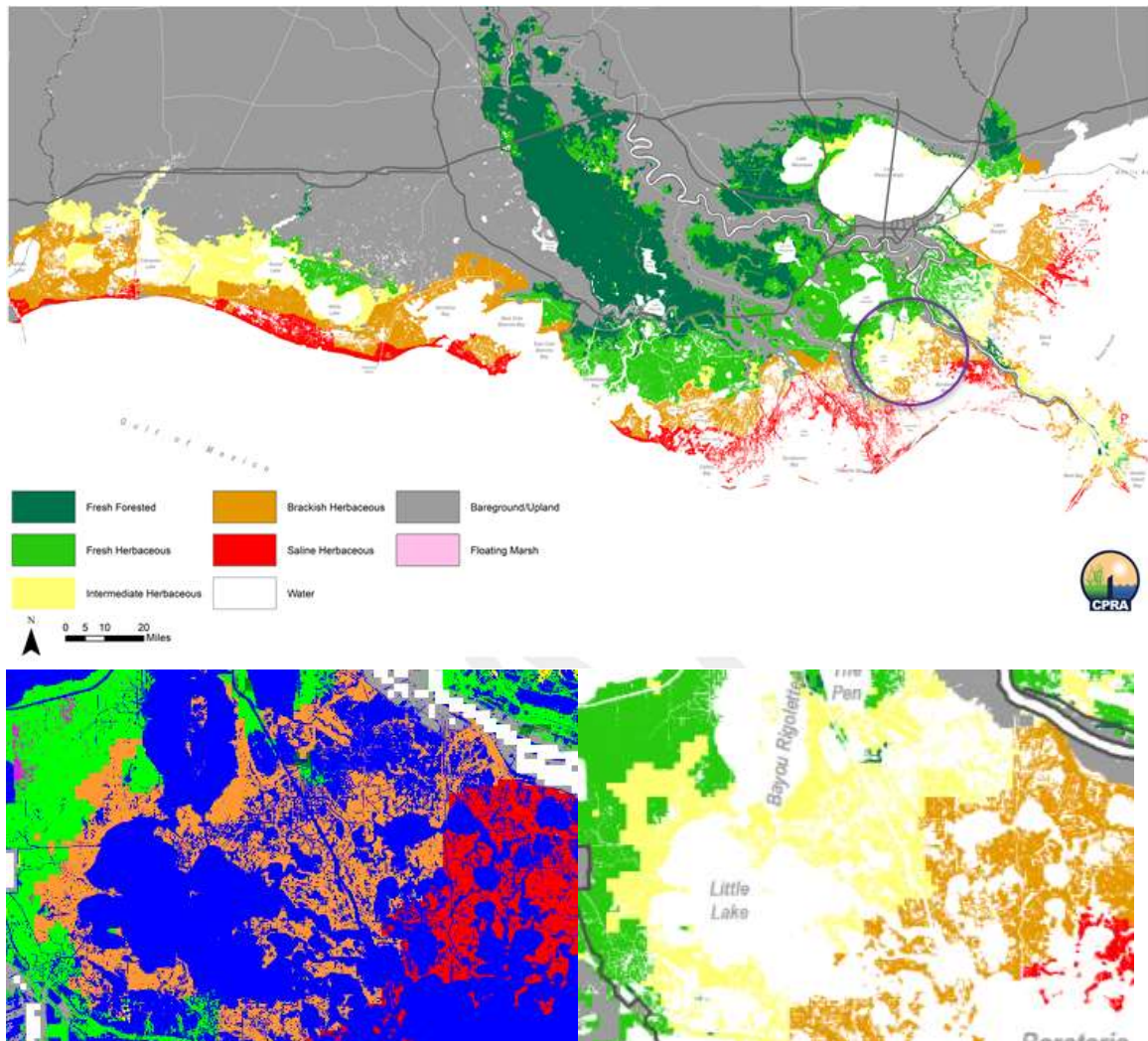
Figure H1. Vegetation coverage for G025 at year 10 with central Barataria Basin circled in purple (top figure); Zoomed in look at vegetation coverage in year 10 using the 2017 ICM FIBS classification system for G400 (left panel) and testing the weighted average approach for the FIBS classification system in G025, (right panel) for Barataria Basin (bottom figure). Note that open water is shown in blue for G400 and in white for GO25.

Figure H2 demonstrated that the proposed 2023 ICM weighted average approach maintained a gradient of habitat types over time. It also showed that the proposed classification system leads to slight differences in land change. At year 40 there was more land loss north of White Lake as well as reduced land loss east of Freshwater Bayou in G025. However, the differences were relatively minor. The area north of White Lake was fresh marsh throughout year 40 in G400. However, in G025 large

areas north of White Lake were classified as Intermediate marsh in early decades; this was most pronounced in year 10 with the area of intermediate marsh diminishing by year 40. Intermediate marshes would be more tolerant of salinity and not subject to collapse based on a high two-week salinity (see Activity 1). This may account for why more land loss was experienced when the marsh is classified as fresh in early decades in G025. The area west of Freshwater Bayou with slightly reduced land loss in G025 was classified as brackish in G025 but is saline marsh by year 10 in G400. Saline marshes have higher bulk densities and lower soil organic matter content in the Mermentau Basin in the 2017 ICM (see Activity 2) which could lead, depending on mineral sediment deposition, to lower accretion rates. Thus, brackish marshes in G025 might be higher in elevation than saline marshes in G400 and brackish marshes can tolerate more flooding (a higher collapse threshold – see Activity 1) in the 2017 ICM. These factors could lead to a change in land loss rates and point to a reduction as seen in Figure H2.
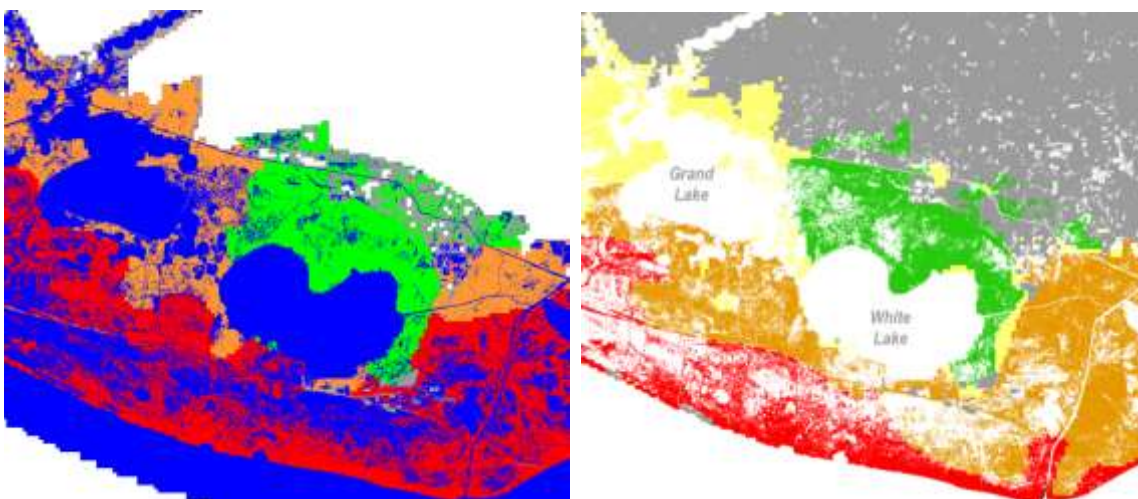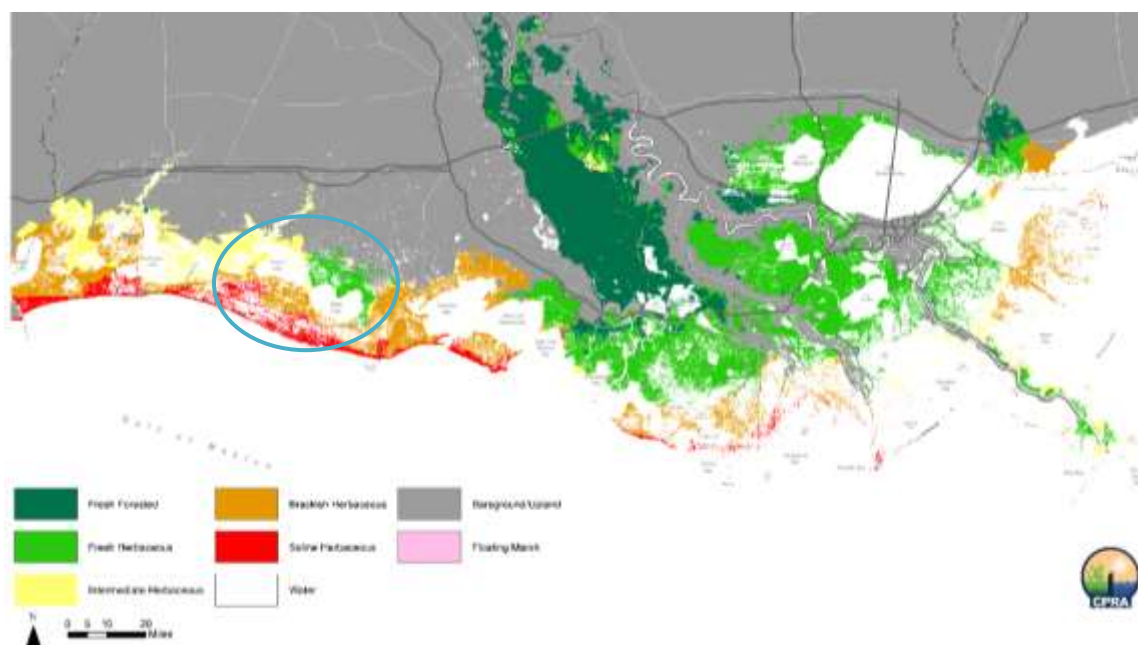
Figure H2. Vegetation coverage for G025 at year 40 with the Mermentau Basin circled in teal (top figure); Zoomed in look at vegetation coverage in year 40 using the 2017 ICM FIBS classification system for G400 (left panel) and testing the weighted average approach for the FIBS classification system in G025, (right panel) for the Mermentau Basin (bottom figure). Note that open water is shown in blue for G400 and in white for GO25.

Although it was hypothesized that the major differences in habitat type area would be from the fresh to intermediate marshes, the greatest changes in habitat type area were from changes in the

intermediate to brackish and brackish to saline marshes. This was due to the 2017 ICM classification being based on just one dominant species, while the proposed approach used all available species calculated by ICM-LAVegMod and provides a weighted average. For example, saline marsh was dominated by *S. alterniflora* and is typically a monoculture. However, when it is co-dominated by *S. patens* and *Distichlis spicata,* it was generally classified as brackish marsh in the 2017 ICM output. If the species cover was 45% *S. alterniflora*, 40% *S. patens*, and 15% *D. spicata* of an area, it would be classified as saline marsh using the 2017 ICM approach; with the proposed approach tested in GO25, it was correctly classified as brackish marsh.

APPENDIX I: VEGETATION CLASSIFICATION (ACTIVITY 5)

1. METHODOLOGY FOR UTILIZING SELF-ORGANIZING MAPS TO CLASSIFY VEGETATION INTO 11 GROUPS

An unsupervised vegetation community classification approach rooted in artificial neural networks, called self-organizing maps (SOMs), holds a key advantage over traditional, distribution-based statistical approaches to classification in that it is robust to strongly skewed distributions that are typical of species abundance datasets (e.g., Snedden, 2019). More importantly, once a SOM is trained, new samples can be projected onto it without altering the existing clustering scheme. The SOMs are particularly attractive approach for classifying samples obtained from ongoing and long-term ecological monitoring programs like CRMS.

The SOMs are also robust to missing data. For example, even though the SOM trained to classify CRMS vegetation communities uses 49 species to make the classifications (Snedden, 2019), in theory it should still perform well in classifying sites based on 23 species used in ICM-LAVegMod, provided most or all of the ICM-LAVegMod species are important in governing the ordination in Snedden (2019).

The performance of the CRMS vegetation communities SOM can be tested by classifying communities based on relative abundance data for the taxa modeled in ICM-LAVegMod and to assemble a confusion matrix that depicts what community types are classified into the 49 species used for CRMS versus the 23 species used for ICM-LAVegMod (Figure I1).

| | Classified as, with only LAVegMod taxa included | | | | | | | | | | | | |
	Maidencane	Three-Square	Roseau Cane	Paspalum	Wiregrass	Bulltongue	Needlerush	Bulrush	Brackish Mix	Oystergrass	Saltgrass	Total	% correct
Maidencane	144	2	0	0	0	40	0	0	0	0	0	186	77
Three-Square	0	122	0	0	4	8	0	0	0	0	0	134	91
Roseau Cane	0	0	99	0	0	0	0	0	0	0	0	99	100
Paspalum	0	2	0	71	2	9	0	0	0	0	0	84	85
Wiregrass	0	4	0	0	901	0	0	0	0	0	0	905	100
Bulltongue	6	30	1	2	5	404	0	4	0	0	0	452	89
Needlerush	0	0	0	0	0	0	48	0	0	0	0	48	100
Bulrush	0	1	0	0	1	5	4	41	1	0	3	56	73
Brackish Mix	0	0	0	0	0	0	0	0	162	0	0	162	100
Oystergrass	0	0	0	0	0	0	0	0	0	325	0	325	100
Saltgrass	0	0	0	0	0	0	0	0	1	0	74	75	99
Total	150	161	100	73	913	466	52	45	164	325	77	2526	
													95

(Actual (with all 49 taxa) — vertical axis label)

Figure I1. Confusion matrix that compares the number of sites classified into wetland vegetation community types based on 49 taxa that were used initially to develop the CRMS vegetation community self-organizing map (vertical) to the 29 vegetation taxa used by ICM-LAVegMod (horizontal). The correct classification rate (95%) is shown in the lower right-hand cell of the table.

The bold values along the diagonal in Figure K1 indicate the number of sites that were classified into the same community types using all 49 species analyzed in Snedden (2019) versus using only the subset of taxa examined by ICM-LAVegMod. For example, of the 75 sites that were classified as "saltgrass" communities using all 49 species in Snedden (2019), 74 of them were classified identically using only the subset of taxa in LAVegMod. Thus, the correct classification rate for "saltgrass" communities was 99%. Altogether, the correct classification rate was 95% based on using the ICM-LAVegMod species, many misclassifications involved species that commonly co-occur. This high correct classification rate indicates that the SOM will be effective in classifying species composition data from ICM-LAVegMod output into the same vegetation communities delineated in Snedden (2019).

2. REFERENCES

Snedden, G. A. (2019). Patterning emergent marsh vegetation assemblages in coastal Louisiana, USA, with unsupervised artificial neural networks. *Applied Vegetation Science, 22,* 213–229.